NUREG/CR-1489
UCRL-52746

Best Estimate Method vs Evaluation Method: A Comparison of Two Techniques in Evaluating Seismic Analysis and Design

S. E. Bumpus, J. J. Johnson, P. D. Smith

Lawrence Livermore National Laboratory

Prepared for
U.S. Nuclear Regulatory
Commission

This work was supported by the United States Nuclear Regulatory Commission under a Memorandum of Understanding with the United States Department of Energy.

Available from
GPO Sales Program
Division of Technical Information and Document Control
U.S. Nuclear Regulatory Commission
Washington, D.C. 20555

and

National Technical Information Service
Springfield, Virginia 22161

DISCLAIMER

DISCLAIMER

NUREG/CR-1489
UCRL-52746
RD

NUREG/CR--1489

TI86 002747

Best Estimate Method vs Evaluation Method: A Comparison of Two Techniques in Evaluating Seismic Analysis and Design

Manuscript Completed: May 1980
Date Published:

Prepared by:
S. E. Bumpus, J. J. Johnson, P. D. Smith

Lawrence Livermore National Laboratory
7000 East Avenue
Livermore, CA 94550

Prepared for
Division of Reactor Safety Research
U.S. Nuclear Regulatory Commission
Washington, D.C. 20555
NRC FIN NO. A-0130

FOREWORD

Under contract with the Division of Reactor Safety Research of the U.S. Nuclear Regulatory Commission (NRC), Lawrence Livermore National Laboratory (LLNL) is currently studying the seismic contribution to reactor risk. This document reports on the initial efforts that have been made on a calculational concept named the Best Estimate Method vs the Evaluation Method (BE-EM). The authors acknowledge the code development contributions made by Shirley Rompel in this study. The NRC FIN number is A-0130.

CONTENTS

LIST OF FIGURES

PAGE

PAGE

LIST OF FIGURES (Continued)

PAGE

LIST OF FIGURES (Continued)

PAGE

PAGE

LIST OF TABLES

BEST ESTIMATE METHOD VS EVALUATION METHOD: A COMPARISON OF TWO TECHNIQUES IN EVALUATING SEISMIC ANALYSIS AND DESIGN

ABSTRACT

The concept of how two techniques, Best Estimate Method and Evaluation Method, may be applied to the traditional seismic analysis and design of a nuclear power plant is introduced. Only the four links of the seismic analysis and design methodology chain (SMC)--seismic input, soil-structure interaction, major structural response, and subsystem response--are considered. The objective is to evaluate the compounding of conservatisms in the seismic analysis and design of nuclear power plants, to provide guidance for judgments in the SMC, and to concentrate the evaluation on that part of the seismic analysis and design which is familiar to the engineering community. An example applies the effects of three-dimensional excitations on a model of a nuclear power plant structure. The example demonstrates how conservatisms accrue by coupling two links in the SMC and comparing those results to the effects of one link alone. The utility of employing the Best Estimate Method vs the Evaluation Method is also demonstrated.

SUMMARY

The primary purposes of this report are to introduce the concept of Best Estimate Method vs Evaluation Method (BE-EM) as it applies to the seismic analysis and design of nuclear power plants, to demonstrate BE-EM with an illustrative example coupling two links in the Seismic Methodology Chain (SMC), and to demonstrate the effects of three-dimensional excitations. The term BE-EM was introduced to represent the comparison of any two seismic analysis methodologies. BE-EM is limited to a systematic evaluation of the SMC only; i.e., seismic input, soil-structure interaction, major structural response, and subsystem response, whereas the Seismic Safety Margins Research Program (SSMRP) treats the SMC along with the failure of systems and components and their functional interdependence. The example considered in this study links two phases of the SMC--seismic input and structural response. All of the results demonstrate three-dimensional effects.

The Best Estimate Method (BE) and Evaluation Method (EM) analysis considered two links in the SMC. The EM procedure was composed of synthetic time histories generated to meet the design criteria of R.G. 1.60, the square-root-of-the-sum-of-the-squares (SRSS) rule of combination for response due to three components of motion, and broadening of in-structure response spectra to account for uncertainties in the dynamic characteristics of structures. Corresponding elements in the BE procedure were recorded time histories--three components with recorded phasing, and probability distributions on structural dynamic characteristics which were sampled repetitively to incorporate structural uncertainties directly. Response was in the form of in-structure response spectra.

Two quantities were used in the comparison of BE and EM response. Factors of Comparison (FOC) were computed as the quotient of the mean EM response spectra and the mean (or the mean-plus-one-standard-deviation) BE response spectra. In addition, Probabilities of Exceedance (POE) were computed representing the probability of a BE response exceeding the corresponding EM response. Both FOC and POE vary over the frequency range

of interest. The results demonstrated the apparent conservatism of the EM design criteria subject to the assumptions of the study.

The results of the present investigation were compared with a previous study which considered only the seismic input phase. The comparison demonstrated a compounding of effects through coupling two links in the SMC as compared to computing one link alone.

1. INTRODUCTION

1.1 BACKGROUND

Performing the seismic analysis of a nuclear power plant and designing that plant to resist earthquakes requires a significant multidisciplinary effort.[1] This effort includes contributions from geologists, seismologists, and engineers specializing in structural, mechanical, and electrical design and in soils. For some time there has been a strong motivation to reexamine the traditional process of seismic analysis and design of nuclear power plants in an overall system context. This motivation comes principally from the widely held belief that a compounding of conservatisms occurs in the current process. That is, at each stage of the current process, conservatisms are introduced to account for uncertainties, and these conservatisms compound from one stage to the next. However, in each stage only minimal compensations are made for the compounding of conservatisms because they are not quantified. The result may be an overconservative seismic design.

A methodology that will examine the current seismic analysis and design process of nuclear power plants in an overall system context is being developed in the Seismic Safety Margins Research Program (SSMRP) at Lawrence Livermore National Laboratory (LLNL).[2] Figure 1 depicts the seismic analysis and design methodology chain (SMC) and its relationship to the SSMRP systems model. The traditional SMC is shown separated from the SSMRP systems analysis by a segmented line to emphasize that the overall seismic analysis and design problem is treated in two parts calculationally in the SSMRP. The systems analysis (under the dashed line) represents reactor systems using an event tree/fault tree methodology, and it also employs an overall computational procedure to compute the probability of failure of structures, components, and systems, the probability of radioactive releases, and variations in these probabilities due to uncertainties in the SMC. (The specially developed SEISIM code is used for these computations.) Clearly, examining the nuclear power plant system in total, including the functional requirements of safety systems and their interdependence, is the most complete

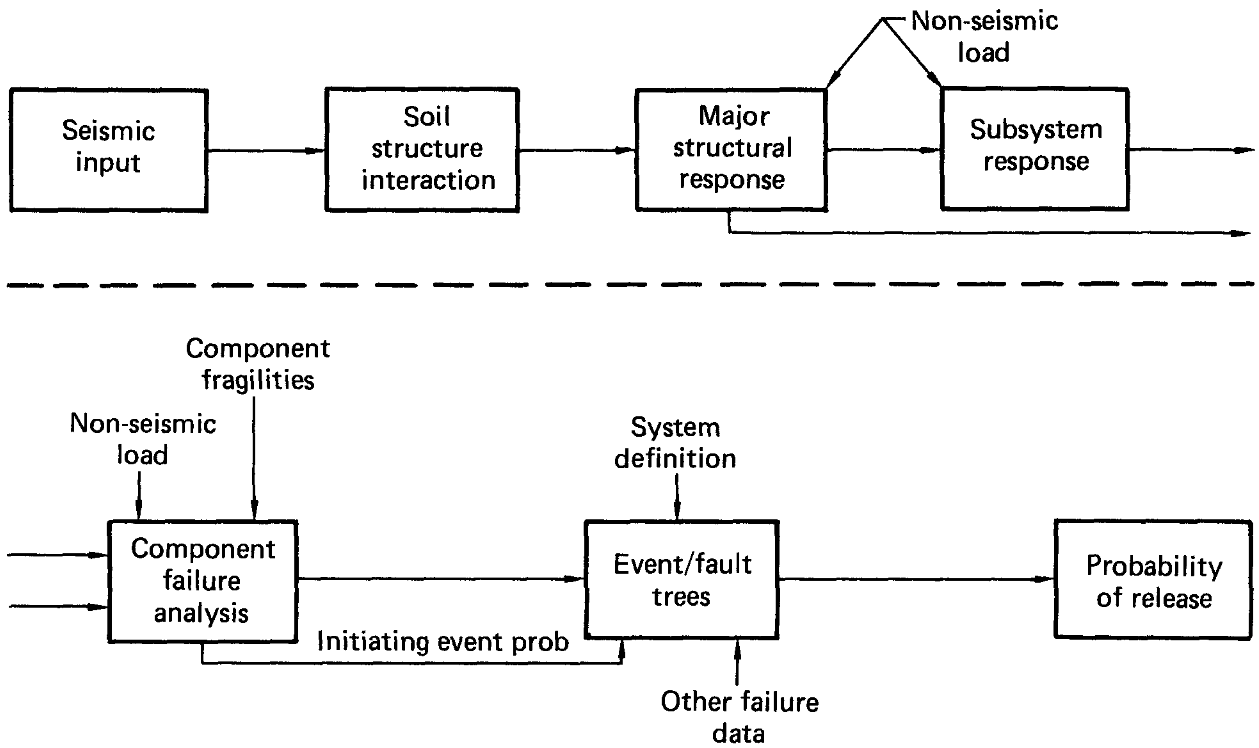

FIG. 1. Key elements of a seismic analysis and design calculational procedure for nuclear power plants. In evaluating possible compounding of conservatisms in such a procedure the Seismic Safety Margins Research Program (SSMRP) calculates values in the entire system, from seismic input to probability of release. The Best Estimate Method vs Evaluation Method procedure, however, reduces the problem by coupling the four traditional elements of seismic analysis and design (boxes above the dashed line) and analyzing them independent of the probabilities of failure and radioactive release.

manner of treating the problem--and this is the SSMRP approach. However, it is possible to consider only the four elements of the SMC (seismic input, soil-structure interaction, major structural response, and subsystem response) in a coupled or "system" fashion independent of the calculation of probabilities of failure or radioactive release. The quantities of interest then become response parameters and their statistics; for example, in-structure response spectra, displacements, velocities, accelerations, forces, rather than probabilities of failure or radioactive release. The concept for such a simplification is introduced in this report.

1.2 PURPOSE AND SCOPE

We simplify in this report the systematic evaluation of the seismic analysis and design of a nuclear power plant to encompass only the four links of the SMC: seismic input, soil-structure interaction, major structural response, and subsystem response. The term Best Estimate Method vs Evaluation Method (BE-EM) is introduced to identify this simplification. The objective of BE-EM is to develop a basis for the comparison of any two seismic analysis procedures. One comparison would be between a Best Estimate Method (BE) and an Evaluation Method (EM); hence, the term BE-EM. However, comparison possibilities are not limited to BE-EM--any two seismic analysis methodologies may be compared. Examples include any combination of best estimate, standard review plan (SRP), design methodologies of older plants, proposed new techniques, erroneous methods of analysis, and so forth. There are two key points to be emphasized in the BE-EM concept. The methodology comparison should include as many links of the SMC as possible and appropriate. For example, in the BE-EM concept, it could be misleading to compare a soil-structure interaction result such as base-mat response instead of a design parameter including structural and subsystem response. Second, the basis of comparison will, in most cases, be statistical; that is, mean vs mean, mean vs mean-plus-one-standard-deviation, mean vs point estimate, etc. When calculating a Best Estimate response, this will always be the case since Best Estimate by definition includes a measure of uncertainty. The Evaluation Method may or may not be statistical.

The term BE-EM is not new. A similar concept was applied to postulated loss-of-coolant accidents (LOCA).[3] Thermal conditions resulting from a LOCA as predicted by a "best estimate" or realistic model were compared with those predicted by an "evaluation model." The comparison provided a measure of the margin between best estimate and design.

The objectives, then, of the present study are:

1. To introduce and apply the BE-EM concept to the seismic analysis and design of nuclear facilities.
2. To demonstrate BE-EM through an illustrative example showing the coupling effects between two links in the SMC.
3. To indicate the sensitivity of response to three components of input motion.

1.3 ANALYSIS OVERVIEW

The present investigation is an extension and coupling of two previous studies,[4,5] which will be briefly reviewed.

Reference 4 addressed the topic of synthetic time histories and their combination vs recorded ground motions. A suite of synthetic time histories was sought and obtained from firms active in the nuclear power industry.[6] These time histories had been generated to match the design ground response spectra of the U.S. Nuclear Regulatory Commission's Regulatory Guide 1.60[7] (R.G. 1.60). The recorded ground motions were from the original data base used to develop R.G. 1.60. Three structural models were analyzed for the synthetic time histories and the recorded ground motions. The responses, in the form of in-structure response spectra, were compared. The mean of the responses due to the synthetic motions was compared to the mean-plus-one-standard-deviation (MSD) of the responses due to the recorded motions. This reflects the assumption that the design criteria of R.G. 1.60 were based on a goal of the MSD. In the notation of this report, the use of recorded ground motions would be considered the Best Estimate Method and the use of synthetic time histories the Evaluation Method.

Reference 5 addressed the practice of enveloping and broadening in-structure response spectra to account for uncertainties. Calculations of two types were performed on a relatively simple structural model using only one-dimensional excitations. The excitations used were the suite of synthetic time histories discussed above and two cases of analyses were considered:

Case 1: A dynamic analysis was performed for each of the synthetic time histories. Structural frequencies and damping were held constant at their nominal values for each analysis. Each resulting in-structure response spectrum was broadened by $\pm$ 15%. The mean spectra were computed for comparison purposes.

Case 2: Dynamic analyses were performed with the excitation randomly selected from the suite of synthetic time histories. The frequency and damping of the structural model were also randomly selected from hypothesized distributions. These distributions were obtained from the open literature and represent dispersion about the nominal values used in Case 1. In-structure response spectra were generated. The MSD spectra were computed for comparison.

Again, in the notation of this report, Case 1 would be considered the Evaluation Method and Case 2 the Best Estimate. The present investigation is an extension and coupling of the two studies just described. The structural model analyzed here is the same as the model of Ref. 4. This model has a large degree of asymmetry; that is, it has coupling of responses in all degrees of freedom.

Key elements of the Best Estimate Method are:

1. Excitations are the three components of recorded ground motion applied simultaneously and with their recorded phasing.
2. Variability in stiffness and damping are incorporated in the analysis by random sampling from distributions.
3. Mean and MSD response specta were generated.

The corresponding elements of the Evaluation Method are:

1. Excitations are synthetic time histories applied in each of the horizontal and vertical directions independently, the resulting

in-structure response spectra being combined by the square-root-of-the-sum-of-the-squares rule (SRSS); i.e., the spectral ordinate S at a point in direction 1 is computed by

$$S_1 = (S_{11}^2 + S_{12}^2 + S_{13}^2)^{1/2} ,$$

where

S_1 = response spectrum ordinate in direction 1 due to three components of motion (1,2,3) and

S_{1j} = response spectrum ordinate in direction 1 due to an excitation in direction j (j = 1,2,3).

2. Variability in stiffness and damping is incorporated by peak-broadening of in-structure response spectra. Nominal values of frequency and damping are assumed in each analysis.
3. Mean response spectra are generated.

This study demonstrates the coupling and compounding of effects through two links in the SMC: seismic input and structural response. The results should be interpreted in the context of this coupling and in the suggestion of one way of comparing two alternative methodologies. For a number of reasons, the significance of the quantitative results is limited. All of the ingredients of the analysis were selected to be compatible with the previous studies.[4,5] The same time histories, structural model, and variability of structural dynamic characteristics were used in the present study as in the previous uncoupled analyses. Hence, the parameter selections and, in particular, their variability do not reflect information available in the interim. For example, the uncertainty in structural damping was represented by a normal distribution with a coefficient of variation of 0.1. Recent information[8] indicates that a minimum coefficient of variation of 0.2 for structural damping is more appropriate. In addition, the present investigation considers only seismic input and structural response and thus neglects soil-structure interaction and its associated uncertainties. Hence, in the most useful situation, the quantitative results would only apply to structures founded on extremely stiff soils or rock where soil-structure interaction effects can be considered negligible.

Chapter 2 describes the Best Estimate Method and Evaluation Method procedures used herein. Chapter 3 presents results for the Best Estimate Method and Evaluation Method both separately and in comparison. Chapter 4 discusses our conclusions and recommendations.

2. THE BEST ESTIMATE METHOD AND EVALUATION METHOD (BE-EM) ANALYSIS

2.1 GENERAL

The Best Estimate Method and Evaluation Method analysis, in the example presented here, couples two links (seismic input and structural response) in the seismic analysis and design methodology chain (SMC), as described in Sec. 1.3. The key ingredients for the Best Estimate Method and Evaluation Method are described in this chapter. They include the excitations in the form of free-field acceleration time histories, structural model, variations of the structure dynamic characteristics, combination of three-dimensional response, and broadening of in-structure response spectra to account for uncertainties.

2.2 STRUCTURAL MODEL

The structural model for the BE-EM analysis is of a main steam valve house and quench spray area (MSVH and QSA) for a pressurized water reactor. It was supplied by the U.S. NRC and is identical to one of the models analyzed in Ref. 4. It is fully three-dimensional with a high degree of asymmetry. Figure 2 shows the model: six nodes with six active degrees of freedom (three translational and three rotational) per node. Modal analysis was performed throughout using the first fourteen modes. The first three frequencies of the structural model were 3.45 Hz, 3.97 Hz, and 8.03 Hz. For convenience' sake we discuss the Evaluation Method first.

2.3 EVALUATION METHOD

The Evaluation Method (EM) for the present study includes three major items:

1. Generation of synthetic time histories that essentially envelope the design ground response spectra of Regulatory Guide 1.60 (R.G. 1.60).
2. Determination of three-dimensional responses due to three directions of excitation.
3. Modification of computed in-structure response spectra to account for uncertainties (broadening).

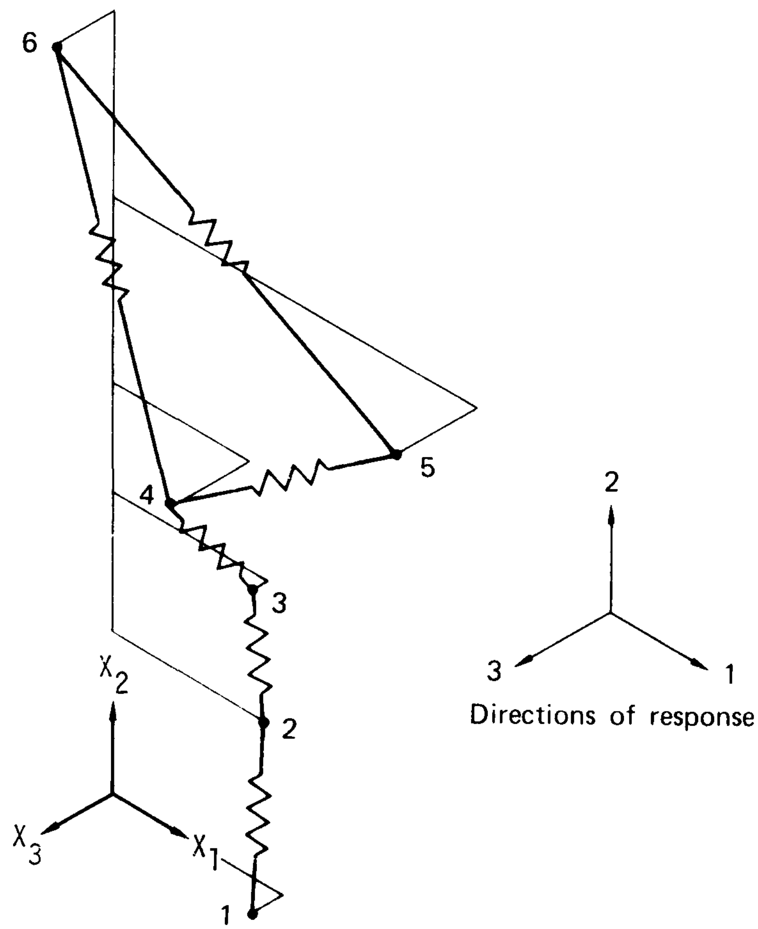

FIG. 2. Structural model of a main steam valve house and quench spray area (MSVH and QSA). 1 and 3 are the horizontal components and 2 is the vertical. This study analyzes responses at nodes 2 and 6.

Each of these items and the resulting combinations are discussed below.

2.3.1 Excitation

2.3.1.1 Time Histories. Specification of the seismic input for the analysis and design of nuclear power plants includes three parameters for the earthquake motion: (1) a measure of the size of the earthquake; (2) the frequency content of the motion; and (3) the duration of the strong motion. In this study, the size of the earthquake is measured by the peak acceleration. The frequency content is specified by the design response spectra of R.G. 1.60. Duration of the ground motion was determined by synthetic time histories obtained from industry.[6]

The peak acceleration of each of the two horizontal components were taken equal. The corresponding peak acceleration of the vertical component is two-thirds of the peak horizontal as defined by R.G. 1.60. For convenience, the peak horizontal acceleration was assumed to be 1.0 g. Since a linear analysis is performed throughout, the results may be scaled linearly to any other excitation level.

It is helpful to review the process by which R.G. 1.60 response spectra were constructed: (1) A data base of strong-motion earthquake time histories was established; (2) displacement, velocity, and acceleration scaling was performed on the data base time histories; (3) the mean and mean-plus-one-standard-deviation (MSD) response spectra were constructed, frequency point by frequency point; and (4) the resulting MSD response spectra were smoothed and served as the basis for R.G. 1.60. In many cases, the seismic analysis of structures is performed using time histories rather than the design response spectra of R.G. 1.60. One way of performing such an analysis would be to utilize the earthquake data base of R.G. 1.60, performing multiple analyses, and interpreting the results in a statistical manner; e.g., MSD. In the design process, this could be prohibitively expensive. However, for a limited number of comparative cases, this approach is feasible, and, in fact, comprises the Best Estimate model used herein. To circumvent using all the time histories, it is common practice to generate synthetic time histories whose response spectra essentially envelope the corresponding response spectra of R.G. 1.60.

The synthetic time histories were obtained from the nuclear industry as reported in Ref. 6. Obviously, this data base does not represent all such histories used in seismic design. However, it is the most complete data base presently available. The goodness of fit of these histories to R.G. 1.60 was not assessed; the entire set, however, met the requirement of essentially enveloping the target spectra. Sixteen horizontal and 12 vertical time histories were obtained. For this study, the assumption was made that each of the 16 horizontal histories could be combined with any other horizontal history and with any of the 12 vertical histories. This assumption led to 16 x 16 x 12 = 3072 possible combinations. All such combinations were calculated.[9] Further, each such combination of two horizontals and one vertical was assumed equally likely.

The excitations, both Best Estimate Method and Evaluation Method, were applied to the structure in the principal coordinate directions of Fig. 2. Coordinates X_1 and X_3 correspond to the horizontal directions and X_2 to the vertical. Other assumptions and sensitivity studies could have been made; for example, azimuth variation of the motions with respect to the structural coordinate system. However, additional assumptions were beyond the scope of this study.

2.3.1.2 <u>Three-Dimensional Response</u>. Nuclear power plants are designed to resist the three translational components of ground motion. When using synthetic time histories, it is common practice to analyze the structure for each component of ground motion separately and combine the results. The Evaluation Method followed this practice. The combination rule applied is the square-root-of-the-sum-of-the-squares (SRSS).[10] That is, in-structure response spectra were generated at nodal degrees of freedom of interest for each component of motion. The resulting spectra were combined by the SRSS rule:

$$S_1 = (S_{11}^2 + S_{12}^2 + S_{13}^2)^{1/2} ,$$

where

S_1 = response spectrum ordinate in direction 1 due to three components of motion (1,2,3) and

S_{1j} = response spectrum ordinate in direction 1 due to an excitation in direction j (j = 1,2,3).

The SRSS rule was applied separately at each frequency point. The SRSS rule is based on statistical considerations; namely, that the peak spectral responses at a given frequency due to three independent motions are not expected to occur at the same instant of time.

2.3.2 Structural Variability

The in-structure response spectra computed for the Evaluation Method were modified to account for uncertainties in the modeling procedure and in the degree of accuracy of the basic material properties.[9] The in-structure response spectra were broadened ± 15% at all frequencies. Figure 3 shows typical broadened and unbroadened response spectra. Note that the broadened spectrum is smoother than the unbroadened spectrum and envelopes it.

2.3.3 Analysis Process

The calculational process for the Evaluation Method is depicted in Fig. 4. Repeated time history analyses were performed to encompass all possible combinations of horizontal and vertical synthetic time histories; i.e., 16 x 16 x 12 = 3072 combinations. Nominal values of frequency and damping were used for the structural model. In-structure response spectra were generated at all points and directions of interest. The analysis for each direction of excitation was performed separately and the resulting in-structure response combined by the SRSS rule. The spectra were broadened by ± 15% to account for uncertainties. After completion of the repeated analyses, the mean response spectra were computed.

2.4 BEST ESTIMATE

The Best Estimate method (BE) for the present investigation includes:

1. Recorded ground motion time histories from the data base for R.G. 1.60;
2. Three components of ground motion applied simultaneously and with their recorded time phasing;
3. Variability in the stiffness and damping of the structure incorporated by random sampling on hypothesized distributions.

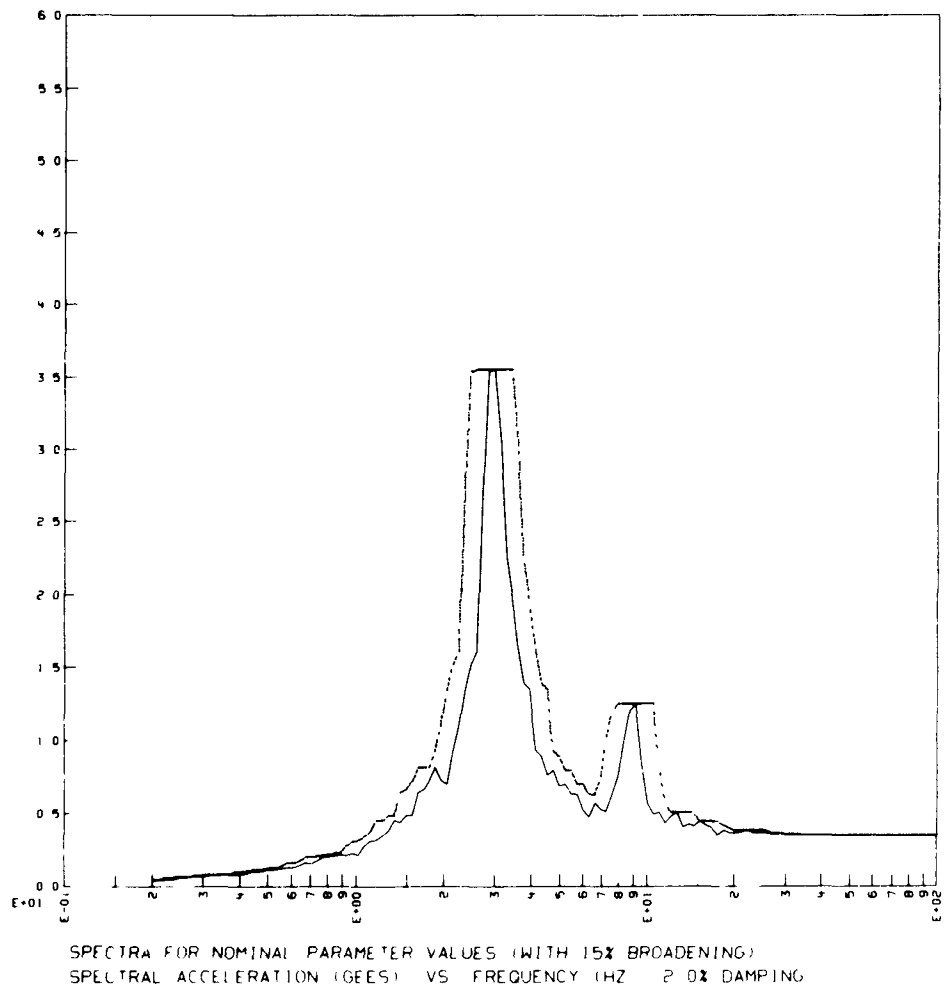

FIG. 3. Typical peak-broadened response spectrum (broken line).

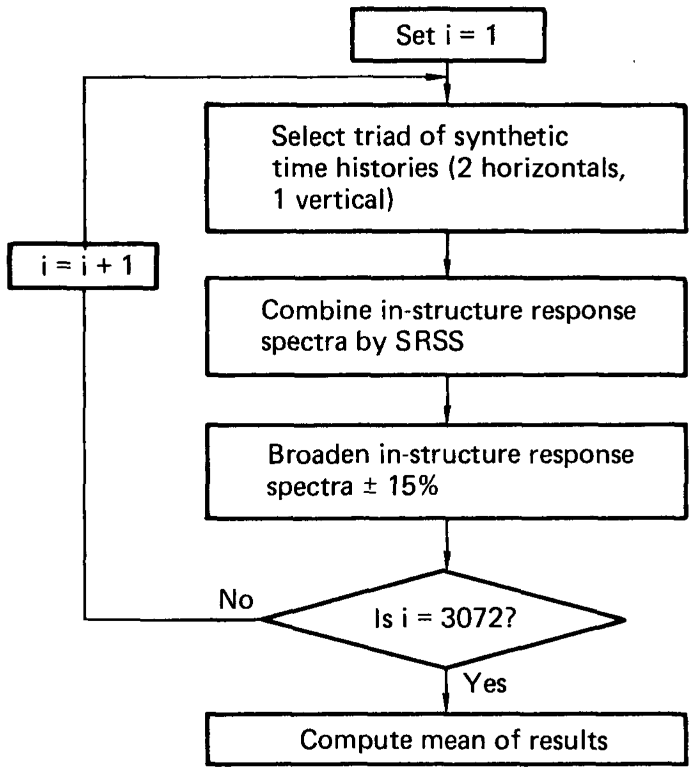

FIG. 4. Flow diagram for the EM calculations.

2.4.1 Excitation

Recorded time histories from the California Institute of Technology (CALTECH) earthquake data base [11] were used in the analysis. These records are identified in Table 1 and include 23 of the earthquakes used to develop R.G. 1.60 design response spectra. The so-called corrected or Vol. II version of the records was used. In constructing the design response spectra of R.G. 1.60, the recorded motions were scaled with respect to displacement, velocity, and acceleration. The present investigation only scaled the accelerations. The three components of motion were scaled by a common factor such that the horizontal component with the largest recorded peak acceleration was scaled to 1.0 g. The resulting peak accelerations are shown in Table 1.

As a point of interest, Table 1 also shows the change in peak acceleration between uncorrected (Vol. I) and corrected (Vol. II) accelerograms.

Structural response was calculated assuming the three components of recorded motion act simultaneously and with their recorded phasing. Therefore, no additional processing of the in-structure response spectra (corresponding to the SRSS rule of Sec. 2.3.1.2) was necessary.

2.4.2 Structural Variability

Variability in the structural model was incorporated into the Best Estimate analysis by defining distributions of frequency and damping, sampling from the distributions, and performing response calculations for the selected parameters. For frequency, two probability density functions were assumed. The first addressed the uncertainty introduced by the process of an engineer developing a structural model from engineering drawings. The second addressed uncertainty in material properties. Both distributions were based on experimental information available in the open literature.[12,13] Of the alternative distributions proposed in Ref. 12 which are dependent on the experience of the engineer and complexity of the structure, the distribution representing an experienced engineer modeling a complex structure was assumed. Figures 5 and 6 show the appropriate distributions. It is important to recognize that these two functions were applied sequentially in the

TABLE 1. Earthquake records used in structural analyses.

Earthquake reference number	Component	Peak acceleration, g Vol. I	Peak acceleration, g Vol. II	Peak velocity,[a] cm/s	Peak displacement,[a] cm	Site/ date	Peak acceleration for this study, g
A001	S00E	0.359g	0.348g	33.4	10.9	El Centro/	1.00
A001	S90W	0.224	0.214	36.9	19.8	May 18, 1940	0.61
A001	Vert	0.278	0.210	10.8	5.6		0.60
A002	S44W	0.123	0.104	4.8	2.4	Ferndale/	0.93
A002	N46W	0.120	0.112	7.4	2.7	October 7, 1951	1.00
A002	Vert	0.031	0.027	2.2	1.6		0.24
A004	N21E	0.177	0.156	15.7	6.7	Taft/	0.87
A004	S69E	0.196	0.179	17.7	9.2	July 21, 1952	1.00
A004	Vert	0.123	0.105	6.7	5.0		0.59
A006	S00W	0.058	0.055	6.1	5.1	Hollywood Stor./	1.00
A006	N90E	0.045	0.044	9.4	5.9	July 21, 1952	0.80
A006	Vert	0.024	0.023	4.2	2.2		0.42
A007	S00W	0.062	0.059	6.6	4.5	Hollywood P.E./	1.00
A007	N90E	0.044	0.042	8.9	6.4	July 21, 1952	1.00
A007	Vert	0.022	0.021	3.0	3.4		
A008	N11W	0.175	0.168	31.6	12.4	Eureka Fed./	0.61
A008	N79E	0.283	0.258	29.4	14.1	December 21, 1954	1.00
A008	Vert	0.116	0.083	8.2	4.7		
A009	N44E	0.166	0.159	35.6	14.2	Ferndale C.H./	0.79
A009	N46W	0.209	0.201	26.0	9.6	December 21, 1954	1.00
A009	Vert	0.045	0.043	7.6	3.9		0.21
A011	S00W	0.035	0.033	4.0	2.4	El Centro/	0.65
A011	S90W	0.054	0.051	7.0	4.1	February 9, 1956	1.00
A011	Vert	0.017	0.013	2.9	1.6		0.20
A015	N10E	0.105	0.083	4.9	2.3	San Fran. GG/	0.79
A015	S80E	0.127	0.105	4.6	0.8	March 22, 1957	1.00
A015	Vert	0.015	0.038	1.2	0.7		0.36

[a]The peak velocities and displacements correspond to Vol. II acceleration values.

TABLE 1. (continued).

Earthquake reference number	Component	Peak acceleration, g Vol. I	Vol. II	Peak velocity, cm/s	Peak displacement, cm	Site/ date	Peak acceleration for this study, g
A018	S01W	0.076	0.065	7.8	2.8	Hollister/	0.36
A018	N89W	0.189	0.179	17.1	3.8	April 8, 1961	1.00
A018	Vert	0.055	0.050	4.7	2.2		0.28
A019	S00W	0.142	0.130	25.8	12.2	El Centro/	1.00
A019	S90W	0.061	0.057	14.7	11.0	April 8, 1968	0.44
A019	Vert	0.036	0.030	3.4	3.9		0.23
B024	N00E	0.169	0.160	20.5	4.2	El Centro/	0.87
B024	N90E	0.184	0.183	11.5	3.7	December 30, 1934	1.00
B024	Vert	0.074	0.069	8.8	5.6		0.38
B025	N00E	0.141	0.146	7.3	1.4	Helena/	1.00
B025	N90E	0.156	0.145	13.3	3.7	October 31, 1935	0.99
B025	Down	0.099	0.089	9.7	2.8		0.61
B029	S04E	0.183	0.165	21.4	8.5	Olympia/	0.59
B029	S86W	0.306	0.280	17.0	10.4	April 13, 1949	1.00
B029	Down	0.111	0.092	7.0	4.0		0.33
B032	S04E	0.161	0.137	8.0	2.7	Olympia WHTL/	0.69
B032	S86W	0.229	0.198	12.7	3.8	April 13, 1949	1.00
B032	Vert	0.083	0.061	3.0	1.7		0.31
B033	N65E	0.509	0.489	77.9	26.3	Parkfield/	1.00
B033	N25W	NA	NA	NA	NA	June 27, 1966	N/A
B033	Down	0.349	0.206	14.1	4.3		0.42
B034	N05W	0.403	0.355	22.5	5.2	Cholame/	0.82
B034	N85E	0.467	0.434	25.4	7.1	June 27, 1966	1.00
B034	Down	0.181	0.119	7.3	3.4		0.27
B037	N65W	0.282	0.269	14.5	4.7	Temblor/	0.78
B037	S25W	0.411	0.347	22.5	5.5	June 27, 1966	1.00
B037	Down	0.165	0.132	4.4	1.4		0.38

TABLE 1. (continued).

Earthquake reference number	Component	Peak acceleration, g Vol. I	Vol. II	Peak velocity, cm/s	Peak displacement, cm	Site/ date	Peak acceleration for this study, g
C041	S16E	1.242	1.170	113.2	37.7	Pacoima dam/	1.00
C041	S74W	1.251	1.075	57.7	10.8	February 9, 1971	0.92
C041	Down	0.718	0.709	58.3	19.3		
C048	N00W	0.258	0.255	30.0	14.9	8244 Orion, LA/	1.00
C048	S90W	0.140	0.134	23.9	13.8	February 9, 1971	0.92
C048	Down	0.178	0.171	32.0	14.6		0.61
D056	N21E	0.335	0.315	16.5	4.2	Castaic/	1.00
D056	N69W	0.289	0.271	27.2	9.3	February 9, 1971	0.86
D056	Down	0.180	0.156	6.4	3.5		0.50
H115	N11E	0.225	0.225	28.2	13.4	15250 Ventura LA/	1.00
H115	N79W	0.152	0.149	23.5	10.3	February 9, 1971	0.66
H115	Down	0.108	0.096	9.4	4.3		0.43
L166	N00E	0.181	0.167	12.3	4.9	3838 Lkshm. LA/	1.00
L166	S90W	0.154	0.150	15.0	5.4	February 9, 1971	0.90
L166	Down	0.085	0.071	5.0	2.4		0.42
Mean	Horizontal	0.241	0.223			Mean of horizontals with lesser peak acceleration standard deviation	0.73
MSD	Horizontal	0.488	0.445				
Mean	Vertical	0.134	0.114				0.16
MSD	Vertical	0.287	0.256				0.40
							0.14

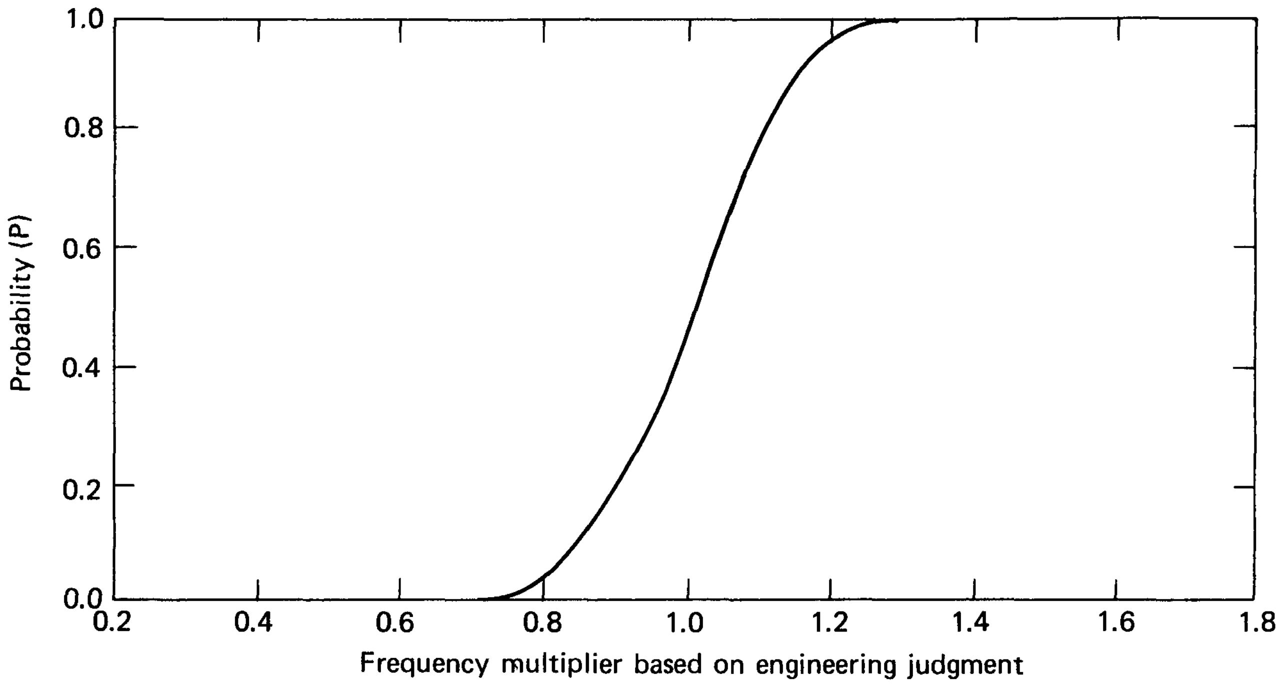

FIG. 5. Cumulative Distribution Function (CDF) on frequency modifier based on engineering judgment.

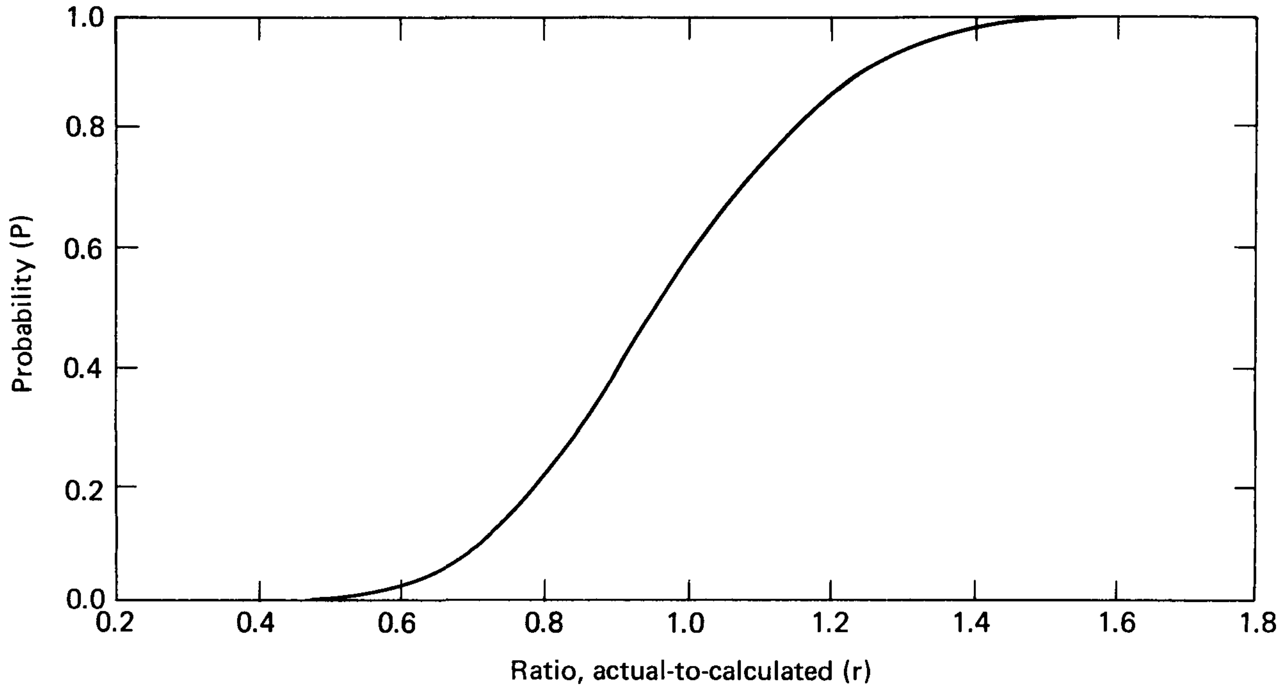

p	r
0.01	0.5854
0.05	0.6726
0.10	0.7243
0.15	0.7615
0.25	0.8200
0.35	0.8700
0.45	0.9176
0.50	0.9416

p	r
0.55	0.9662
0.65	1.0190
0.75	1.0813
0.85	1.1647
0.90	1.2247
0.95	1.3195
0.99	1.5176

FIG. 6. Cumulative Distribution Function (CDF) on stiffness ratios.

analysis process. Their effects were compounded. Figure 7 shows the resulting function. It was this distribution which served as the basis for a random sampling on frequency.

Variability in the energy dissipation characteristics of the structure was incorporated into the analysis through variations in the values of modal damping. Modal damping was assumed to be normally distributed with a mean value of 0.05 or 5% of critical and a coefficient of variation of 0.1

The distributional shapes of both frequency and damping were selected to be identical to those used in Ref. 5. This permits a direct comparison of the results. However, the parameter selections and their variability do not reflect information available in the interim.

2.4.3 Analysis Process

The calculational procedure for the Best Estimate analysis is shown in Fig. 8. As in the Evaluation Method, repeated time history analyses were performed. In-structure response spectra at points of interest were generated. The excitations, however, were the recorded time histories of motion described in Sec. 2.4.1. Twenty-three sets of three components of motion are shown. This data set was expanded to 46 by first analyzing the structural model assuming that horizontal components 1 and 2 align with the model coordinates X_1 and X_3, respectively, and then interchanging them to align 1 with X_3 and 2 with X_1. Variations in frequency and damping characteristics were incorporated by sampling from the distributions described in Sec. 2.4.2. A stratified sampling method was used to span the parameter space. The distributions on frequency and damping characteristics were divided into 46 equal probability segments, each representing a probability of 1/46. Pairs of frequencies and damping were selected through the use of a random two-column selection of the parameters listed in Tables 2 and 3. The resulting pairs are listed in Table 4. After completion of the repeated analyses, the mean and MSD response spectra were computed for comparison purposes.

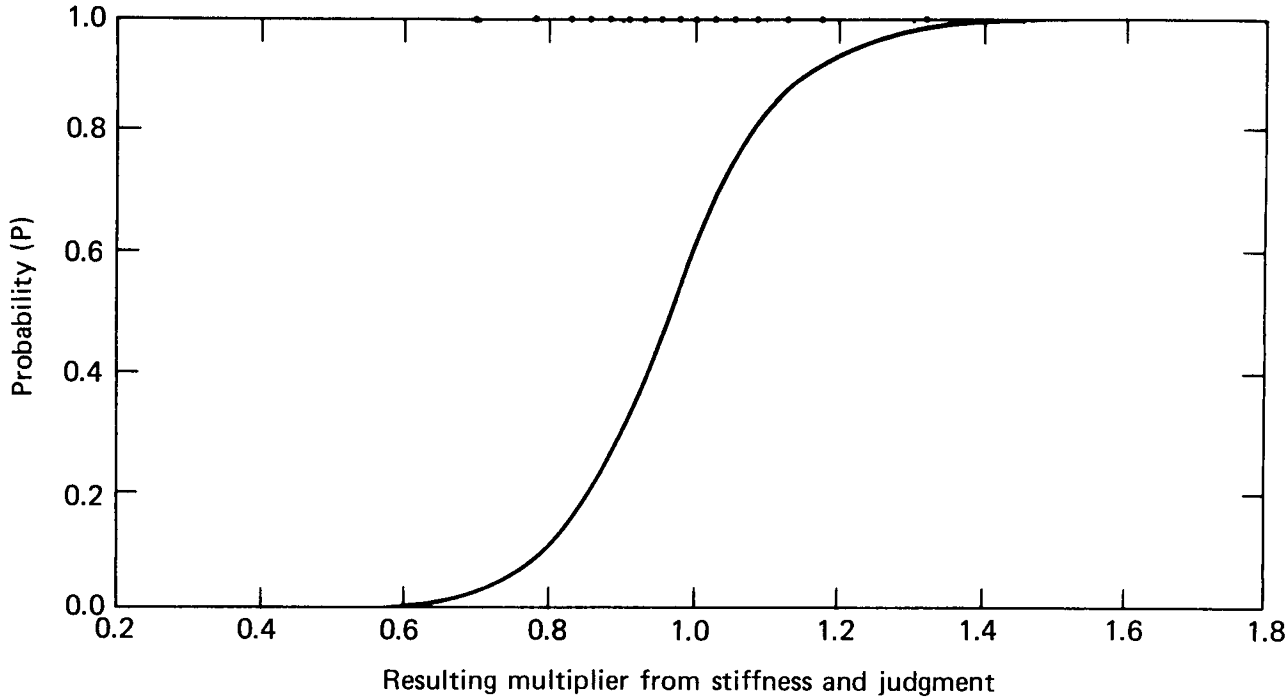

FIG. 7. Expected CDF on frequency modifier.

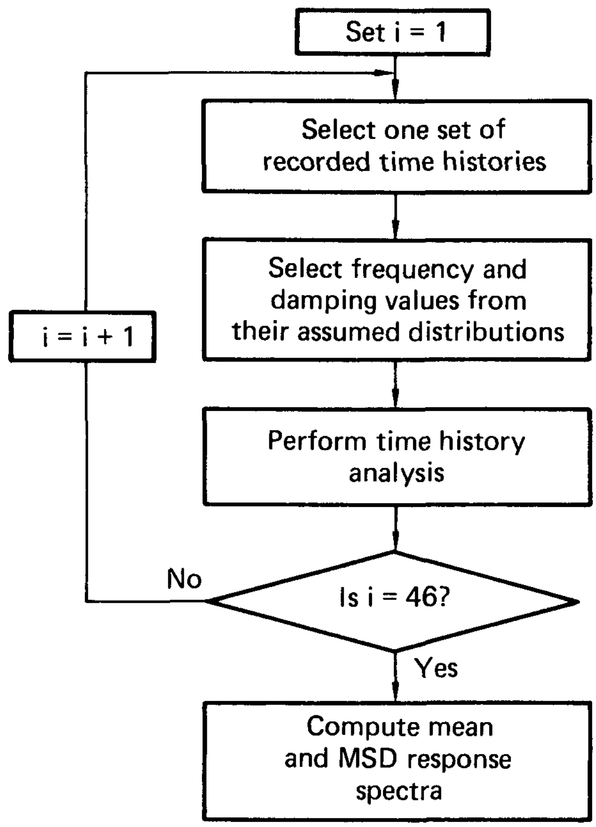

FIG. 8. Flow diagram for the BE calculations.

TABLE 2. Values of damping used in BE analysis.

1.	0.03805	24.	0.05014
2.	0.04074	25.	0.05041
3.	0.04197	26.	0.05068
4.	0.04283	27.	0.05096
5.	0.04353	28.	0.05124
6.	0.04411	29.	0.05152
7.	0.04463	30.	0.05181
8.	0.04509	31.	0.05210
9.	0.04551	32.	0.05241
10.	0.04591	33.	0.05272
11.	0.04628	34.	0.05304
12.	0.04663	35.	0.05337
13.	0.04697	36.	0.05372
14.	0.04728	37.	0.05409
15.	0.04759	38.	0.05449
16.	0.04790	39.	0.05491
17.	0.04819	40.	0.05537
18.	0.04848	41.	0.05589
19.	0.04876	42.	0.05647
20.	0.04904	43.	0.05717
21.	0.04931	44.	0.05803
22.	2.04959	45.	0.05926
23.	0.04986	46.	0.06195

TABLE 3. Values of frequency modifier used in BE analysis.

1.	0.6975	24.	0.9720
2.	0.7393	25.	0.9795
3.	0.7640	26.	0.9870
4.	0.7827	27.	0.9957
5.	0.7978	28.	1.0027
6.	0.8124	29.	1.0106
7.	0.8234	30.	1.0208
8.	0.8362	31.	1.0292
9.	0.8453	32.	1.0372
10.	0.8577	33.	1.0479
11.	0.8651	34.	1.0562
12.	0.8753	35.	1.0678
13.	0.8846	36.	1.0768
14.	0.8922	37.	1.0891
15.	0.8998	38.	1.1017
16.	0.9083	39.	1.1154
17.	0.9163	40.	1.1306
18.	0.9246	41.	1.1441
19.	0.9321	42.	1.1639
20.	0.9408	43.	1.1820
21.	0.9486	44.	1.2102
22.	0.9562	45.	1.2494
23.	0.9628	46.	1.3195

TABLE 4. Pairs of damping and frequency modifiers used in BE analysis.

	Damping value	Frequency modifier		Damping value	Frequency modifier
1.	0.04551	0.8922	24.	0.04353	0.9246
2.	0.05647	0.8124	25.	0.04663	1.1441
3.	0.05491	0.6975	26.	0.04697	0.9083
4.	0.05096	1.2494	27.	0.06195	0.7827
5.	0.05409	1.0678	28.	0.04074	1.1639
6.	0.05717	0.8362	29.	0.04931	0.9486
7.	0.05304	1.0106	30.	0.04463	0.9628
8.	0.05372	0.8651	31.	0.04848	0.8577
9.	0.05241	1.1154	32.	0.05449	1.1017
10.	0.03805	1.0027	33.	0.04283	0.8846
11.	0.04819	0.9795	34.	0.05041	0.7640
12.	0.05181	1.0768	35.	0.05210	1.0891
13.	0.04197	1.0562	36.	0.05926	1.1820
14.	0.04628	0.9957	37.	0.04790	1.0292
15.	0.05068	0.7393	38.	0.04728	0.7978
16.	0.05537	0.9321	39.	0.05014	0.9720
17.	0.04591	0.8453	40.	0.05589	0.9163
18.	0.05337	0.8234	41.	0.04904	1.3195
19.	0.04759	0.9562	42.	0.05803	1.0208
20.	0.05152	0.8998	43.	0.05124	1.2102
21.	0.04986	1.1306	44.	0.04876	0.8753
22.	0.04959	0.9408	45.	0.04411	1.0479
23.	0.05272	1.0372	46.	0.04509	0.9870

2.5 COMPUTER ANALYSIS

The computer program used in the present investigation was an extension of the program LUST developed and used in the studies of Ref. 4. The extended version is denoted LUSTE, an acronym for Limited Understanding of the Statistics of Transients with Extension. A review of several basic elements of LUSTE is appropriate.

LUSTE was assembled using the SAP IV computer program as a basis for the dynamic response calculations and the International Mathematical and Statistical Library of statistical routines. Graphic display capability unique to the Lawrence Livermore Laboratory computer system was incorporated.

LUSTE minimizes the chance for human error in data handling by automating the different stages of the calculations. One execution of LUSTE completes the analysis.

The large amount of data is output in graphical form. Twenty-seven different types of computer plots are available as described in Appendix A and displayed in Appendix B.

Response spectra were computed at 111 frequency points between 0.2 and 33 Hz and one additional value at 100 Hz. Excluding the value at 100 Hz, frequency points were selected according to the rule $f_{i+1} = 1.048\ f_i$ with $f_1 = 0.2$ Hz. This yields $f_{i+3} = 1.15 f_i$ and permits an automated scheme for broadening of response spectra. Note that adjacent frequency points were less than 5% apart. Automation of this type of calculation was essential.

3. RESULTS

3.1 GENERAL

The analysis procedures for the Best Estimate (BE) and Evaluation Method (EM) calculations were described in Sections 2.4.3 and 2.3.3, respectively. The calculations were performed with the computer program LUSTE (Sec. 2.5). The principal dynamic response quantities of interest in this investigation are in-structure response spectra--individual, mean, and mean-plus-one-standard-deviation (MSD) spectra. The majority of the output from LUSTE is in plot form due to the large amount of data generated. Appendix A describes the types of plots produced. Appendix B contains an example of each plot.

Response spectra were generated at node points 2 and 6 of the structural model (Fig. 2). Node point 6 lies at the top of the structure and typically has the largest response. Node point 2 lies at an intermediate elevation. Response spectra were generated in two horizontal directions and the vertical direction. Results are shown herein for one horizontal direction (denoted direction 1) and the vertical direction (denoted direction 2) for node point 6. The response in the other horizontal direction is similar to the first and not shown. The response at node point 2 is similar to node point 6. The principal results for the individual Best Estimate and Evaluation Method analyses are contained in Section 3.2. Comparisons of the BE-EM type are discussed in Section 3.3.

3.2 BE AND EM RESPONSE

Figures 9 through 14 show results from the Evaluation Method analysis. Figures 9 and 10 contain in-structure response spectra at node point 6, direction 1 and direction 2, respectively. Forty-four curves are plotted corresponding to the response due to each of the 44 synthetic time histories. As discussed in Section 2.3.3, each of the 16 horizontal time histories was applied independently in the two horizontal directions and each of the 12 vertical time histories were applied in the vertical direction to yield 44 responses (16 + 16 + 12 = 44). Therefore, Figs. 9 and 10 contain the basic data for the Evaluation Method. These raw spectra were combined by the SRSS rule and then broadened which resulted in 3072 spectral values for each frequency point. All possible combinations were considered (16 x 16 x 12 = 3072). Figures 11 and 12 display the results of the process. The means and the extremes of the combined spectra are shown. Five curves are plotted in each figure and described here in order of increasing magnitude. The lowest curve (dotted) is a compilation of the minimum spectral values before combination, i.e., Fig. 11 (Fig. 12) shows the minimum values from Fig. 9 (Fig. 10). The next highest curve shows the minimum spectral values from the 3072 combined spectra. The middle curve (distinguished by the N over print) is the mean of the 3072 combined spectra. At each spectral frequency, the mean was calculated as the simple arithmetic average of the 3072 spectra values. The two remaining higher curves display the maximum spectral values: the dotted curve shows the maxima for the raw data (Figs. 9 and 10); and the solid curve the maxima for the combined spectra. Figures 13 and 14 repeat the plot of the mean response spectra of the smoothed, broadened, and SRSS combined spectra. The corresponding 95% confidence intervals, assuming a normal distribution, are shown by the dotted curves. Due to the large number of combined spectra comprising the data base, the typical confidence intervals about the estimate of the mean are quite narrow. While the classical statistical meaning and interpretation of such narrow confidence bands is clear, their usefulness for engineering purposes is not.

Figures 15 through 22 show results from the Best Estimate analysis. Figures 15 and 16 contain in-structure response spectra at node point 6, direction 1 and direction 2, respectively. Forty-six curves are plotted, corresponding to the response due to the 46 sets of recorded time histories (Sec. 2.4). The scatter of data in the figures is due to variability in time histories and structural dynamic characteristics (frequency and damping). Figures 15 and 16 contain the basic data for the Best Estimate analysis and are analogous to Figs. 9 and 10. Figures 17 and 18 display the MSD (curve with N over print) response spectra and the extremes (minima and maxima). Figures 19 and 20 show the means of the 46 spectra and the corresponding 95% confidence intervals, assuming a normal distribution for node point 6, direction 1 and direction 2, respectively. The mean curves of Figs. 19 and 20 represent the Best Estimate of the in-structure response spectra due to three-dimensional real earthquakes. Figs. 21 and 22 repeat the plot of the MSD response spectra shown in Figs. 17 and 18 and include 95% confidence intervals.

3.3 BE-EM RESPONSE COMPARISONS

The comparison of the Best Estimate and Evaluation Method response is performed by the computation of two quantities: Factor of Comparison (FOC) and the Probability of Exceedance (POE). The Factor of Comparison for in-structure response spectra is the quotient of the BE and EM computed spectra, frequency point by frequency point. The Probability of Exceedance is the probability a BE response spectral ordinate exceeds the corresponding EM ordinate. The POE was computed by comparing each of the 3072 combined spectra with the first of the 46 spectra from the BE analysis and counting the number of times the latter exceeded the former to yield n_1. The process was repeated for the remaining 45 spectra to yield n, where $n = n_1 + . . . + n_{46}$. The POE was calculated as n/(46 x 3072). The calculation was performed separately for each frequency value.

It is convenient to identify three frequency ranges of the FOC and POE for discussion purposes. A low-frequency range, 0.2 Hz to about 1.3 Hz, in the past, has been called the "time history" section to emphasize that the differences in this range are primarily due to the time histories themselves. The middle-frequency range, 1.3 Hz to about 15 Hz, is associated with amplified structural response. The high-frequency range, above 15 Hz, represents differences in the peak accelerations or the Zero Period Amplitude (ZPA). Of principal interest are the latter two frequency ranges; i.e., middle and high. These ranges profoundly influence the design of structures and equipment.

Two sets of FOCs were generated and are shown in Figs. 23, 24, 27, and 28. Figures 23 (direction 1) and 24 (direction 2) show the FOC computed as the quotient of the mean of the EM response spectra and the MSD of the BE response spectra. This comparison reflects the policy used during the development of the design response spectra of R.G. 1.60; i.e., the resulting design spectra were based on the MSD of the spectra generated from recorded time histories. In addition, the comparison implies this policy is appropriate for a subsequent link in the SMC. Figure 23 shows the FOC for horizontal response at the top of the structure. In the low-frequency range, the minimum FOC is approximately 1.1. The FOC in the mid-frequency range varies from 1.4 to 3.5. In the high-frequency range, the FOC is approximately 1.8 or greater. Hence, the design objective in the frequency range of most interest has been exceeded on the average by a factor of 2 provided the assumptions made herein apply. These assumptions include the definition of the BE and EM procedures and the extension of the MSD policy to multiple links in the SMC. Figure 24 shows similar results for the vertical response.

Figures 25 (direction 1) and 26 (direction 2) show the POEs corresponding to the results of Figures 23 and 24 respectively. The POEs have large variations over the frequency range. In the mid-frequency range, no POEs are greater than 0.1.

Figures 27 (direction 1) and 28 (direction 2) show the FOC computed as the quotient of the means of the EM and BE response spectra. Such a comparison reflects an alternative design objective and is given here for illustrative purposes. The FOCs are obviously higher throughout the frequency range.

3.4 COMPARISON OF COUPLED AND UNCOUPLED RESPONSE

To demonstrate the coupling effects between two links in the SMC, the results of Ref. 4 are compared with the present case. As summarized in Sec. 1.3, the study of Ref. 4 encompassed only the seismic input phase of the SMC; i.e., synthetic vs real time histories. Figures 29 through 32 show a comparison of FOCs as computed for seismic input alone (Ref. 4) and seismic input plus structural uncertainty. The comparison is based on FOCs computed from means of the BE and EM response. Node points 2 and 6 for horizontal and vertical degrees of freedom are shown. As expected, this comparison shows a general trend of increasing FOCs as additional links in the SMC are considered (the results of this study suggest greater FOCs than in Ref. 4). Generally, there is an average factor of about 1.2 due to this compounding effect. This represents a "compounding of conservatism" as hypothesized. Note that minimums occur at frequencies near the limit of the broadened peaks. This could indicate that the broadening rule used (± 15%) may not be accomplishing the desired result. However, further investigation including additional parameter studies would be necessary before a definitive conclusion can be made.

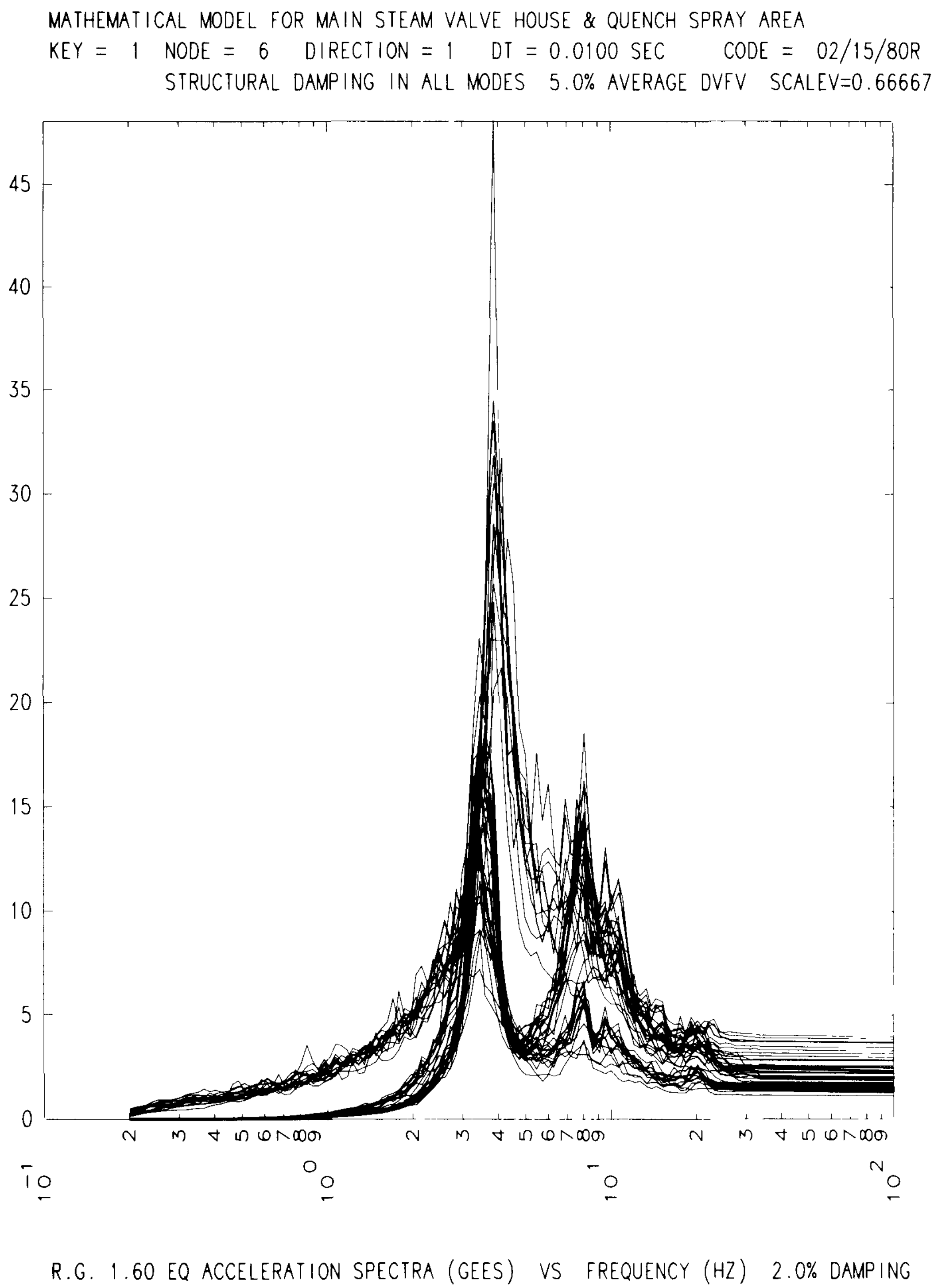

FIG. 9. Mathematical model for main steam valve house and quench spray area (key = 1, node = 6, direction =1).

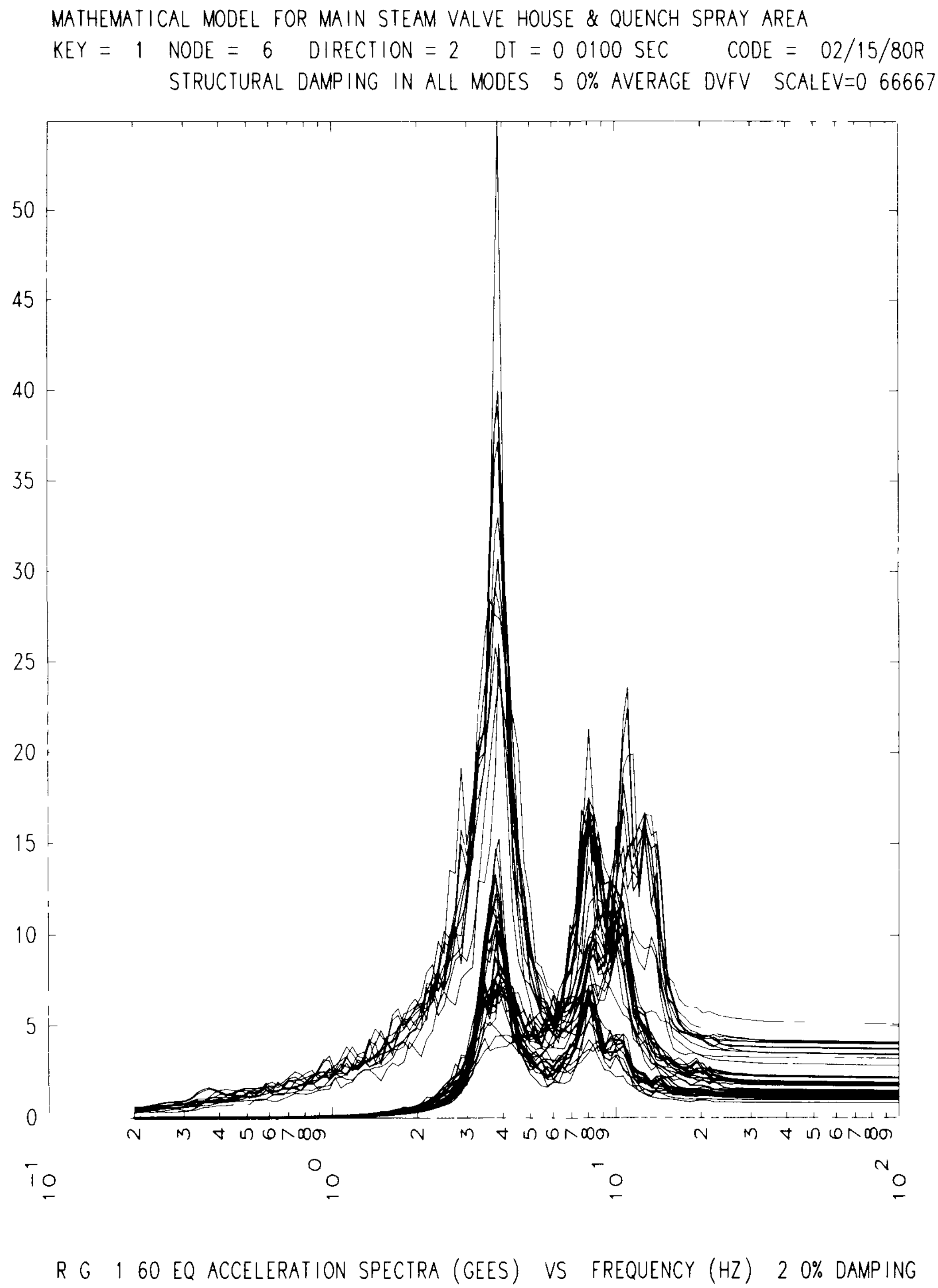

FIG. 10. Mathematical model for main steam valve house and quench spray area (key = 1, node = 6, direction = 2).

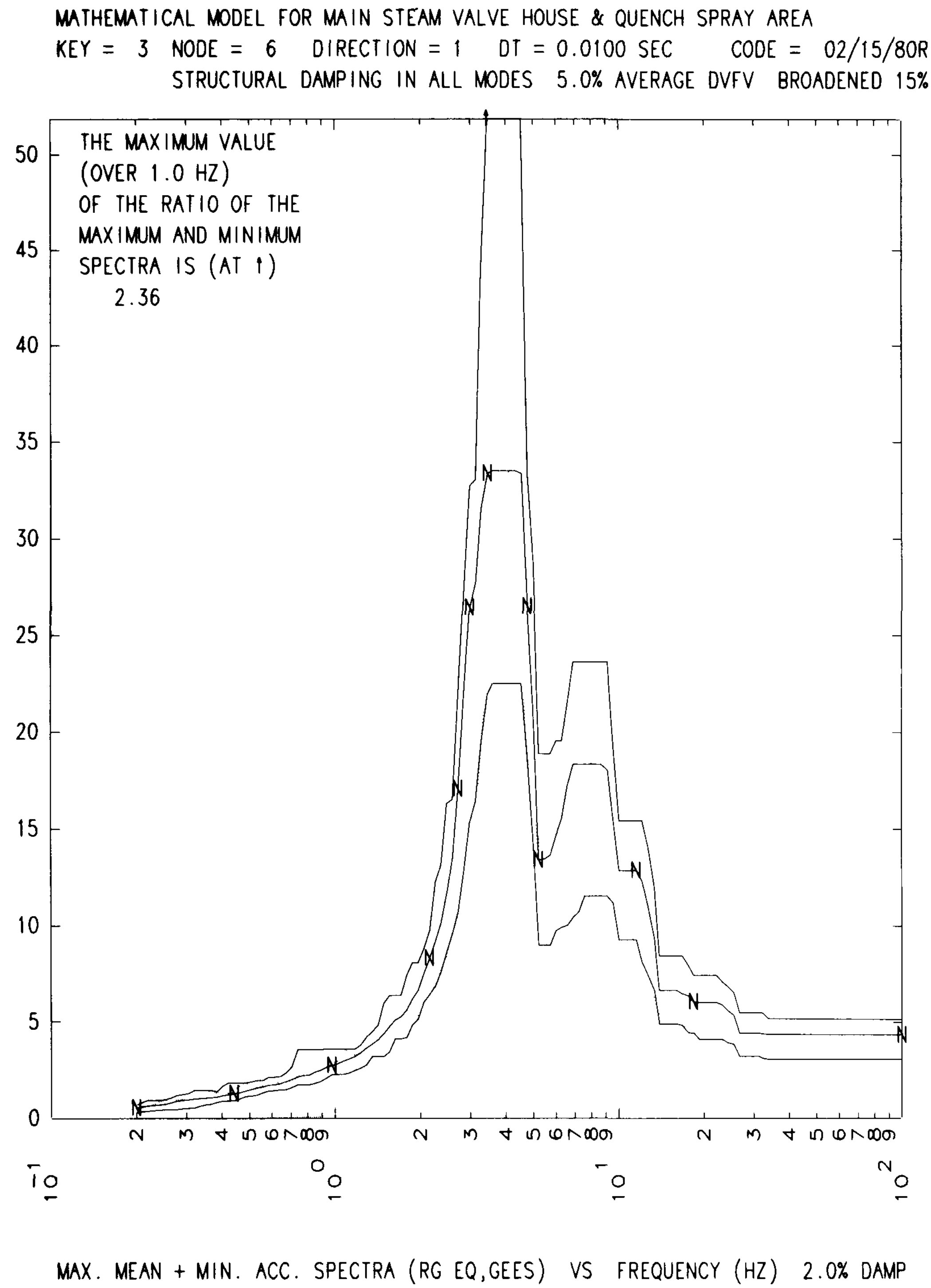

FIG. 11. Mathematical model for main steam valve house and quench spray area (key = 3, node = 6, direction = 1).

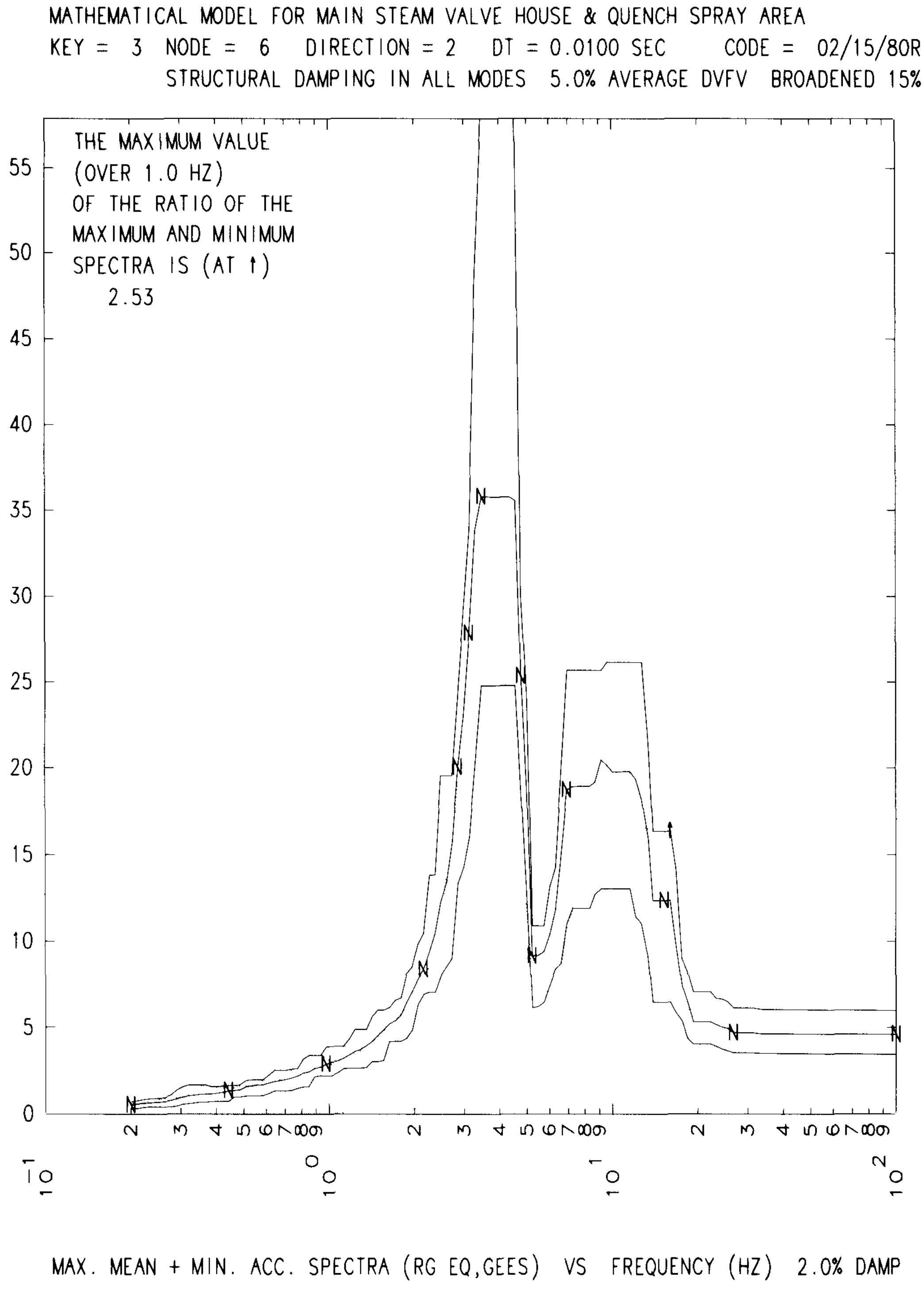

FIG. 12. Mathematical model for main steam valve house and quench spray area (key = 3, node = 6, direction = 2).

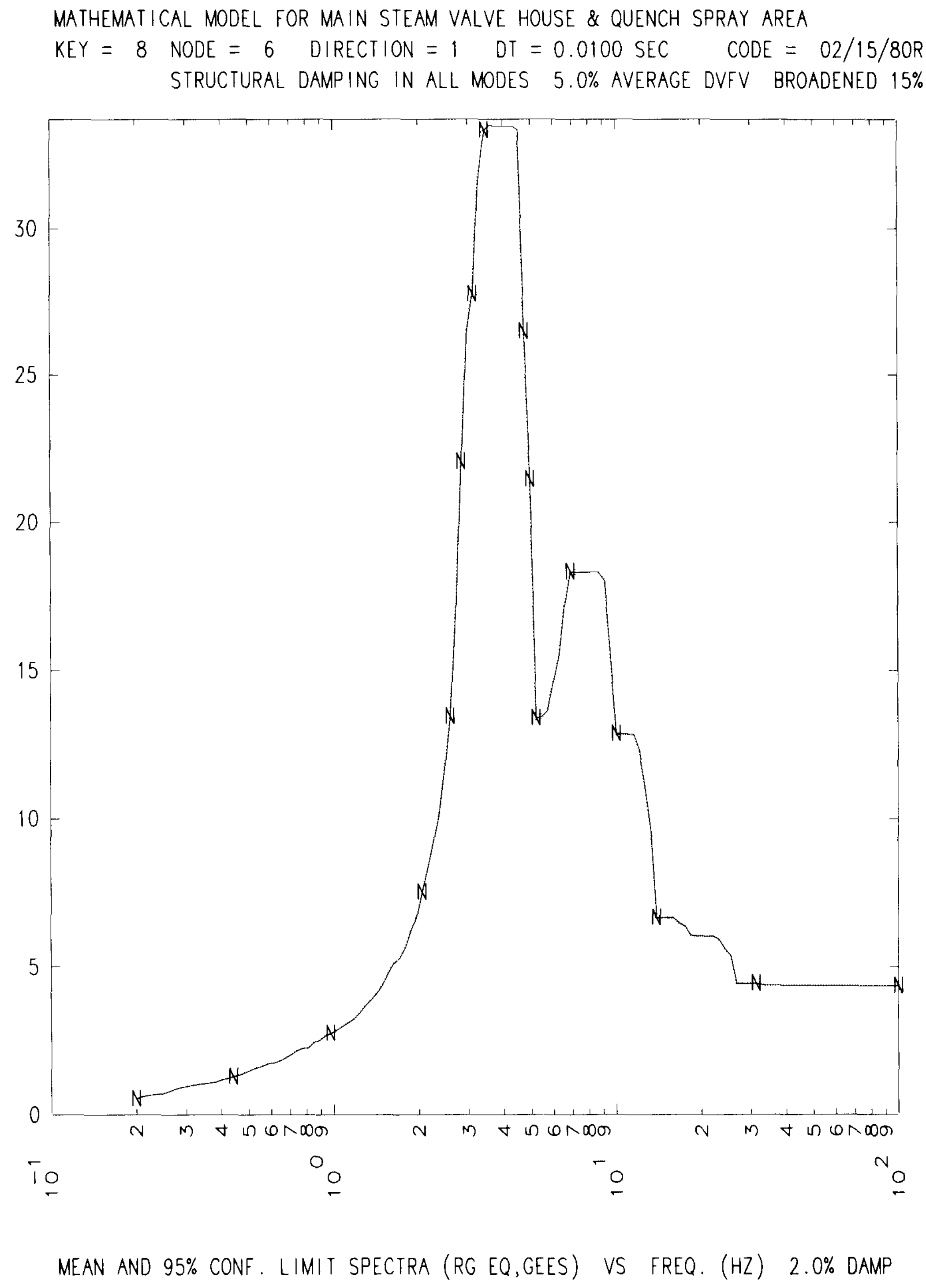

FIG. 13. Mathematical model for main steam valve house and quench spray area (key = 8, node = 6, direction = 1).

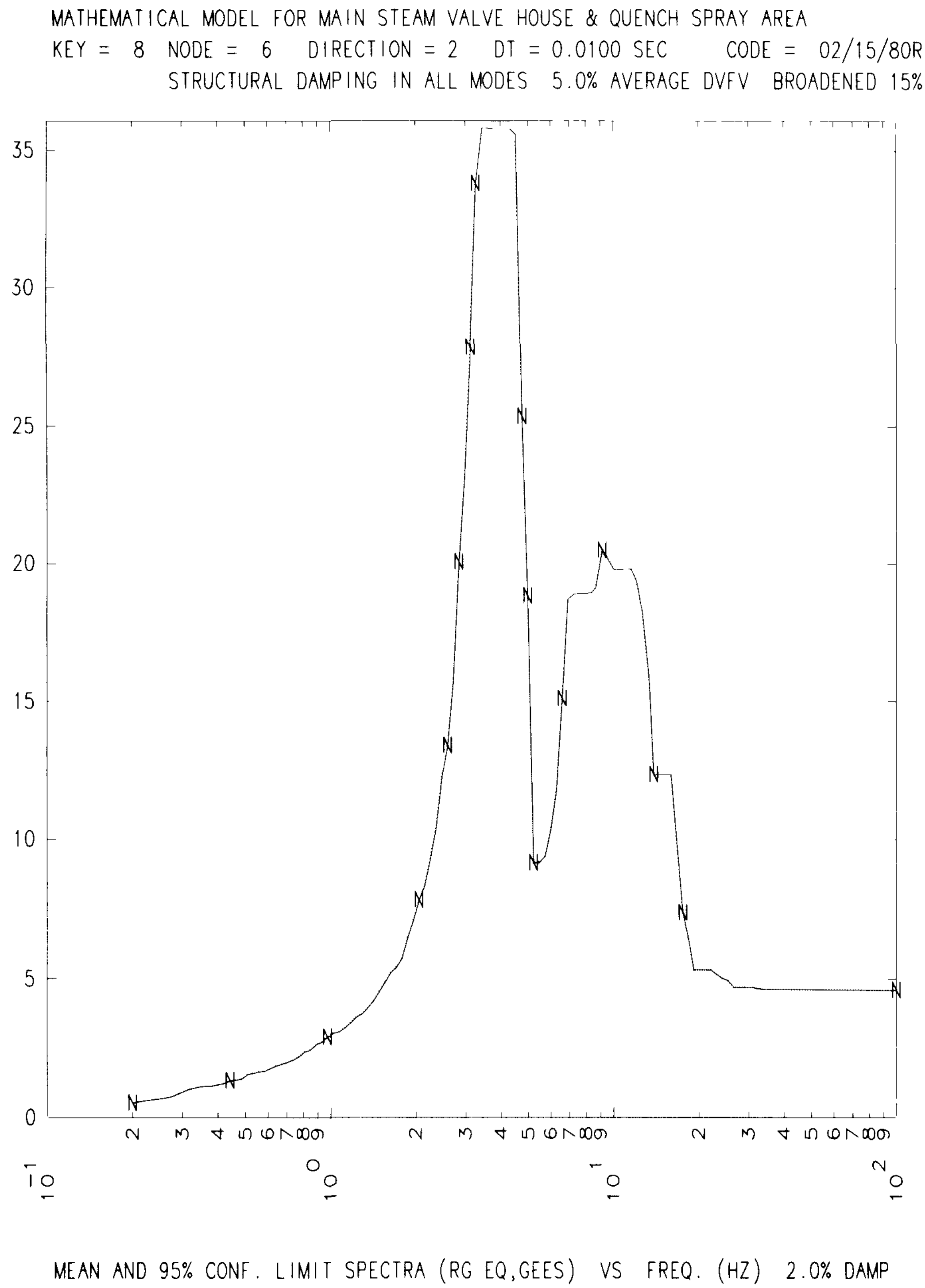

FIG. 14. Mathematical model for main steam valve house and quench spray area (key = 8, node = 6, direction = 2).

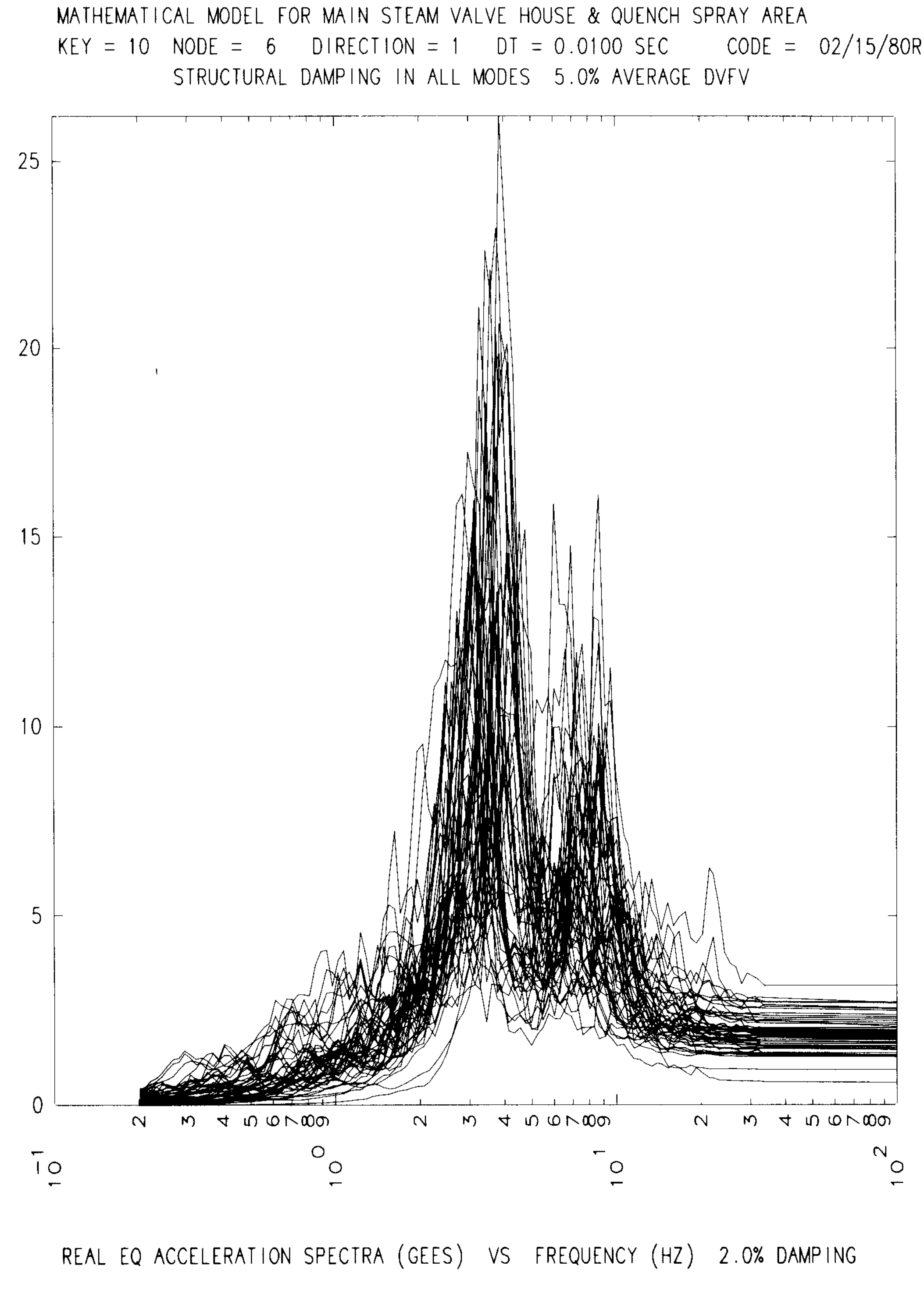

FIG. 15. Mathematical model for main steam valve house and quench spray area (key = 10, node = 6, direction = 1).

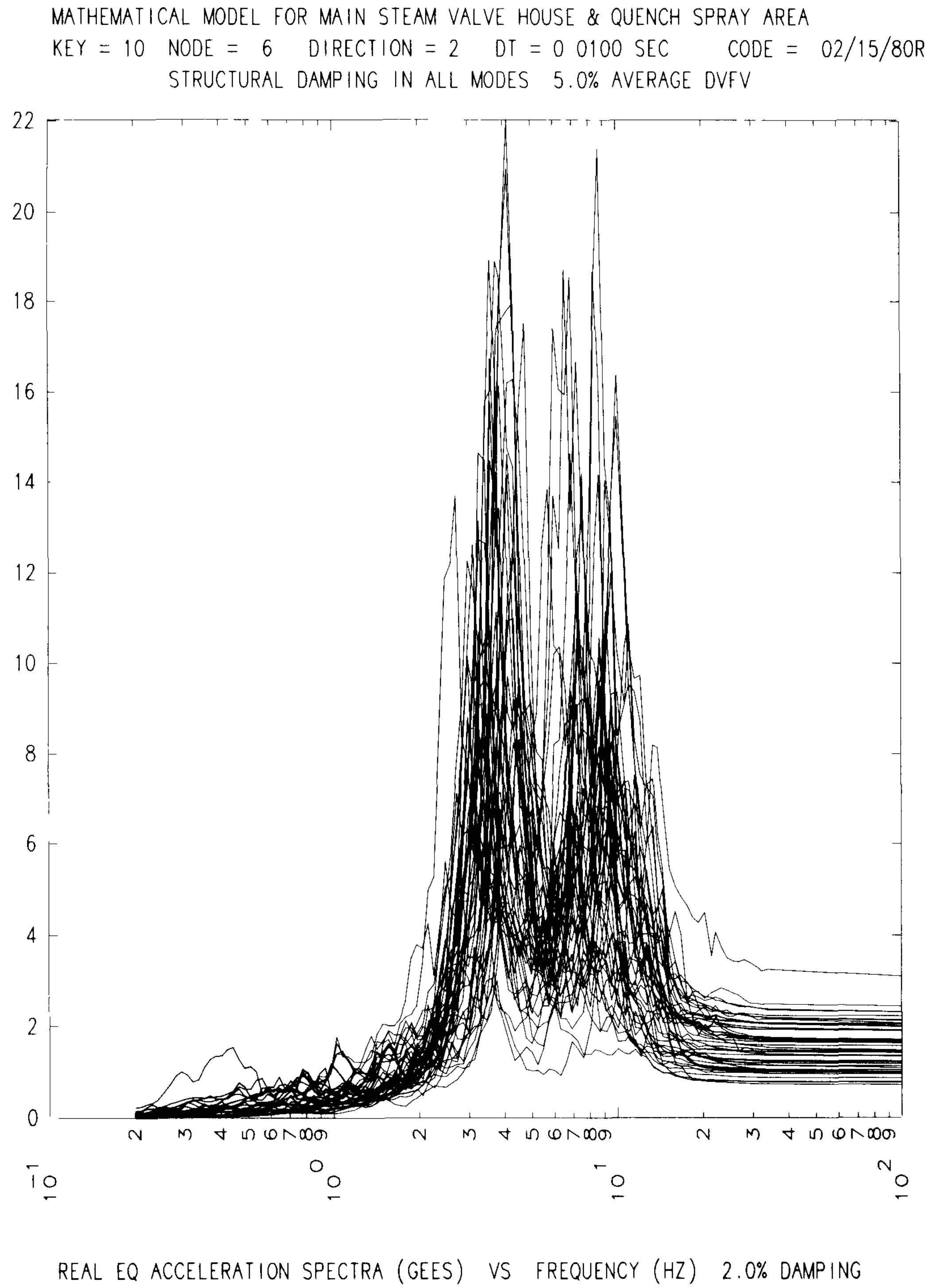

FIG. 16. Mathematical model for main steam valve house and quench spray area (key = 10, node = 6, direction = 2).

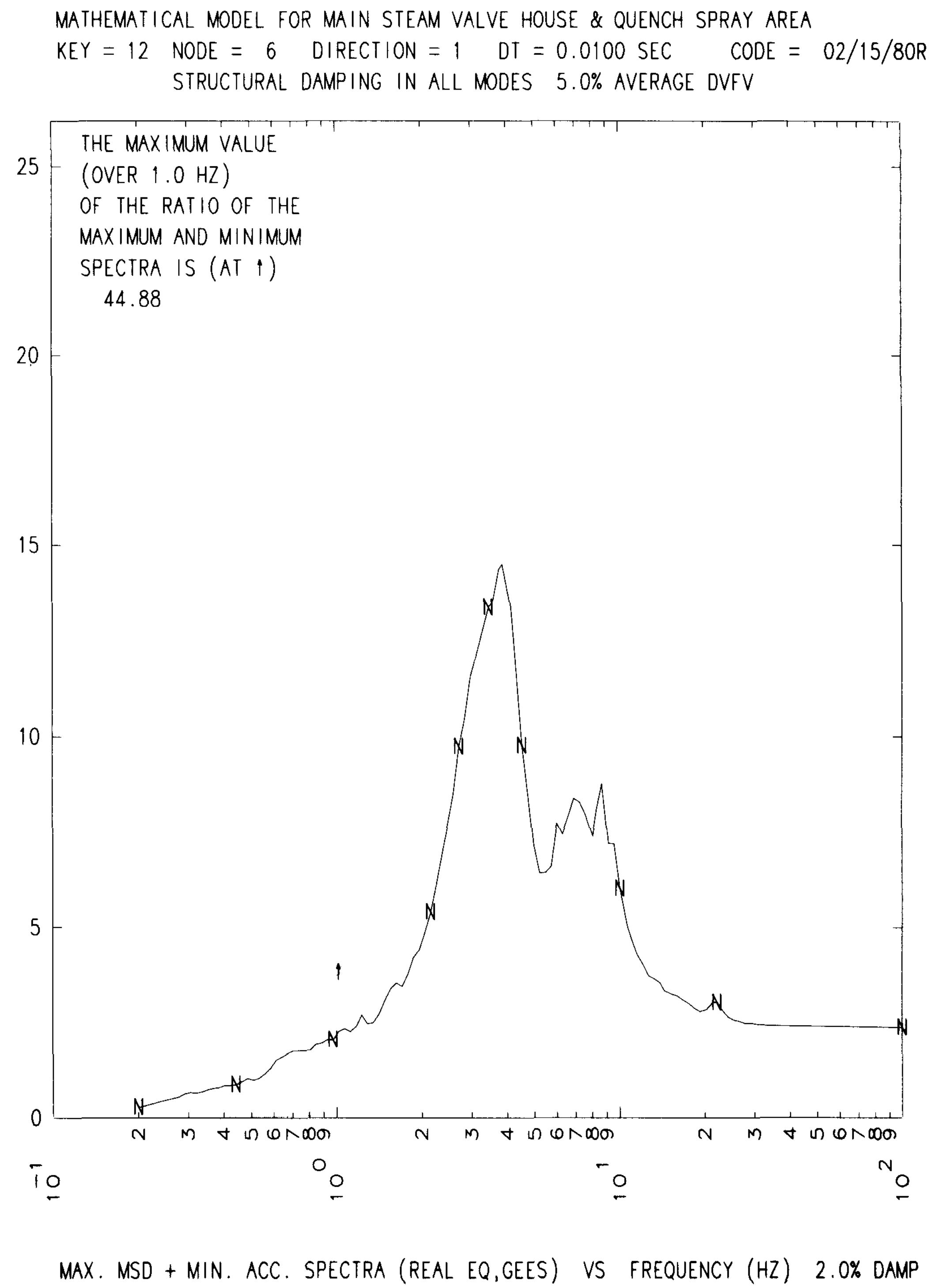

FIG. 17. Mathematical model for main steam valve house and quench spray area (key = 12, node = 6, direction = 1).

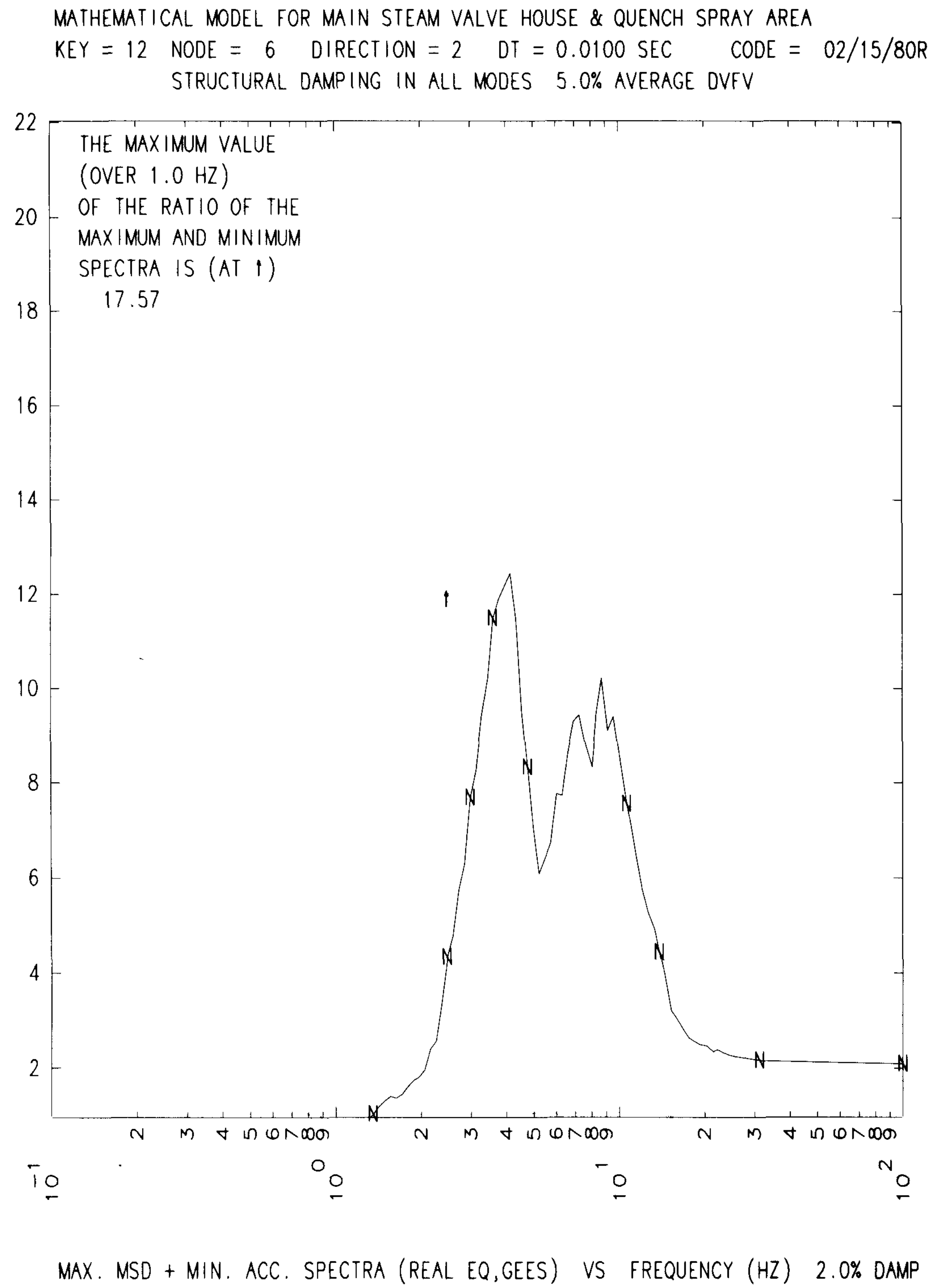

FIG. 18. Mathematical model for main steam valve house and quench spray area (key = 12, node = 6, direction = 2).

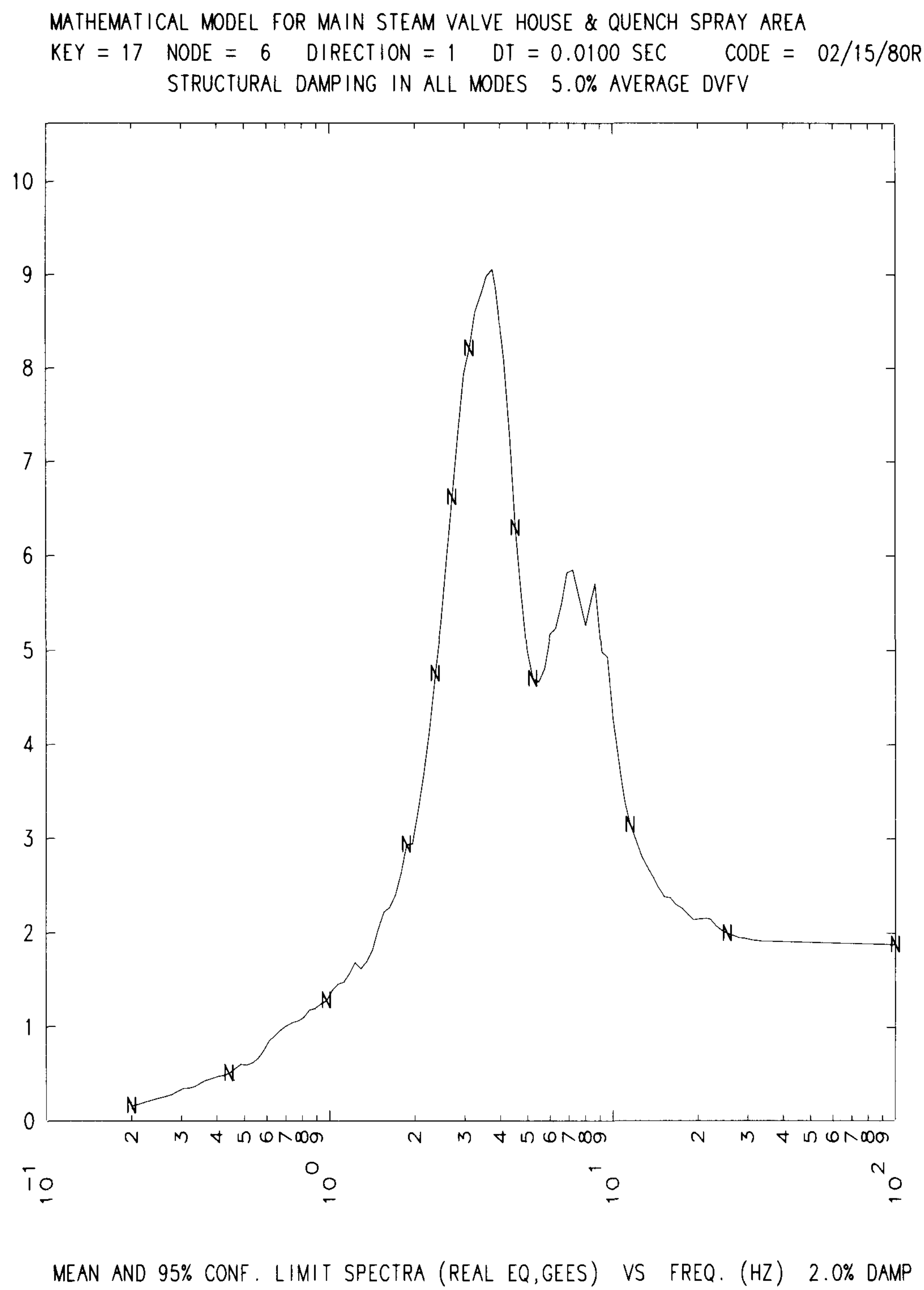

FIG. 19. Mathematical model for main steam valve house and quench spray area (key = 17, node = 6, direction = 1).

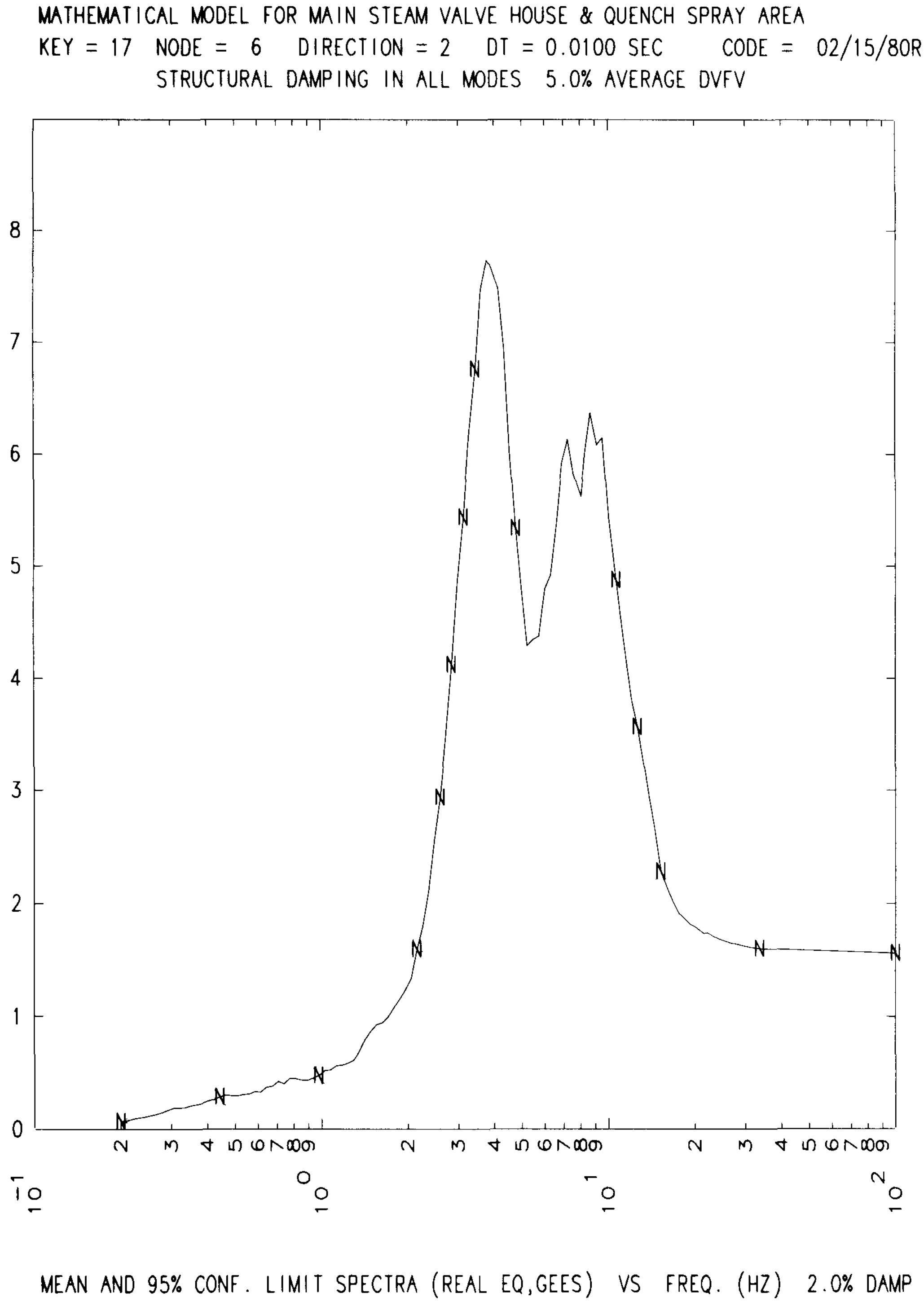

FIG. 20. Mathematical model for main steam valve house and quench spray area (key = 17, node = 6, direction = 2).

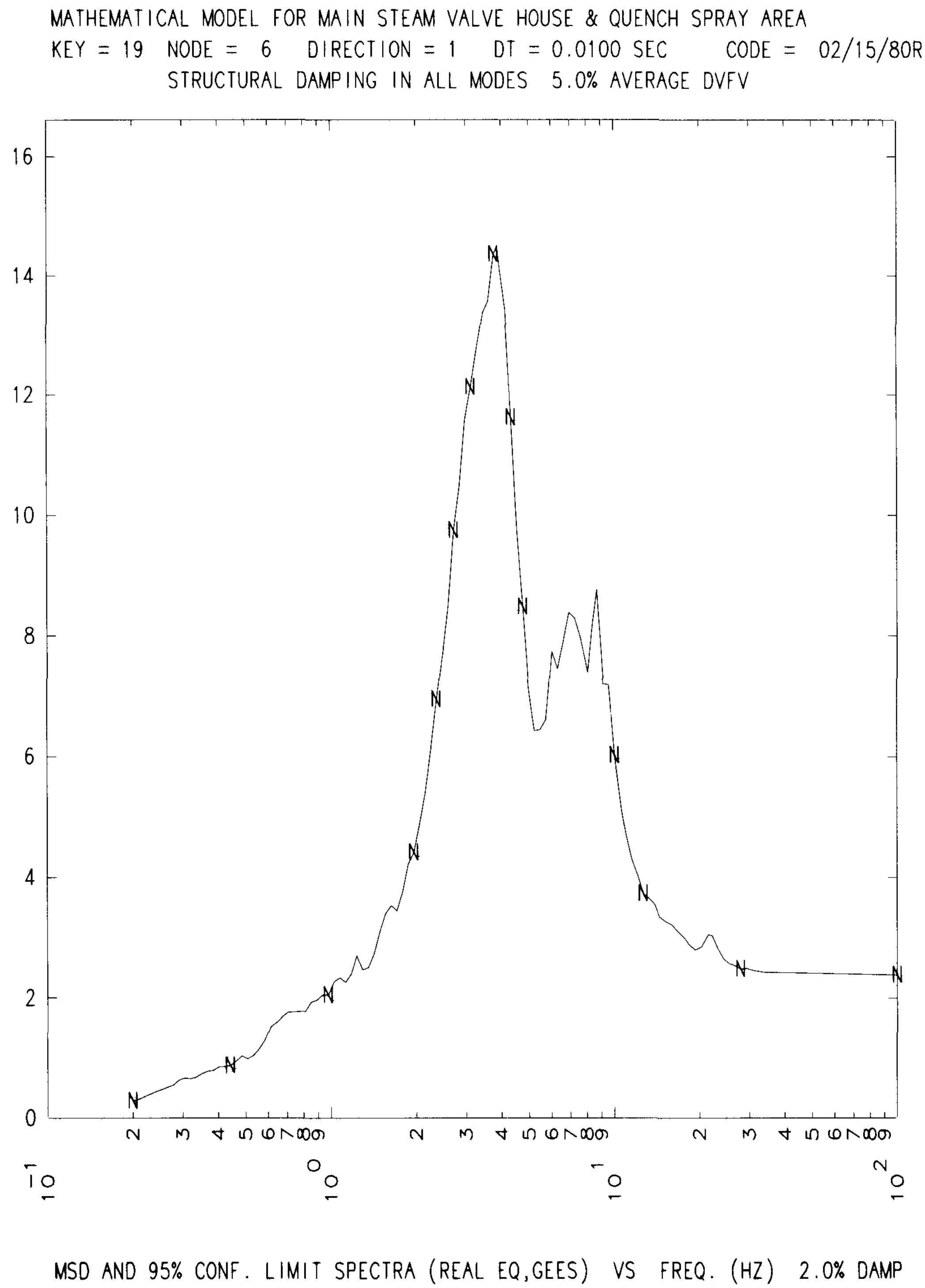

FIG. 21. Mathematical model for main steam valve house and quench spray area (key = 19, node = 6, direction = 1).

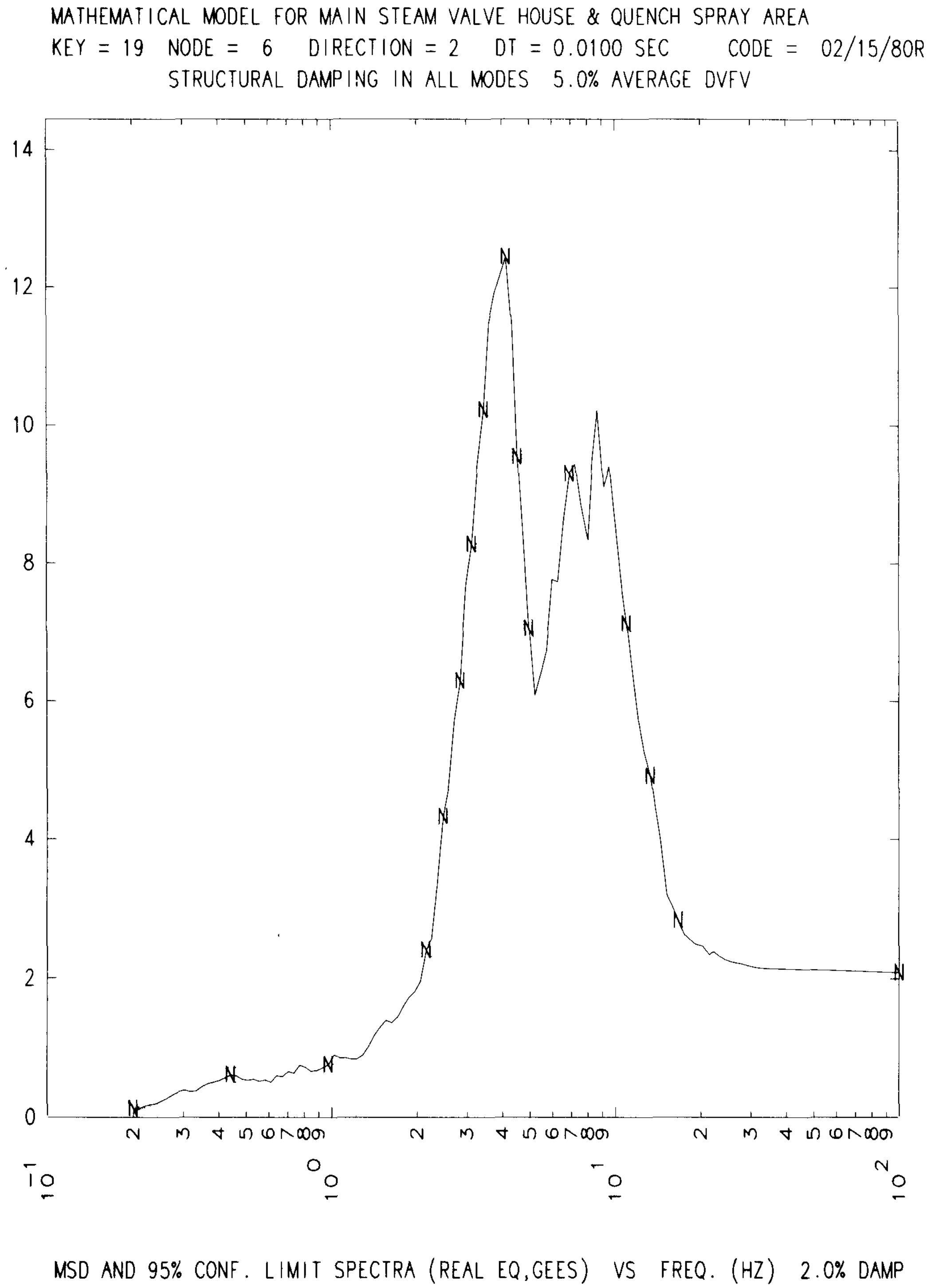

FIG. 22. Mathematical model for main steam valve house and quench spray area (key = 19, node = 6, direction = 2).

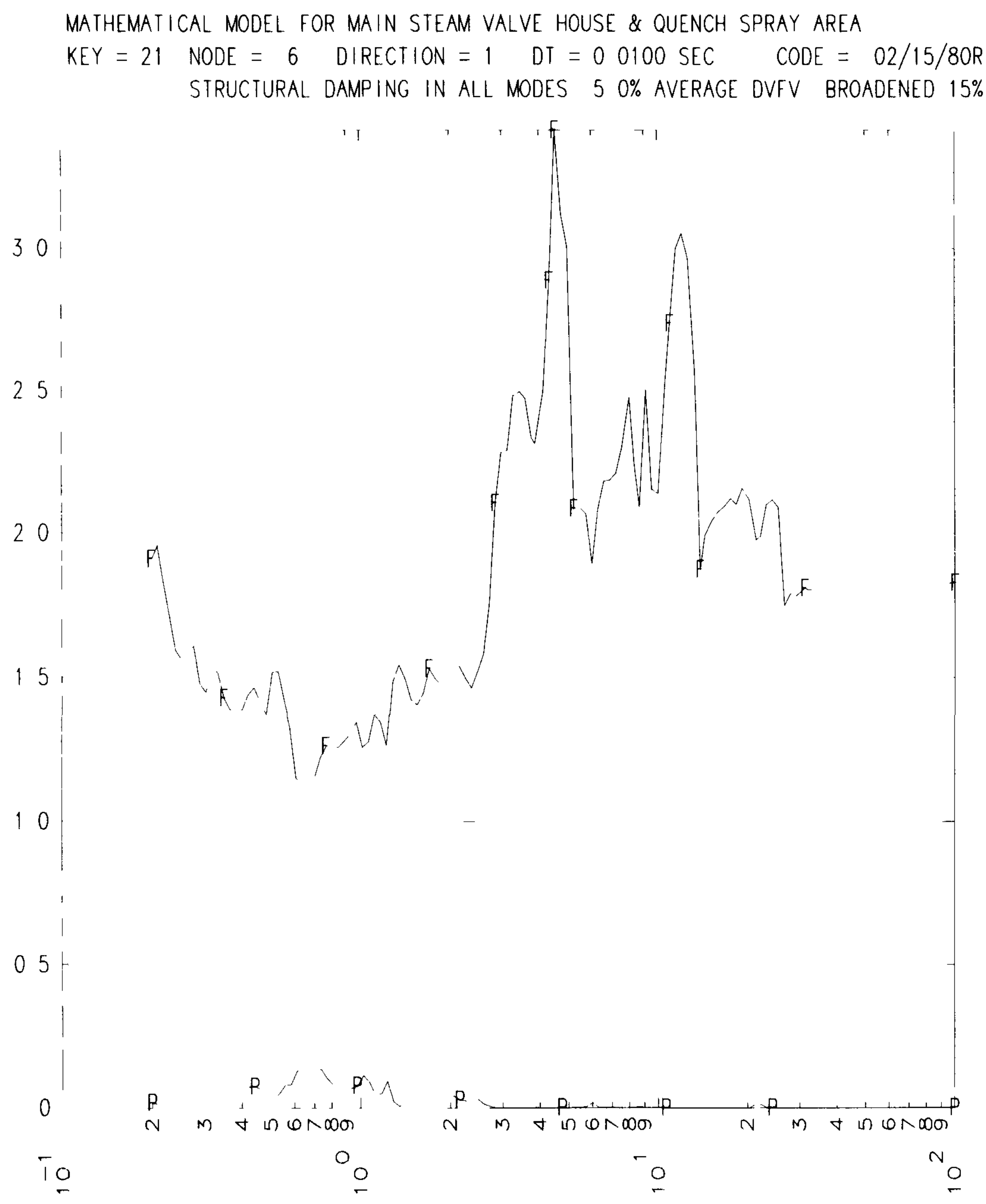

FIG. 23. Mathematical model for main steam valve house and quench spray area (key = 21, node = 6, direction = 1).

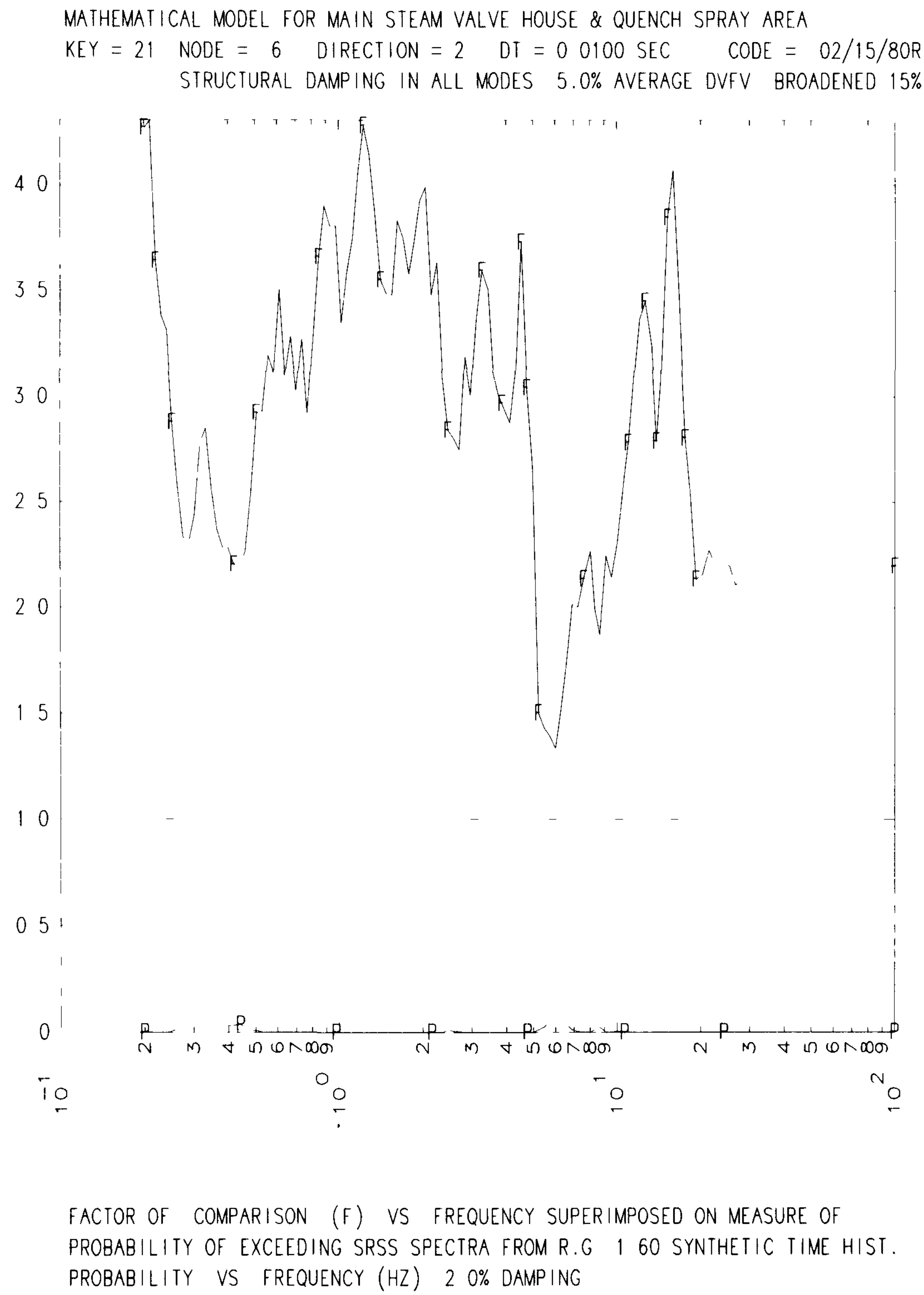

FIG. 24. Mathematical model for main steam valve house and quench spray area (key = 21, node = 6, direction = 2).

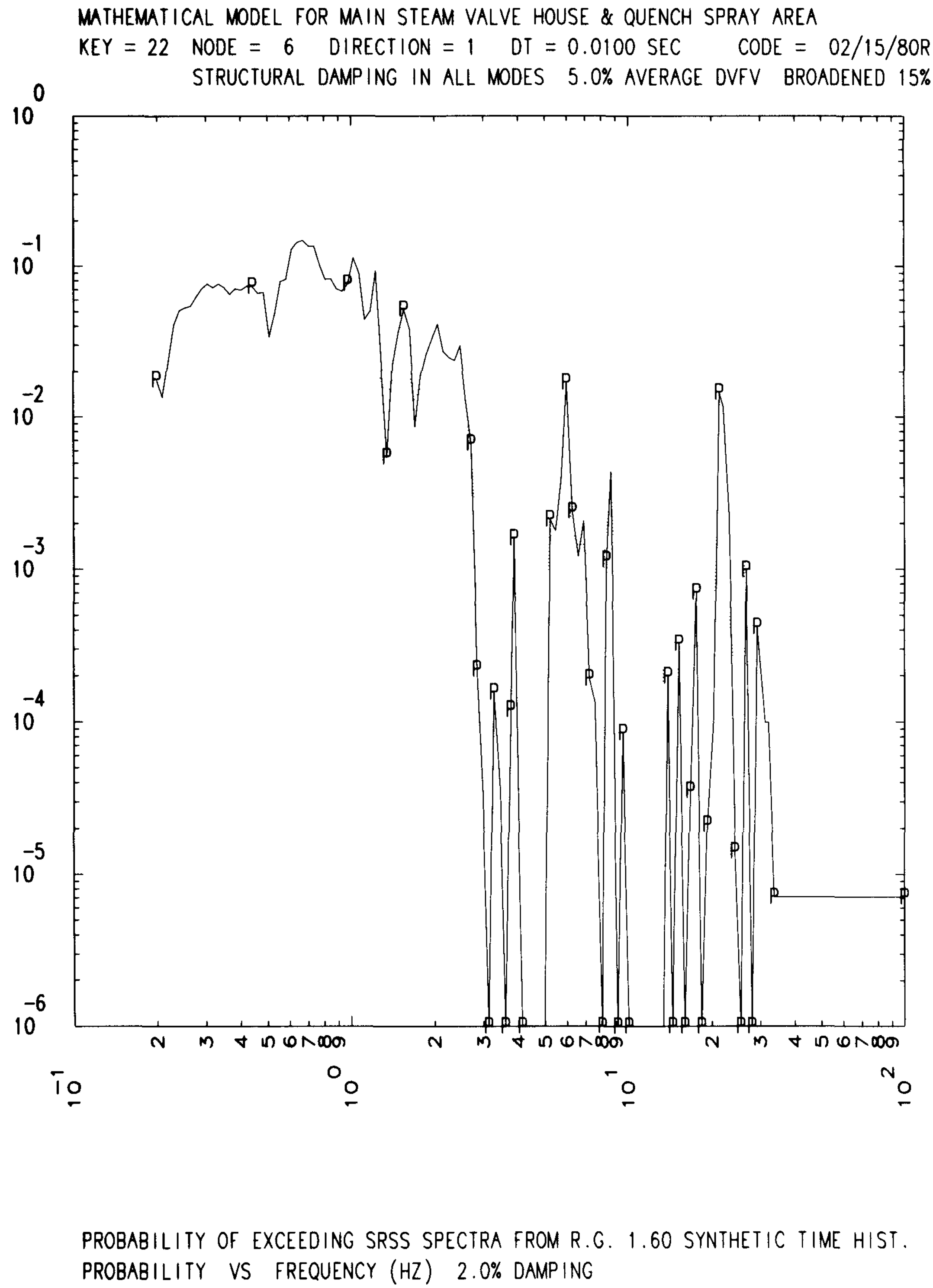

FIG. 25. Mathematical model for main steam valve house and quench spray area (key = 22, node = 6, direction = 1).

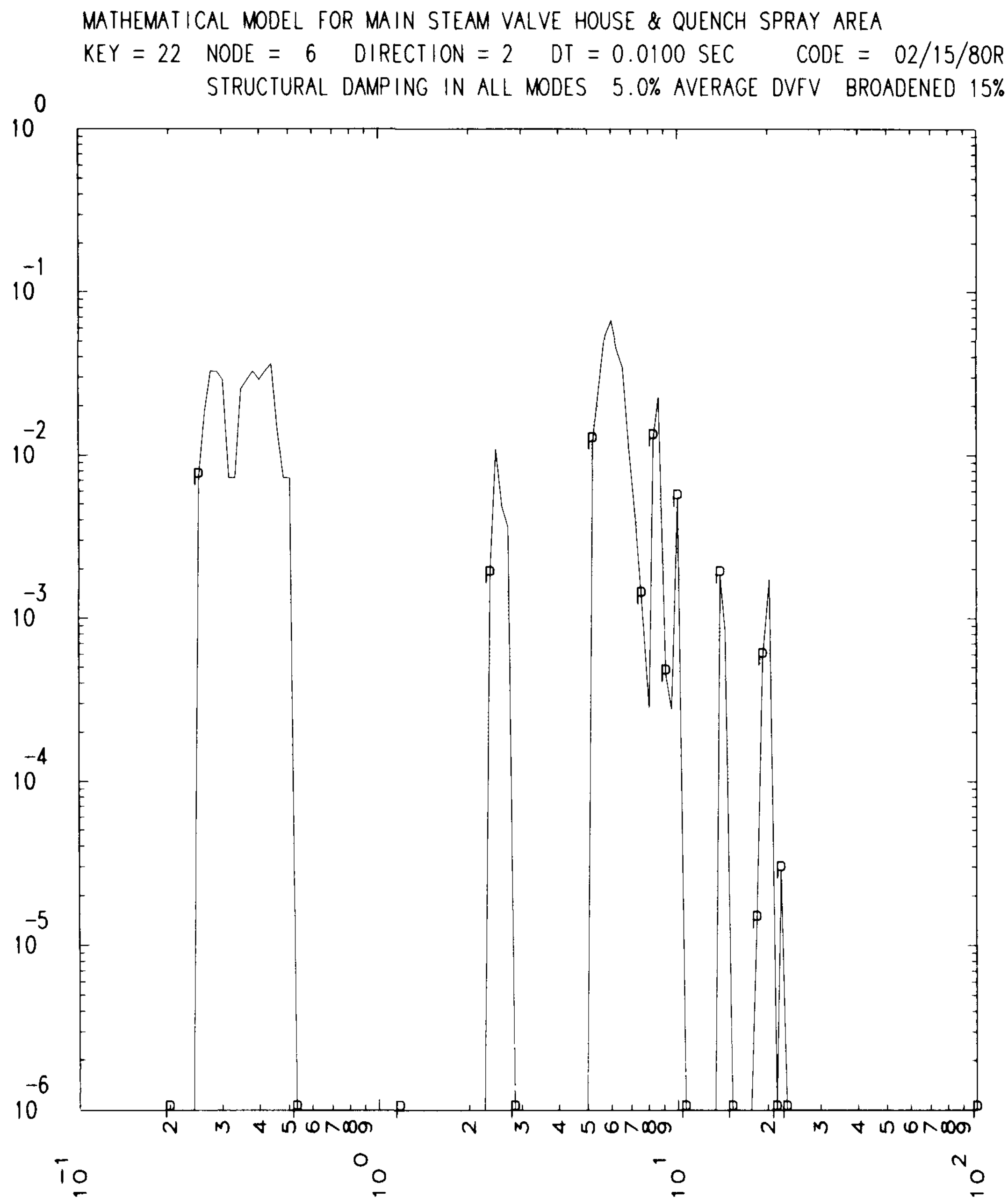

FIG. 26. Mathematical model for main steam valve house and quench spray area (key = 22, node = 6, direction = 2).

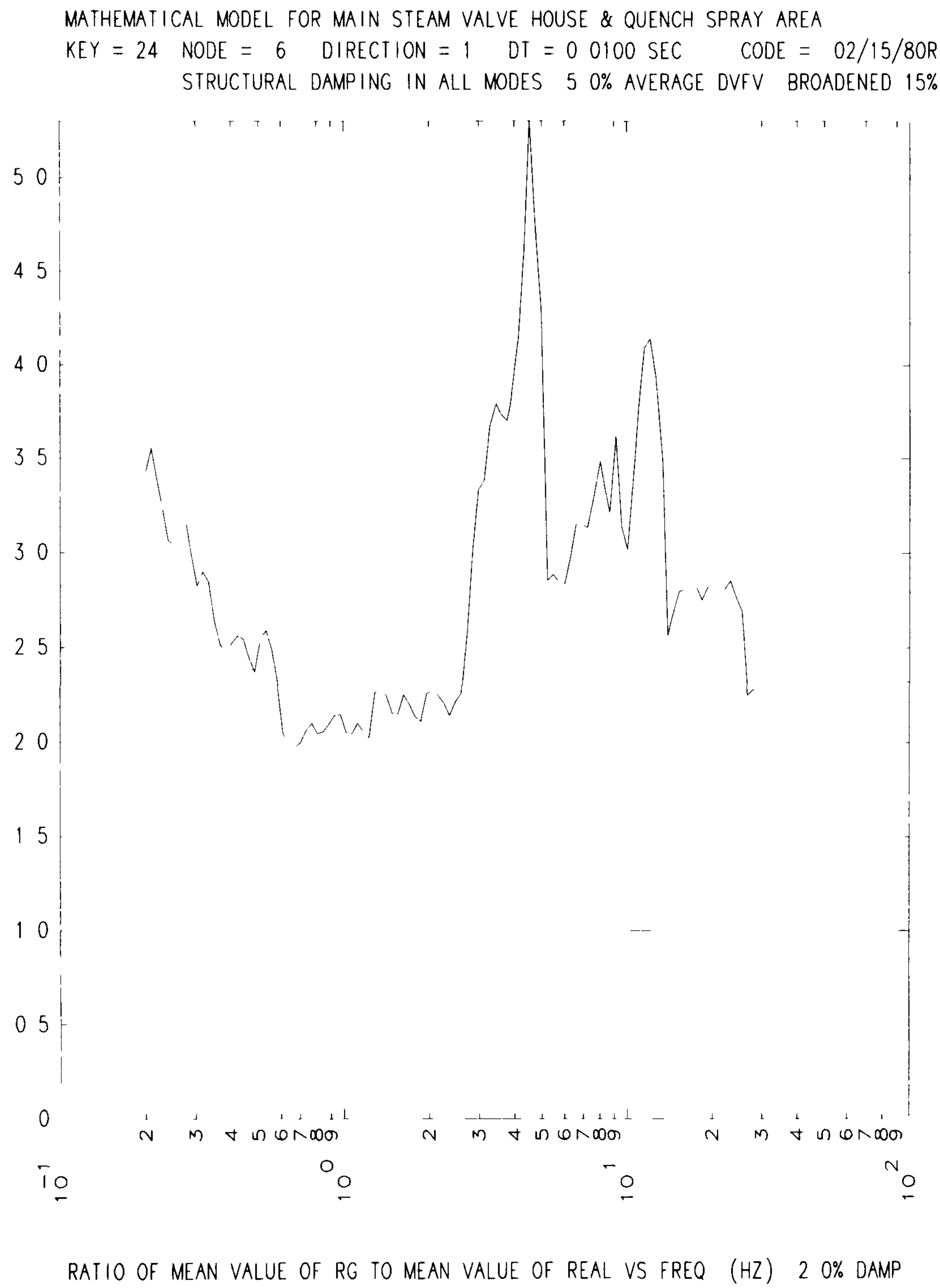

FIG. 27. Mathematical model for main steam valve house and quench spray area (key = 24, node = 6, direction = 1).

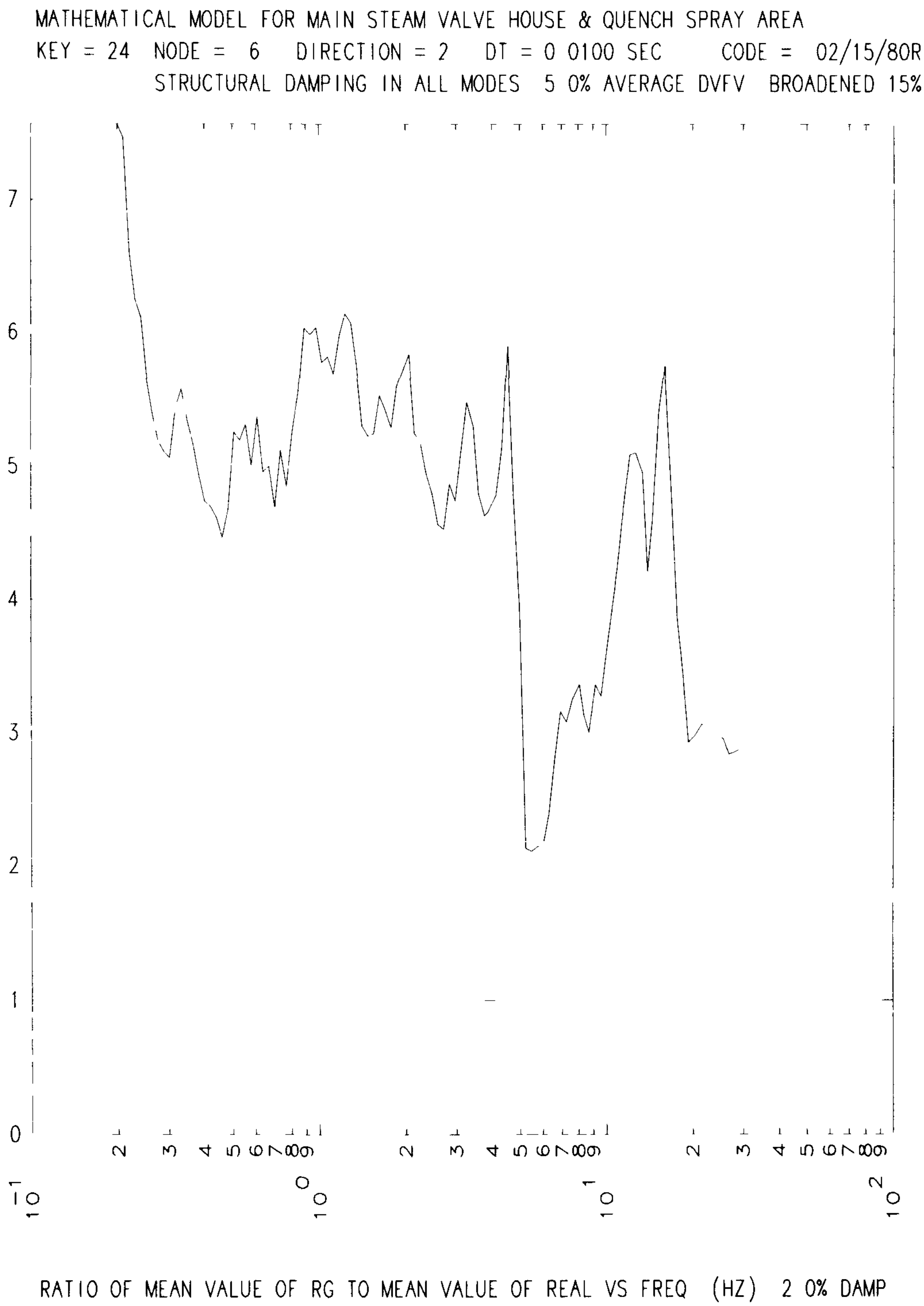

FIG. 28. Mathematical model for main steam valve house and quench spray area (key = 24, node = 6, direction = 2).

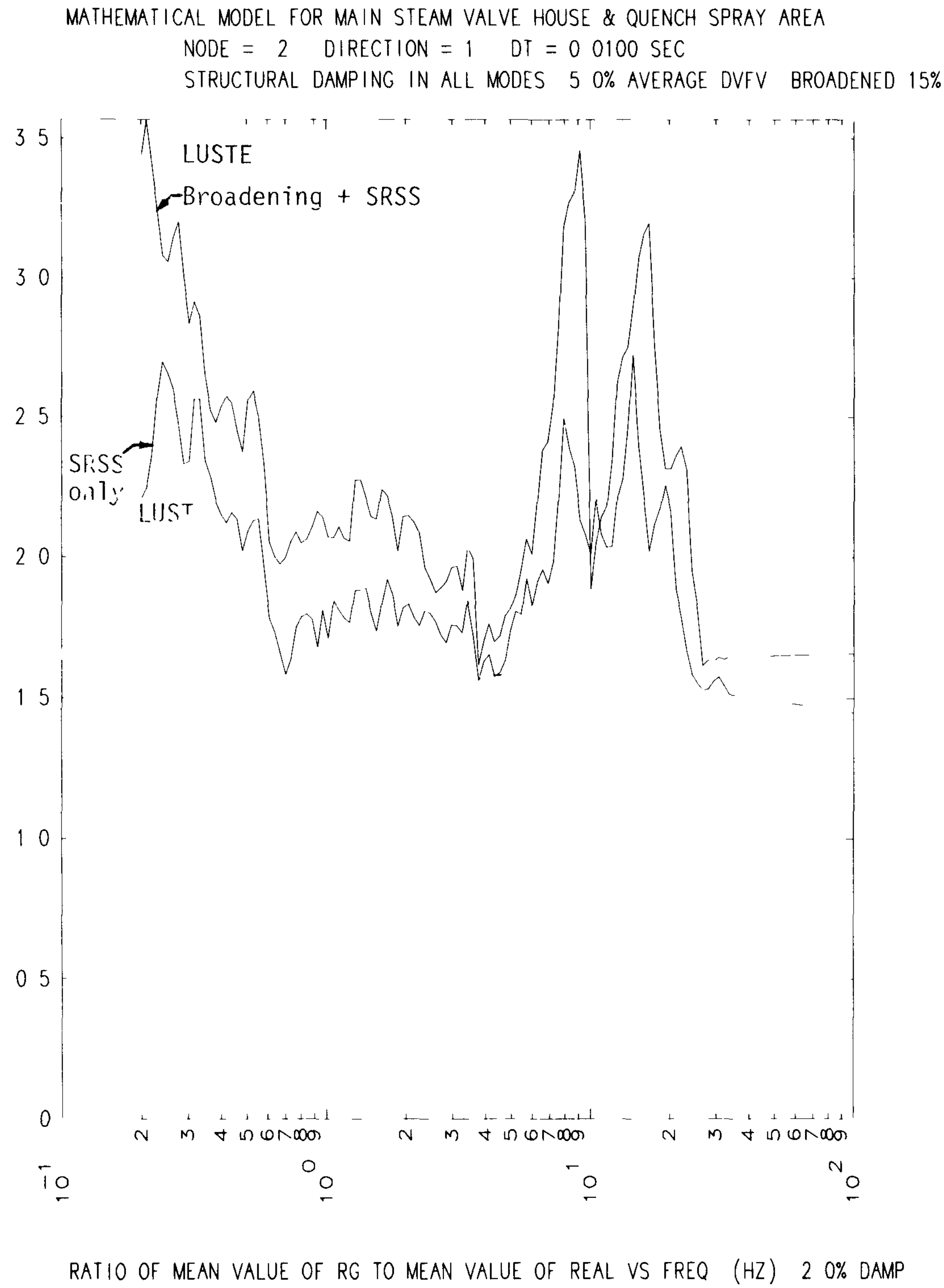

FIG. 29. Mathematical model for main steam valve house and quench spray area (node = 2, direction = 1).

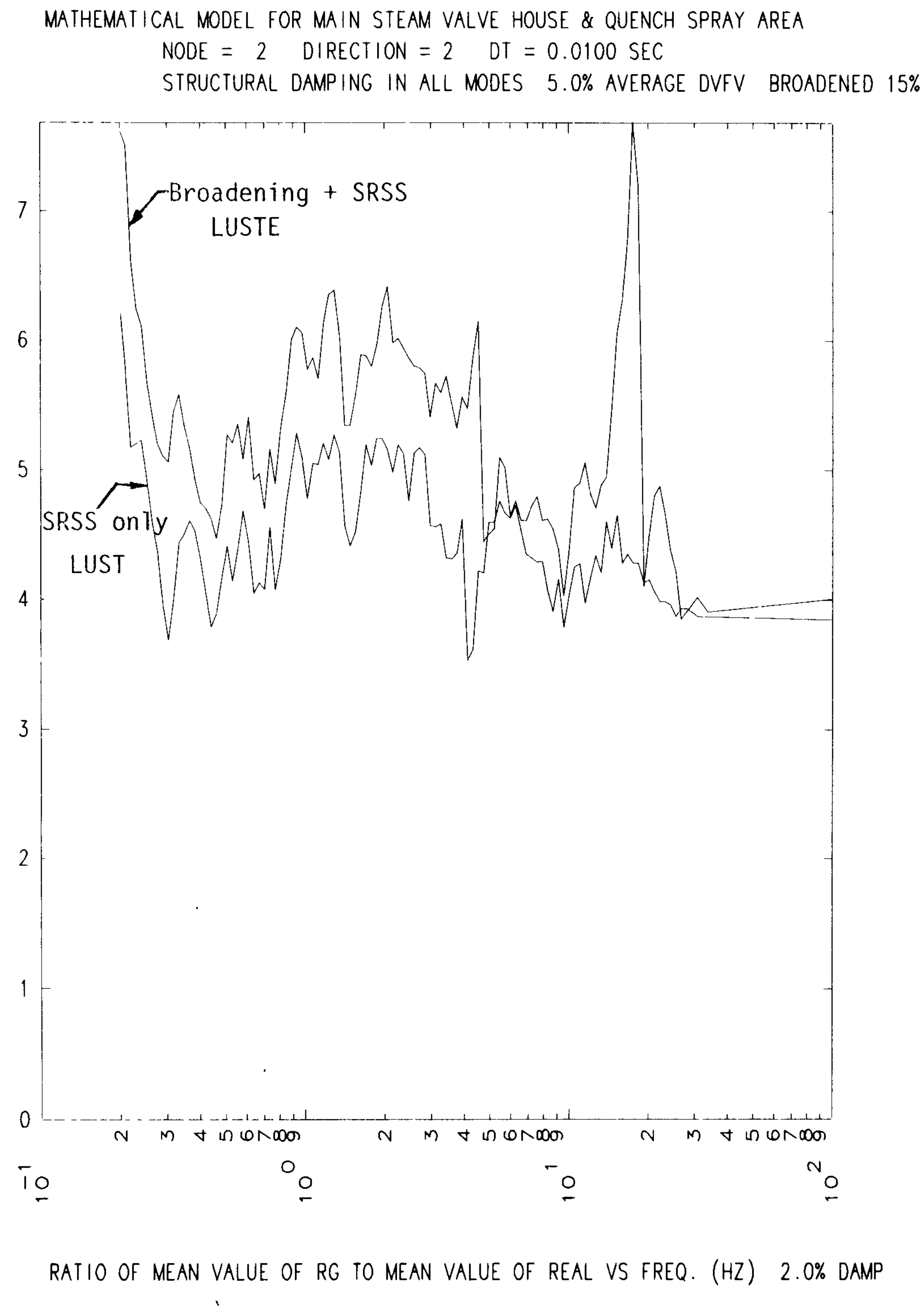

FIG. 30. Mathematical model for main steam valve house and quench spray area (node = 2, direction = 2).

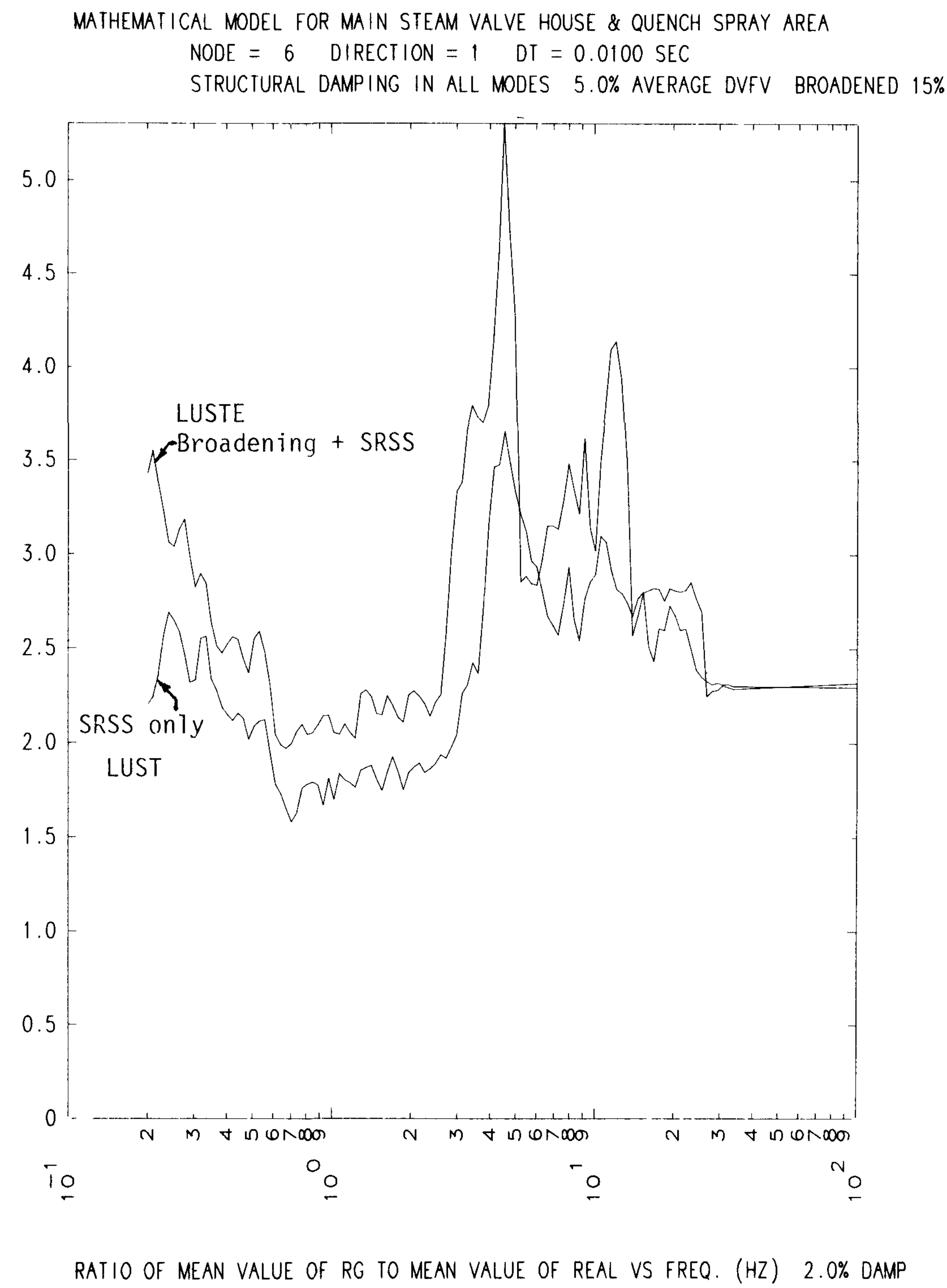

FIG. 31. Mathematical model for main steam valve house and quench spray area (node = 6, direction = 1).

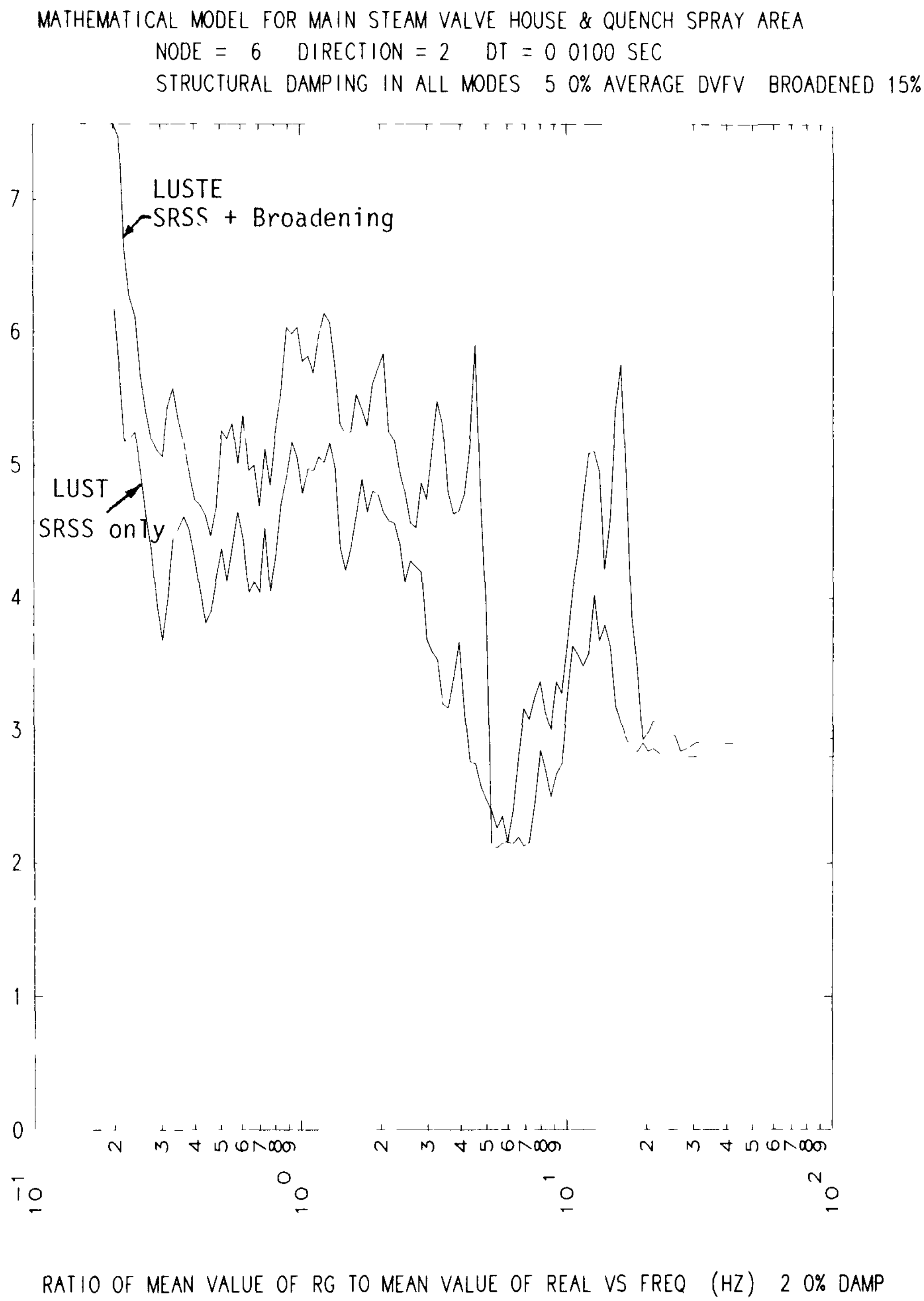

FIG. 32. Mathematical model for main steam valve house and quench spray area (node = 6, direction = 2).

4. CONCLUSIONS AND RECOMMENDATIONS

4.1 CONCLUSIONS

The concept of Best Estimate-Evaluation Method (BE-EM) has been introduced with respect to the seismic analysis and design of nuclear power plants. The concept has been shown to be extremely useful in the evaluation of two alternative methodologies. The illustrative example coupled two links in the SMC and introduced a possible method of comparison. The significance of the quantitative results is limited due to the methodologies selected. However, the results clearly illustrated the utility of such an approach. Compounding of effects through the SMC was shown.

4.2 RECOMMENDATIONS FOR FURTHER STUDY

- Future studies should include as many links of the SMC as appropriate to realistically analyze the phenomenon of interest. For example, structures founded on soil sites should be analyzed including the effects of soil-structure interaction. For subsystem response quantities of interest, the entire SMC should be treated in the analysis.

- The bases of comparison--the Factor of Comparison (FOC) and the Probability of Exceedance (POE)--introduced in this report need to be evaluated for their usefulness and alternatives proposed, if necessary.

- Alternative seismic analysis and design methodologies must be defined for comparison in the future. Each link in the SMC--seismic input, soil-structure interaction, major structural response, and subsystem response--will require the definition of alternative techniques. Initial comparisons should be between Best Estimate (BE) and a design methodology (EM). However, any two alternative approaches may be compared.

- We recommend establishing BE methodologies for each link in the SMC.

REFERENCES

1. J. J. Johnson and R. P. Kennedy, "Earthquake Response of Nuclear Power Facilities, Journal of the Power Division, ASCE, Vol. 105, No. EY1, Proc. Paper 14296 (January 1979).

2. P. D. Smith, et al., Seismic Safety Margins Research Program--Program Plan, Revision II, UCID-17824, Rev. II, Lawrence Livermore Laboratory, Livermore, Calif. (August 1978).

3. G. W. Johnsen, et al., A Comparison of "Best Estimate" and "Evaluation Model" LOCA Calculations: The BE/EM Study, PG-R-76-009, Idaho National Engineering Laboratory (December 1976).

4. P. D. Smith, S. E. Bumpus, and O. R. Maslenikov, LLL/DOR Conservatism Program: Investigations of the Conservatism in the Seismic Design of Nuclear Power Plants. Part VI: Response to Three Input Components, Lawrence Livermore Laboratory, Livermore, Calif., UCID-17959 (1979).

5. P. D. Smith, S. E. Bumpus, and O. R. Maslenikov, LLL/DOR Conservatism Program: Investigations of the Conservatism in the Seismic Design of Nuclear Power Plants. Part VII: Broadening of Floor Response Spectra, Lawrence Livermore Laboratory, Livermore, Calif., UCID-18104 (1979).

6. P. D. Smith, LLL/DOR Seismic Conservatism Program: Investigations of the Conservatisms in the Seismic Design of Nuclear Power Plants. Part I: Synthetic Time History Data Base, Lawrence Livermore Laboratory, Livermore, Calif., UCID-17988 (1979).

7. United States Atomic Energy Commission Regulatory Guide 1.60, "Design Response Spectra for Nuclear Power Plants" (1973).

8. W. Gersch, "On the Achievable Accuracy of Structural System Parameter Estimates," Journal of Sound and Vibration, Vol. 34, No. 1 (1974).

9. United States Nuclear Regulatory Commission, "Combining Modal Responses and Spatial Components in Seismic Response Analysis," Regulatory Guide 1.92, Rev. 1 (December 1974).

10. United States Nuclear Regulatory Commission, "Development of Floor Design Response Spectra for Seismic Design of Floor-Supported Equipment or Components," Regulatory Guide 1.122, Rev. 1 (February 1978).

11. California Institute of Technology, Earthquake Engineering Research Laboratory, "Strong Motion Earthquake Accelerograms," Index Volume, Report NO. EERL76-02, Pasadena, Calif. (August 1976).

12. A. H. Hadjian, et al., "Variability in Engineering Aspects of Structural Modeling," Proceedings Sixth World Conference on Earthquake Engineering, New Delhi, India (1977).

13. C. W. Hamilton and A. H. Hadjian, "Probabilistic Frequency Variations of Structure-Soil Systems," Nuclear Engineering and Design, 38 (1976), 303-322.

APPENDIX A: LUSTE OUTPUT DESCRIPTIONS

The computer program LUSTE, which is an acronym for Limited Understanding of the Statistics of Transients with Extension, provides output in the form of 27 different types of computer plots. Each plot is identified by KEY = 01 to KEY = 26 or KEY = L in the upper left-hand corner. LUSTE automatically produced these plots. The plots have self-descriptive information displayed at the top. This information includes a description of the structure, the key number, the node analyzed, the direction for which output results were obtained (not input analysis direction), the integration time-step, the version (date) of LUSTE used, the average structural damping, the amount of broadening if (applicable), and other data that vary from plot to plot. At the bottom, the ordinate and the abscissa are described, and the spectral damping is given.

We describe now the different types of plots, key number by key number.

KEY = 01

These plots show the response spectra at the indicated node and in the indicated direction for the 44 (16 + 16 + 12) synthetic time histories. Each of the 44 curves resulted from a single time history analysis. The 3072 SRSS-broadened combinations are not shown.

KEY = L

These plots show spectra from plot KEY = 1 but with every spectra broadened by 15%. The plots are for illustrative purposes only to show typical broadened spectra. All subsequent plots and results were obtained by first doing the SRSS combination and then broadening 15%.

KEY = 02

These plots show the cumulative distribution function (CDF) and a 95% confidence interval for the 3072 SRSS-broadened spectral values at frequencies nearest to the indicated mode of the structure. At this frequency the 3072 SRSS spectral responses were sorted according to increasing acceleration and normalized to 1.0 to construct the CDF. The CDF measures the probability of the spectral acceleration being below the value given on the abscissa. Three separate KEY = 02 plots show the results for the first three modal frequencies.

The 95% confidence intervals were calculated by the Kolmogorov-Smirnov (K-S) method. These K-S confidence bands are independent of any assumption of distribution type. Confidence intervals obtained by using an assumption of normality and the K-S method, as well as the point estimates, are printed on these plots.

KEY = 03

These plots show the extremes and means of the SRSS-broadened response spectra derived from the 44 spectra in KEY = 01. The lowest (dotted) curve is a compilation of the minimum spectral values in the KEY = 01 plot. The curve above it is a compilation of the minimum spectral values from the 3072 SRSS-broadened spectra. The middle curve, with the N overprint, is the mean of the 3072 SRSS-broadened spectra. At each spectral frequency, the mean was calculated as the simple arithmetic average of the 3072 spectra values at that frequency. The higher dotted curve is a compilation of the maximum spectral values in the KEY = 01 plot. The highest curve is a similar compilation for the 3072 SRSS-broadened spectra.

KEY = 04 to KEY = 07

These plots basically illustrate a distribution-free statistical test for normal and lognormal distribution assumptions about the 3072 SRSS-broadened spectral curves. These tests were conducted by using a modification of the K-S method.

KEY = 08

These plots show the mean of the 3072 SRSS-broadened spectra and the corresponding 95% confidence intervals, assuming a normal distribution. Because of the large number of SRSS-broadened spectra, typical confidence intervals about the estimate of the mean are quite narrow and as a result the three curves on these plots are typically indistinguishable. While the classical statistical meaning and interpretation of such narrow confidence bands is clear, their usefulness for engineering purposes is not.

KEY = 09

Each of these plots shows the standard deviation of the 3072 SRSS-broadened spectra and the corresponding 95% confidence intervals assuming a normal distribution. Because of the large number of SRSS-broadened spectra, the three curves are again virtually indistinguishable.

KEY = 10

These plots show the response spectra at the indicated node and in the indicated direction for the 46 real earthquake analyses. Each of these 46 spectra is the result of the simultaneous application of three orthogonal real time histories.

KEY = 11

These plots are analogous to KEY = 02, but are based on the analyses using real time histories.

KEY = 12

These plots display the minimum, the MSD (with N overprint), and the maximum of the 46 spectra from the real earthquake analyses.

KEY = 13 to KEY = 16

These plots are analogous to the plots KEY = 04 to KEY = 07.

KEY = 17

These plots show the mean of 46 spectra from the real earthquake analyses and the corresponding 95% confidence intervals, again assuming a normal distribution. These plots thus show the best estimate of the in-structure response spectra due to three-dimensional real earthquakes.

KEY = 18

Each of these plots shows the standard deviation of the 46 spectra from the real earthquake analyses and the corresponding 95% confidence intervals, assuming a normal distribution.

KEY = 19

These plots show the MSD of the 46 spectra from the real earthquake analyses (also shown by KEY = 12) and the corresponding 95% confidence limits. We computed the confidence intervals by assuming a normal distribution and performing 2000 Monte Carlo simulations at each of the 112 spectral frequencies.

KEY = 20

These plots display the Factor of Comparison (FOC) for in-structure response spectra and the corresponding 95% confidence intervals. The FOC is the quotient of the mean of the 3072 SRSS-broadened spectra (KEY = 08) and the MSD of the 46 spectra from the real earthquake analyses (KEY = 19). The 95%

confidence intervals were calculated by assuming a normal distribution and performing 2000 Monte Carlo simulations at each of the 112 spectral frequencies.

KEY = 21

These plots display the FOC from the KEY = 20 plot and a measure of the Probability of Exceedance (POE), which has a P overprint. The POE was obtained by comparing each of the 3072 SRSS-broadened spectra with the first of the 46 spectra from the real earthquake analyses and then counting the number of times that the real spectrum exceeded the SRSS spectrum, to give n_1. We repeated this procedure for the remaining 45 spectra to give n, where $n = n_1 + \ldots + n_{46}$. The POE was calculated as n/(46 x 3072). The calculation was performed separately for each of the 112 spectral frequencies.

KEY = 22

These plots show on a logarithmic scale the same POE from plot KEY = 21 with an overprint P label. Any POE that had been computed to be 0.0 in plot KEY = 21 was set to an arbitrary value of 10^{-6}. Also shown with a dotted line is the POE that can be calculated from the Coefficients of Variation (COVs) of the real and Regulatory Guide (R.G.) analyses as shown in plot KEY = 23, the ratio of the means given in plot KEY = 24, and an assumption that the variables are lognormally distributed. This latter computed POE correlates well with the former POE, which results from strict comparison counting.

KEY = 23

These plots show the calculated COVs for the R.G. (dotted line) and real (solid line) analyses. The COV for the R.G. analyses was computed by dividing the standard deviation in plot KEY = 09 by the mean in plot KEY = 08. Likewise, the COV for the real analyses was computed by dividing the standard deviation in plot KEY = 18 by the mean shown in plot KEY = 17.

KEY = 24

These plots probably provide the most important results of this study. They display the ratio of the means of the R.G. analyses (from plot KEY = 08) and the real analyses (from plot KEY = 17). The plots show the relationship between the BE and the EM types of structural analysis.

KEY = 25

These tables display information similar to that in the plots, but the results pertain only to peak absolute accelerations which closely approximate the spectral accelerations at 100 Hz. Units are ft/s^2.

KEY = 26

These plots show the Cumulative Distribution Functions (CDFs) for the peak absolute accelerations from the 3072 SRSS spectra and from the 46 spectra from real time histories. These CDFs and the corresponding 95% confidence intervals are shown on two separate plots. The first plot shows results for the SRSS spectra, the second plot shows results for the real earthquake spectra.

APPENDIX B: LUSTE OUTPUT PLOTS

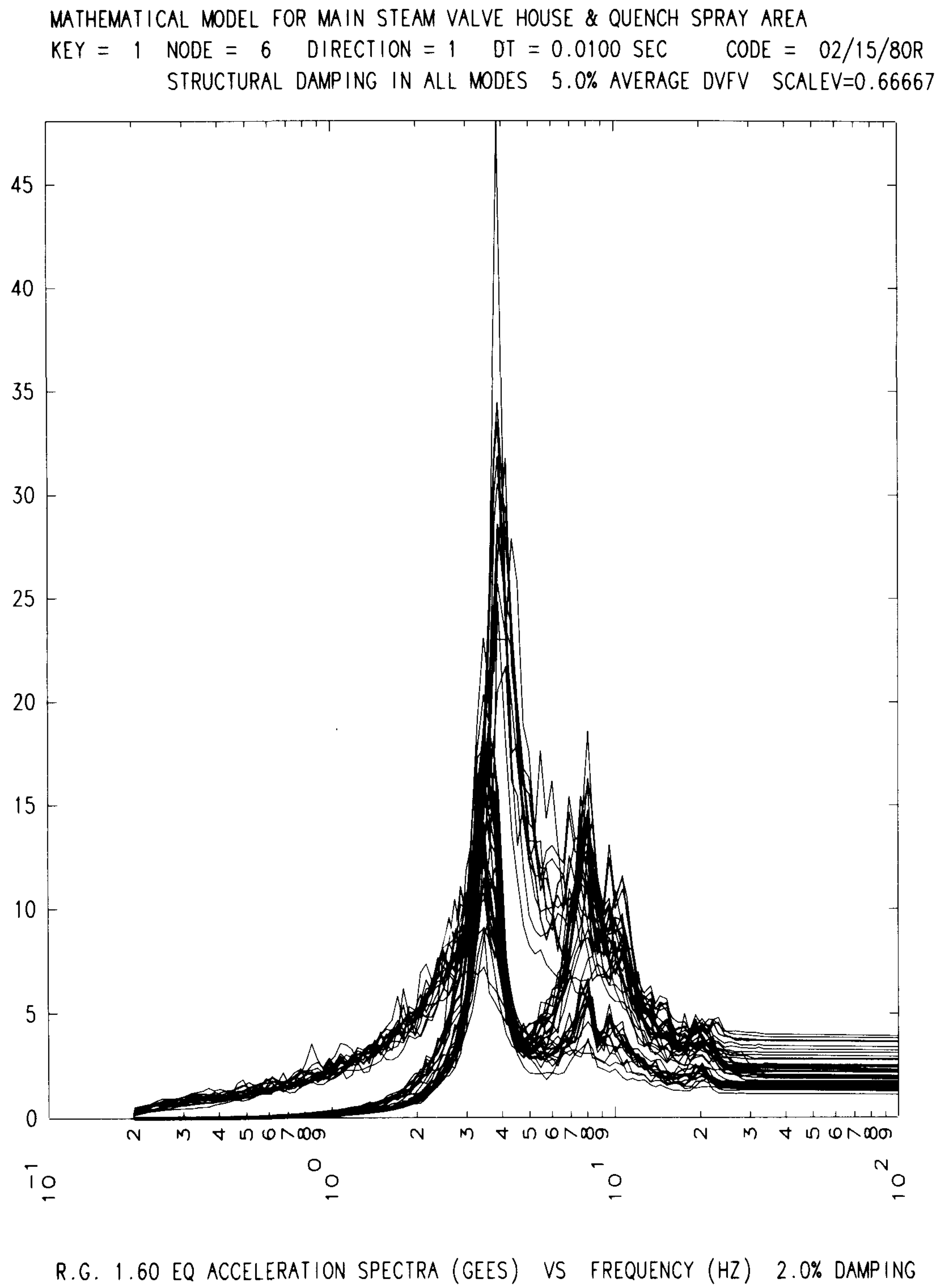

FIG. B-1. Mathematical model for main steam valve house and quench spray area (key = 1, node = 6, direction = 1).

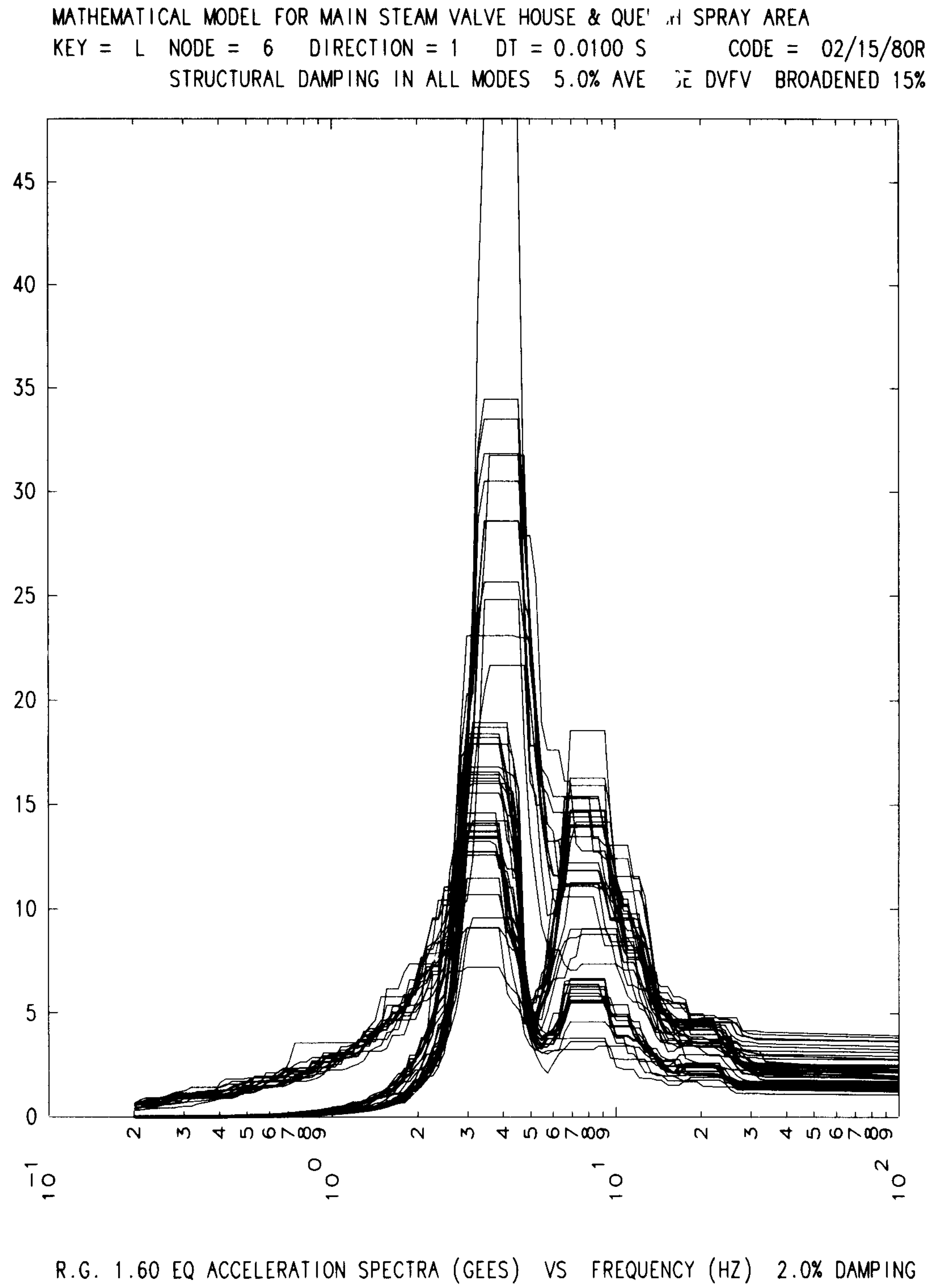

FIG. B-2. Mathematical model for main steam valve house and quench spray area (key = L, node = 6, direction = 1).

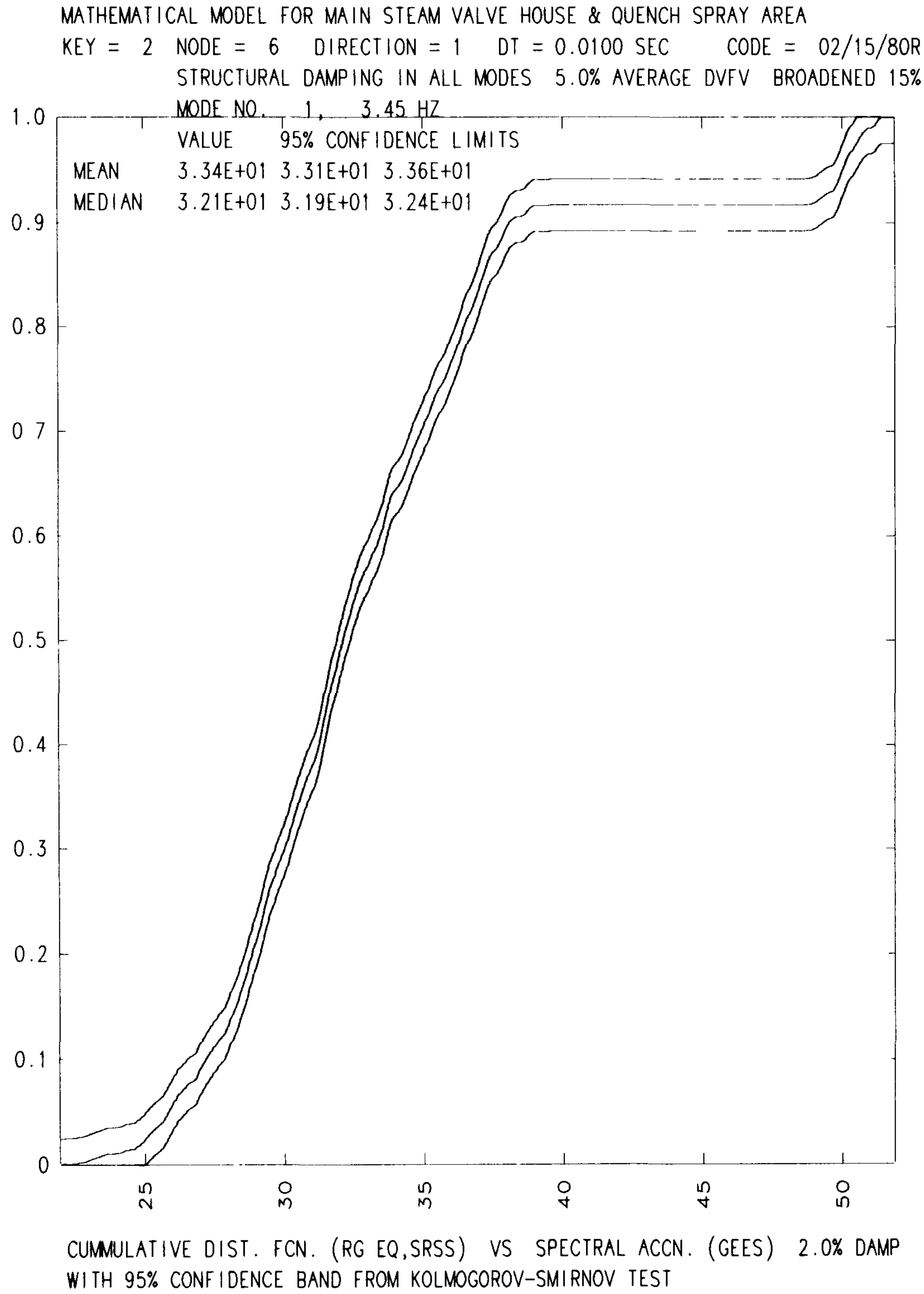

FIG. B-3. Mathematical model for main steam valve house and quench spray area (key = 2, node = 6, direction = 1).

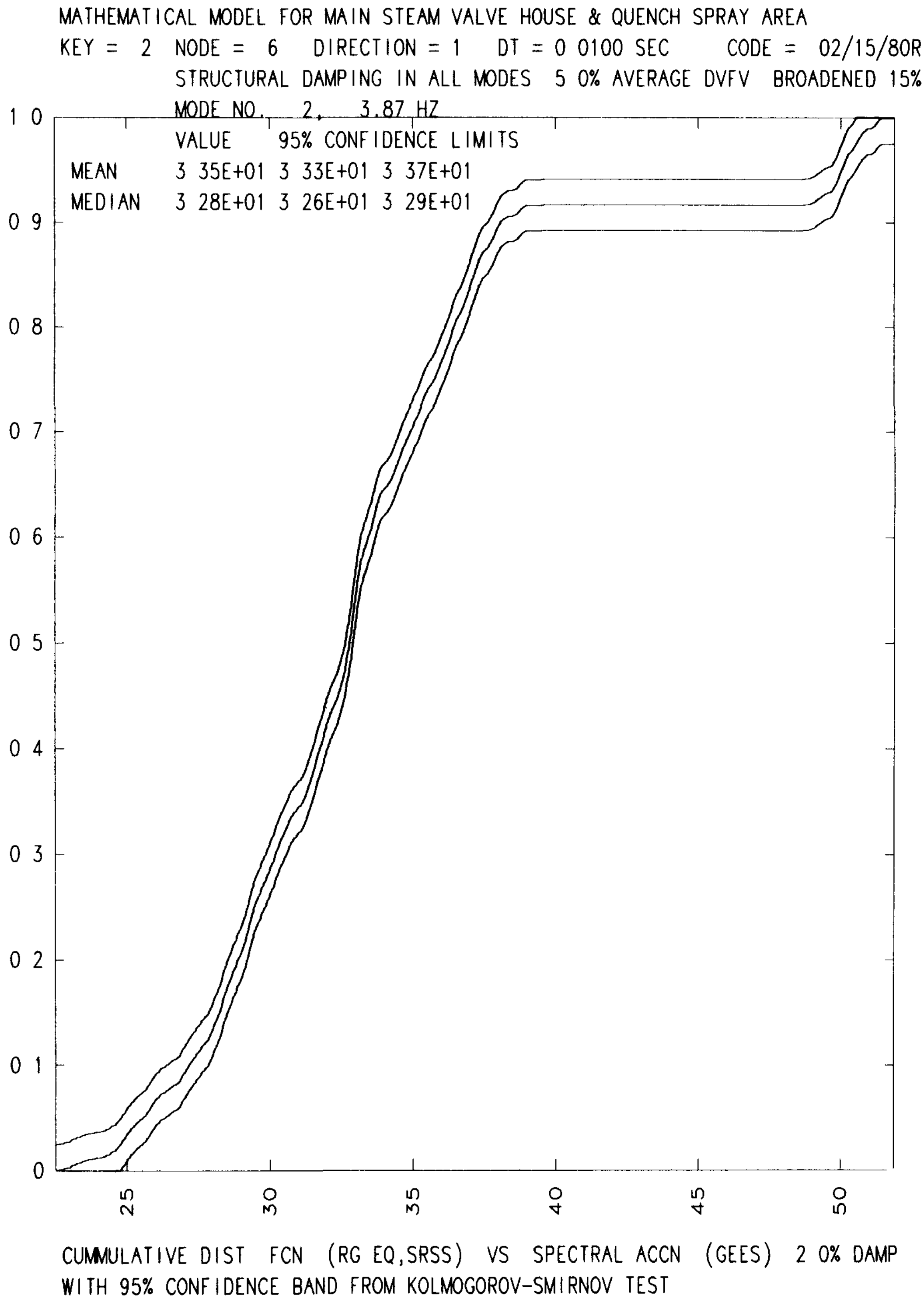

FIG. B-4. Mathematical model for main steam valve house and quench spray area (key = 2, node = 6, direction = 1).

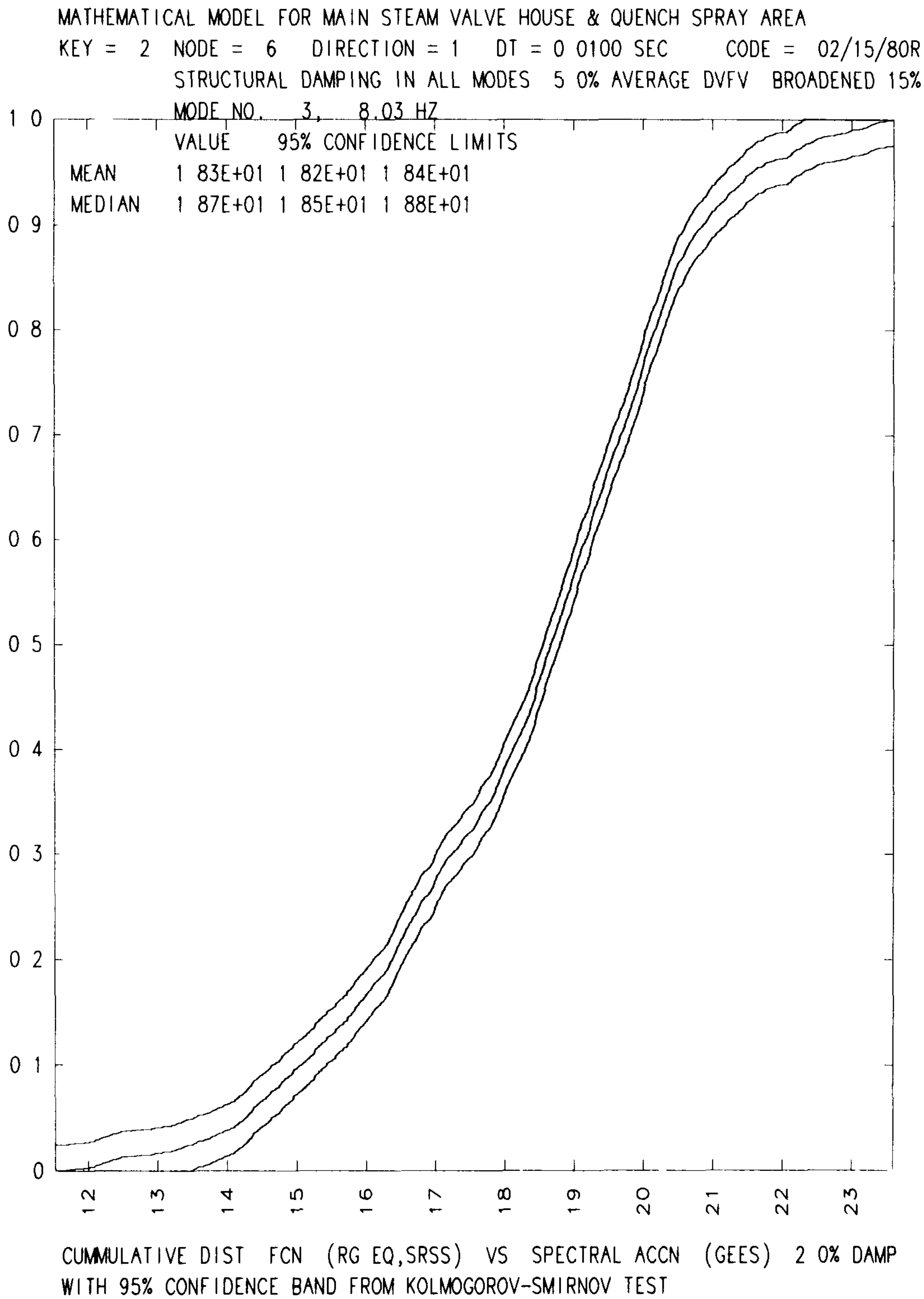

FIG. B-5. Mathematical model for main steam valve house and quench spray area (key = 2, node = 6, direction = 1).

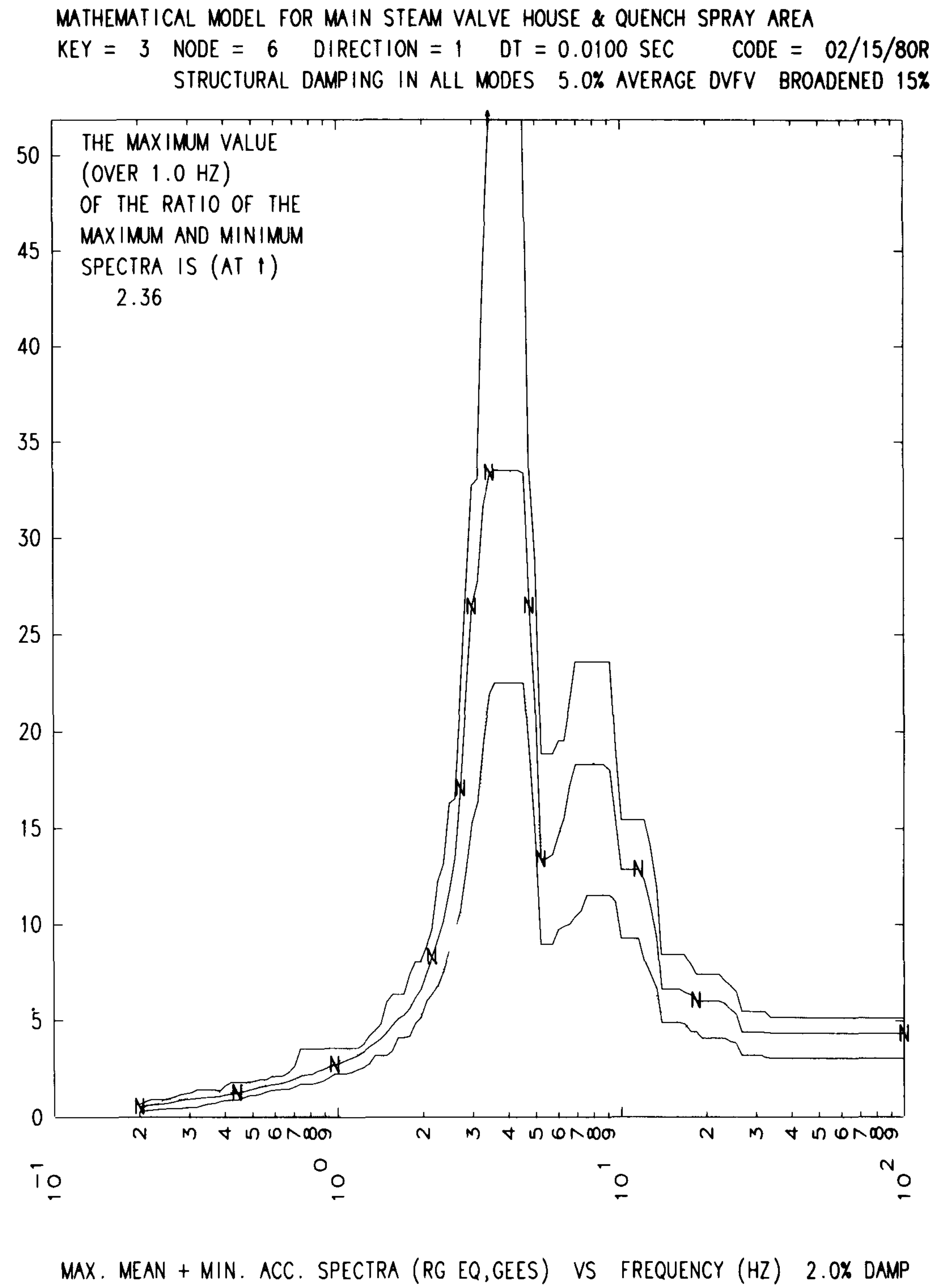

FIG. B-6. Mathematical model for main steam valve house and quench spray area (key = 3, node = 6, direction = 1).

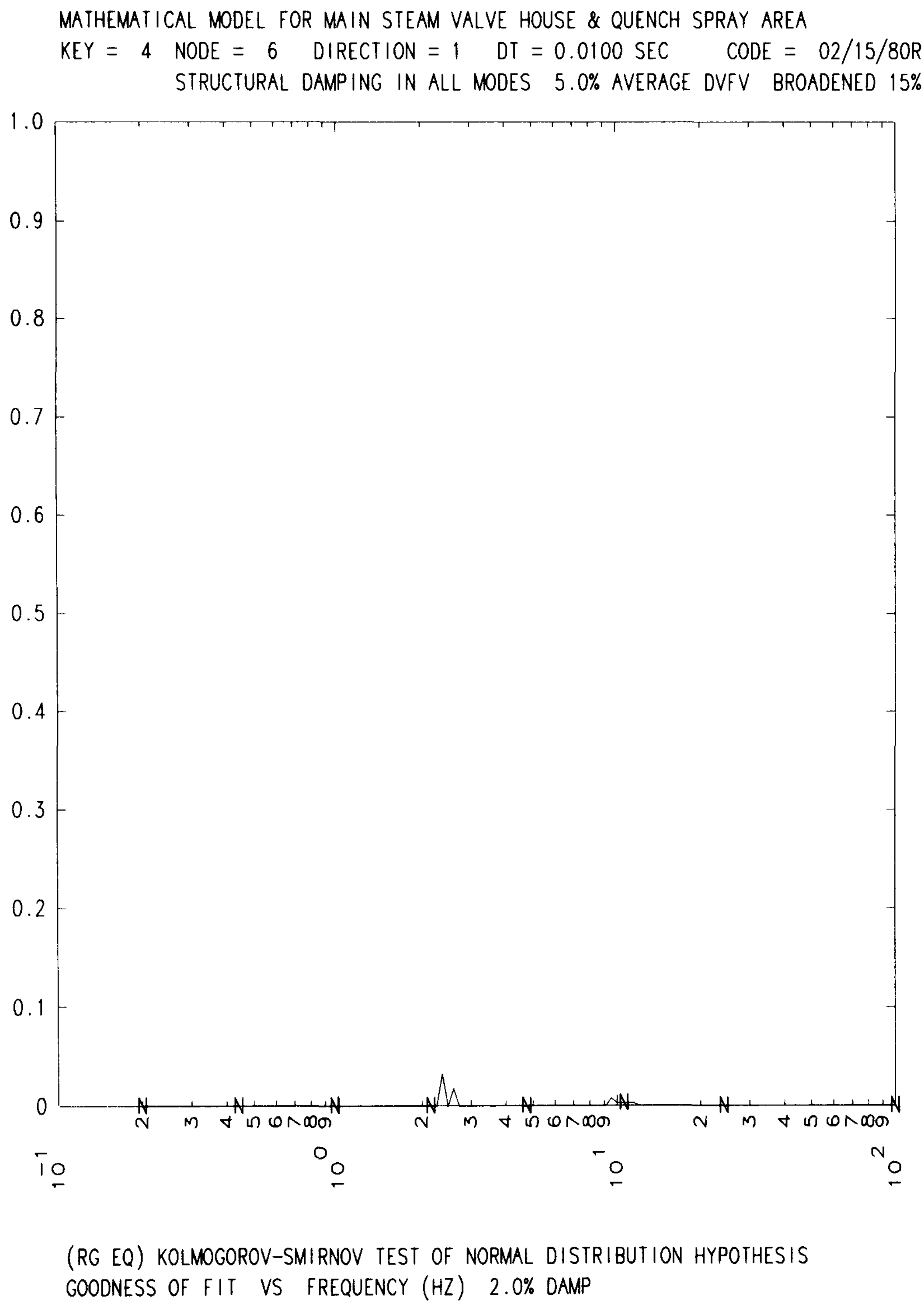

FIG. B-7. Mathematical model for main steam valve house and quench spray area (key = 4, node = 6, direction = 1).

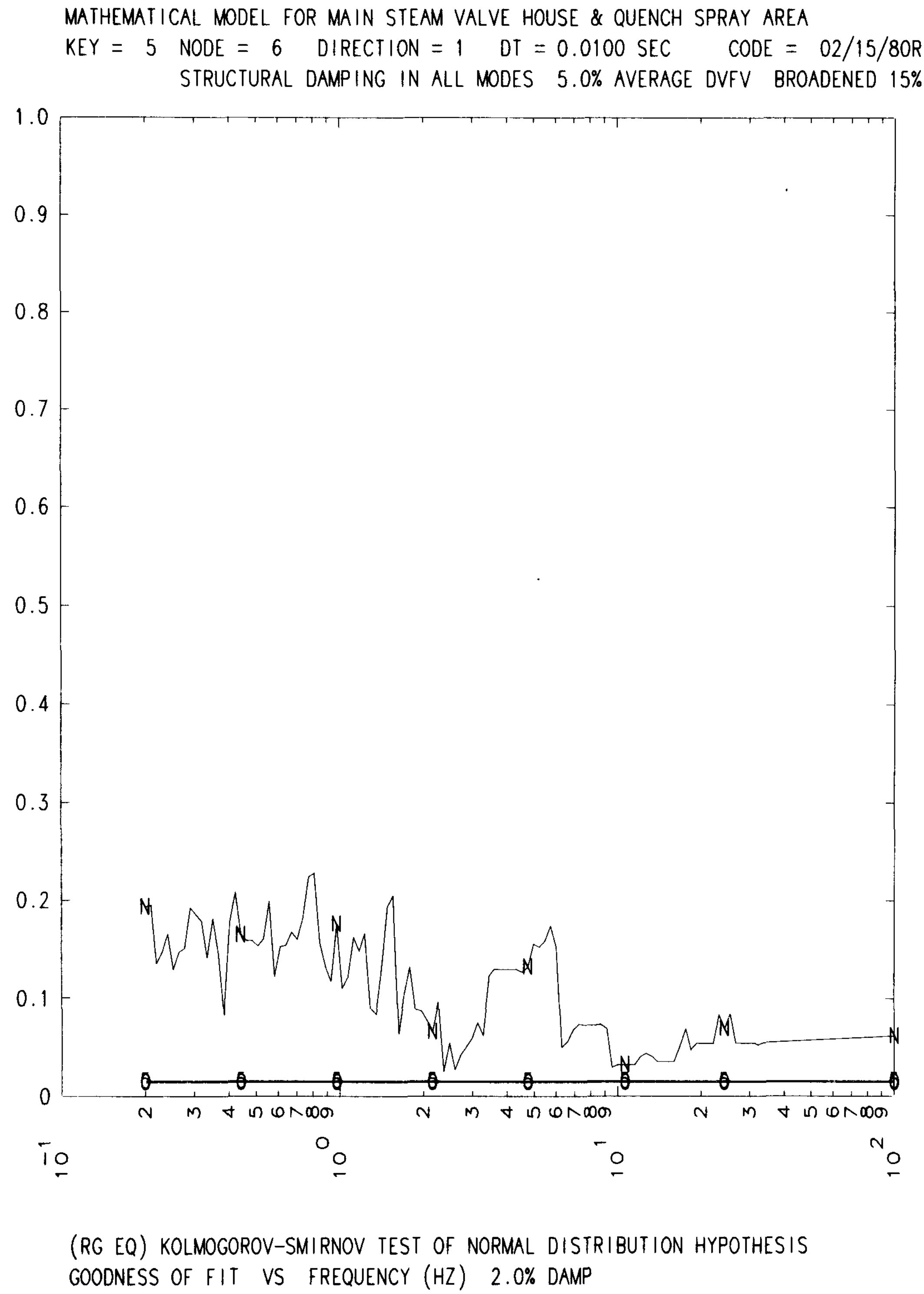

FIG. B-8. Mathematical model for main steam valve house and quench spray area (key = 5, node = 6, direction = 1).

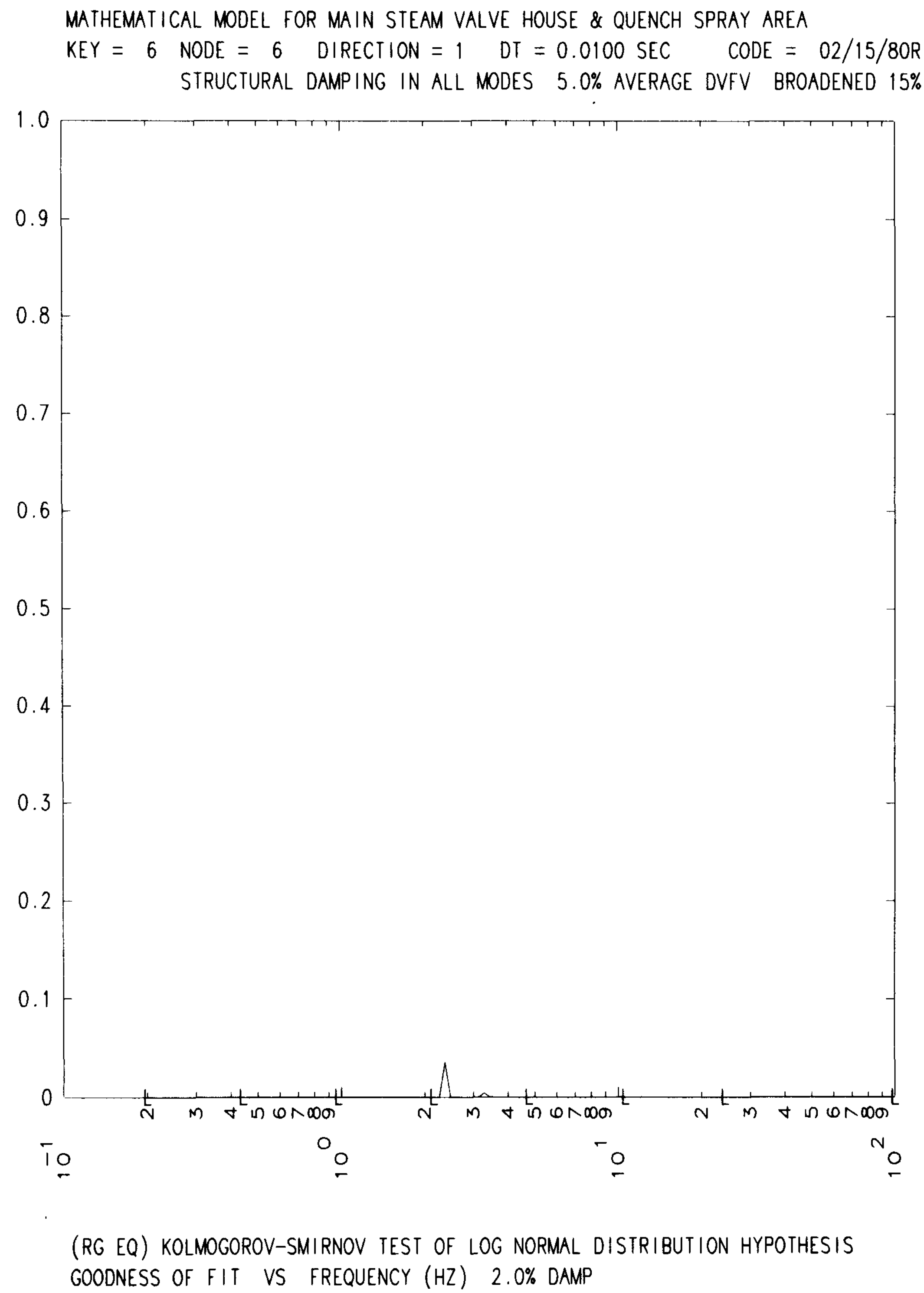

FIG. B-9. Mathematical model for main steam valve house and quench·spray area (key = 6, node = 6, direction = 1).

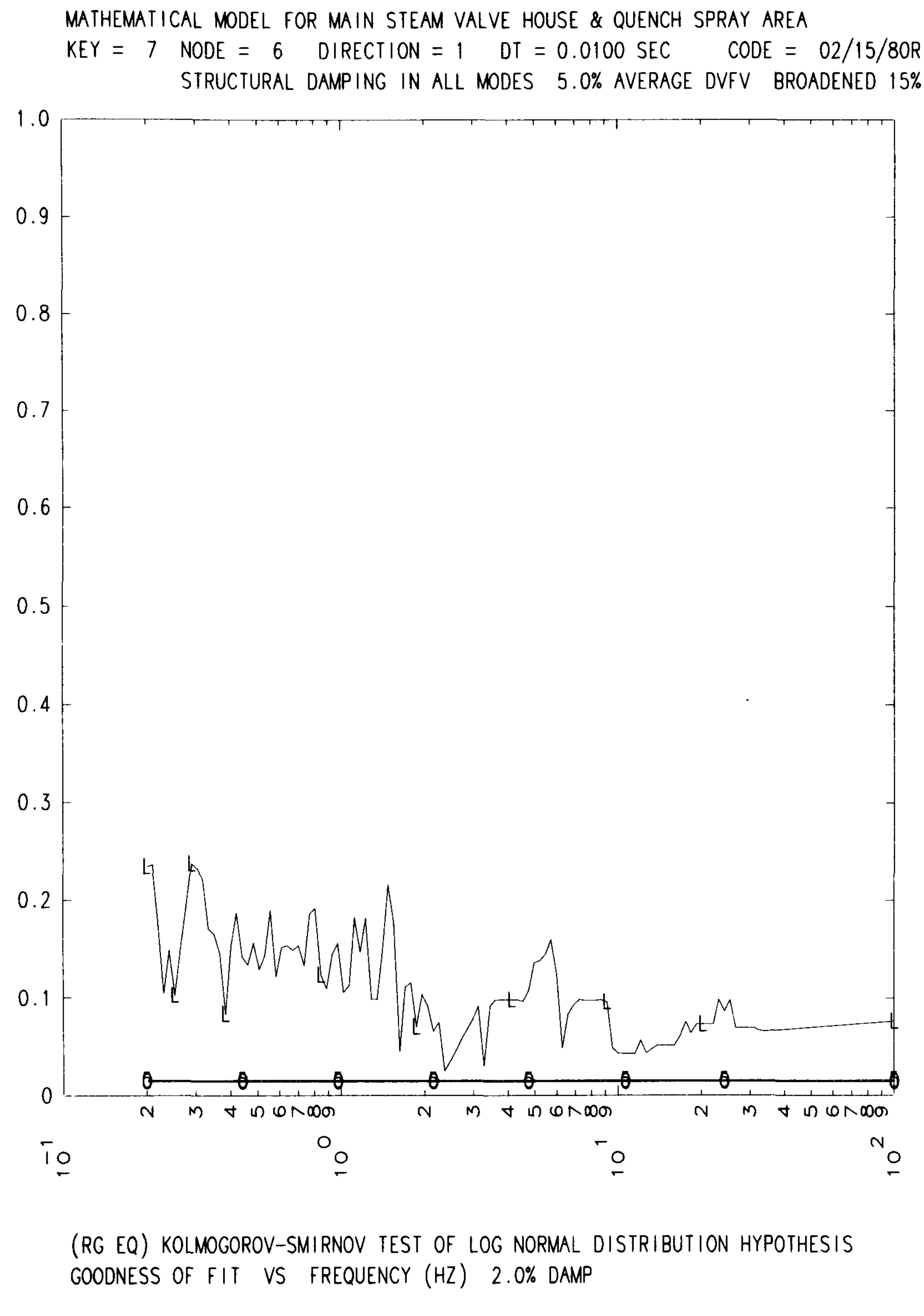

FIG. B-10. Mathematical model for main steam valve house and quench spray area (key = 7, node = 6, direction = 1).

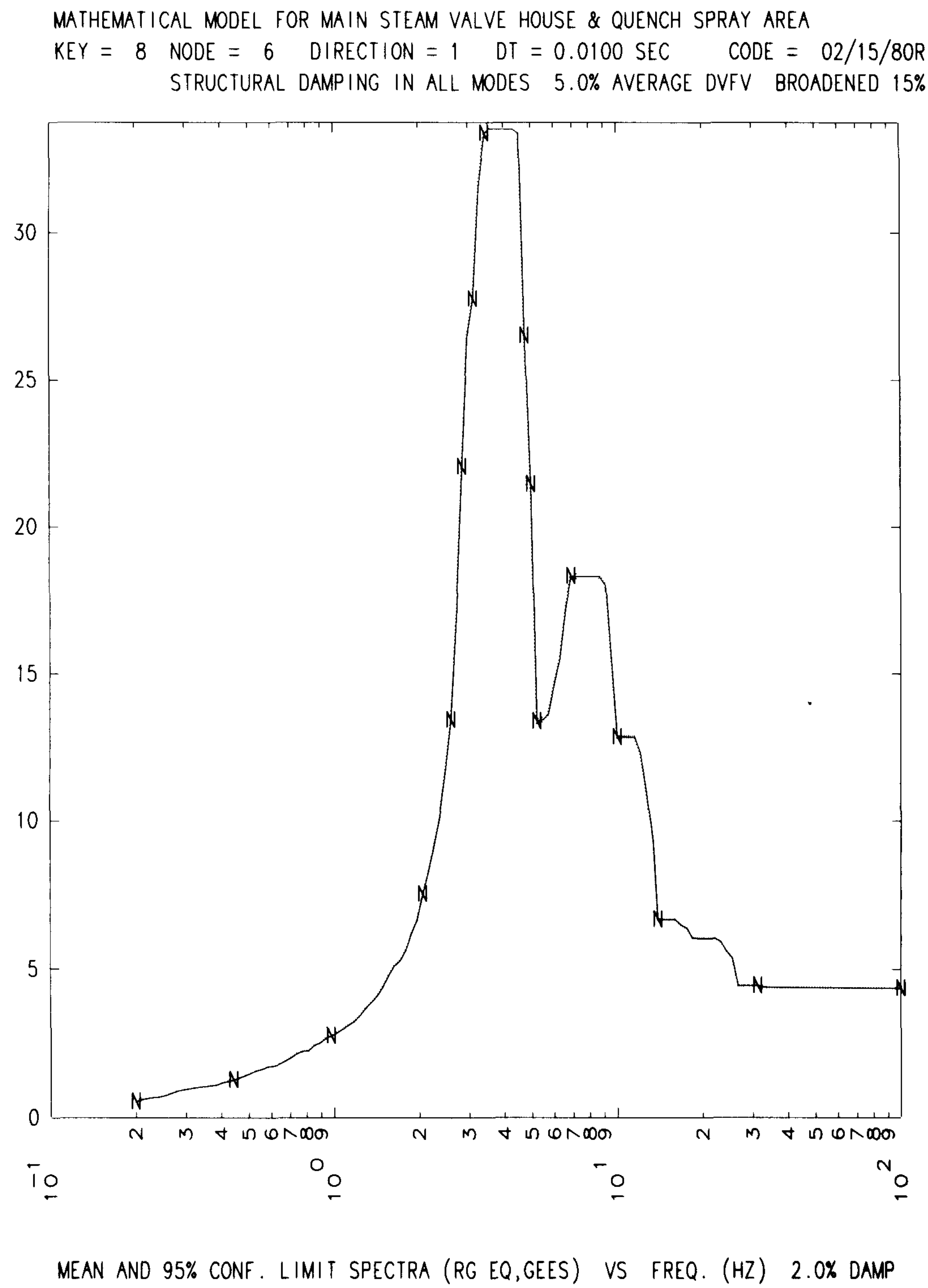

FIG. B-11. Mathematical model for main steam valve house and quench spray area (key = 8, node = 6, direction = 1).

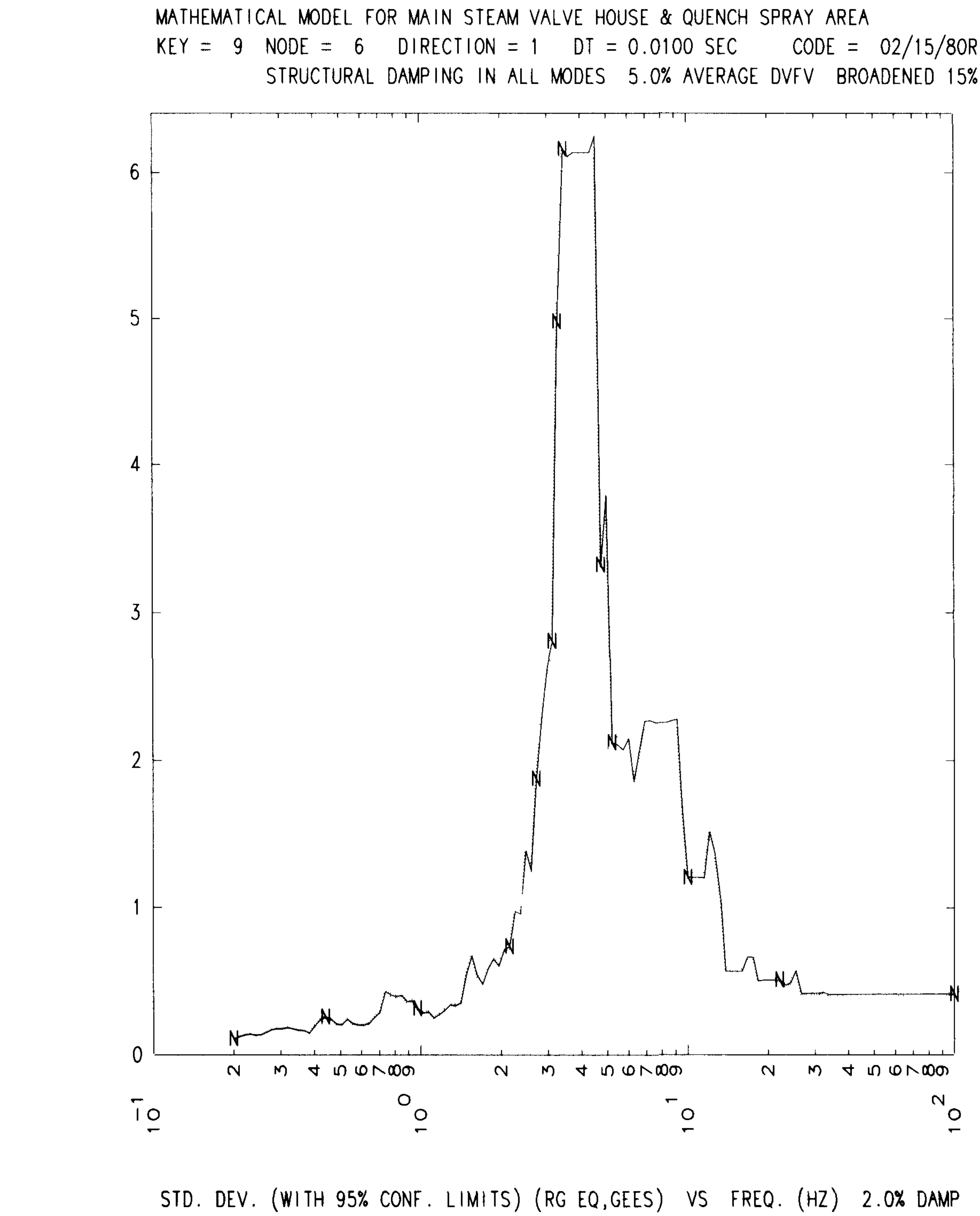

FIG. B-12. Mathematical model for main steam valve house and quench spray area (key = 9, node = 6, direction = 1).

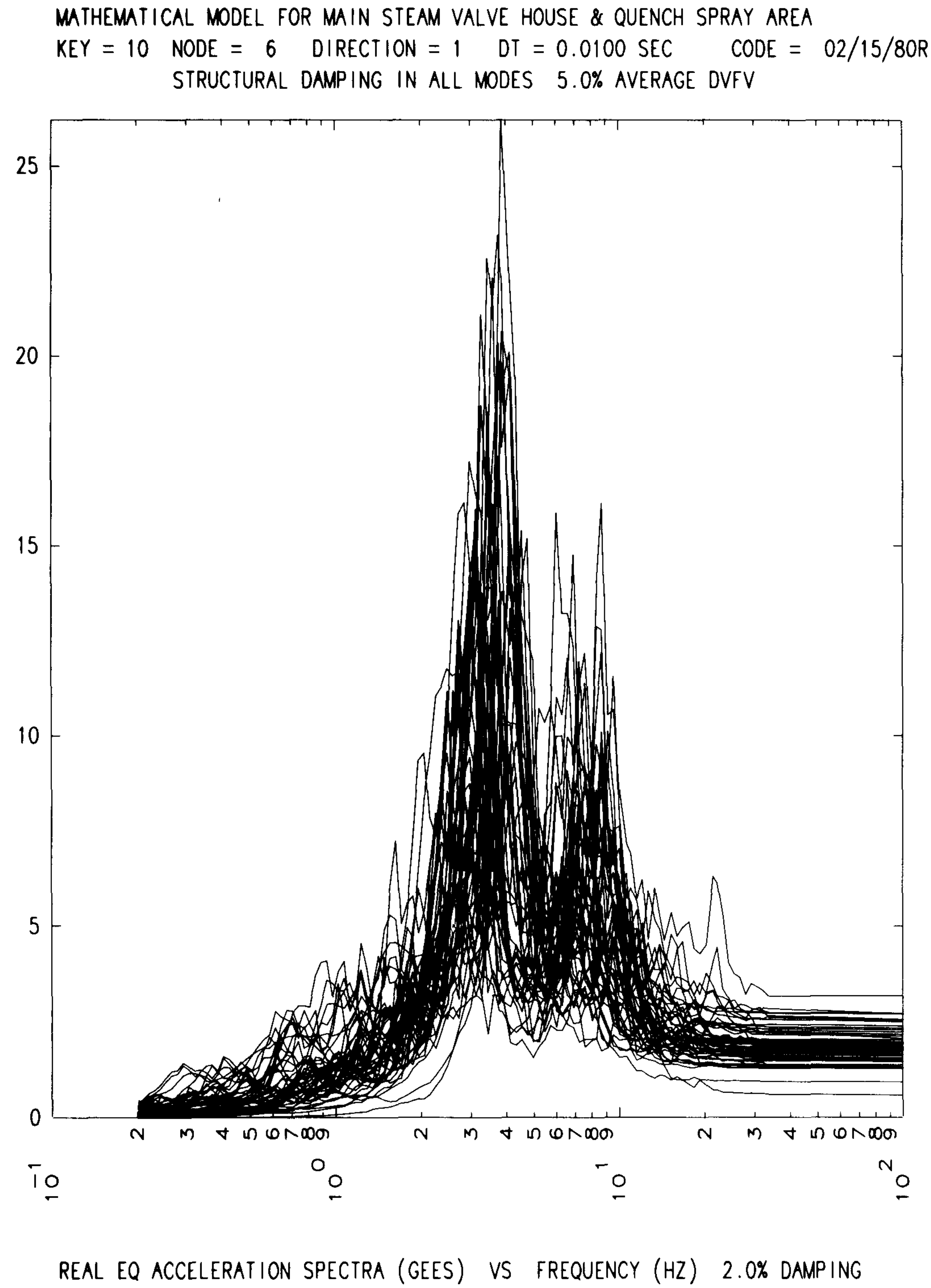

FIG. B-13. Mathematical model for main steam valve house and quench spray area (key = 10, node = 6, direction = 1).

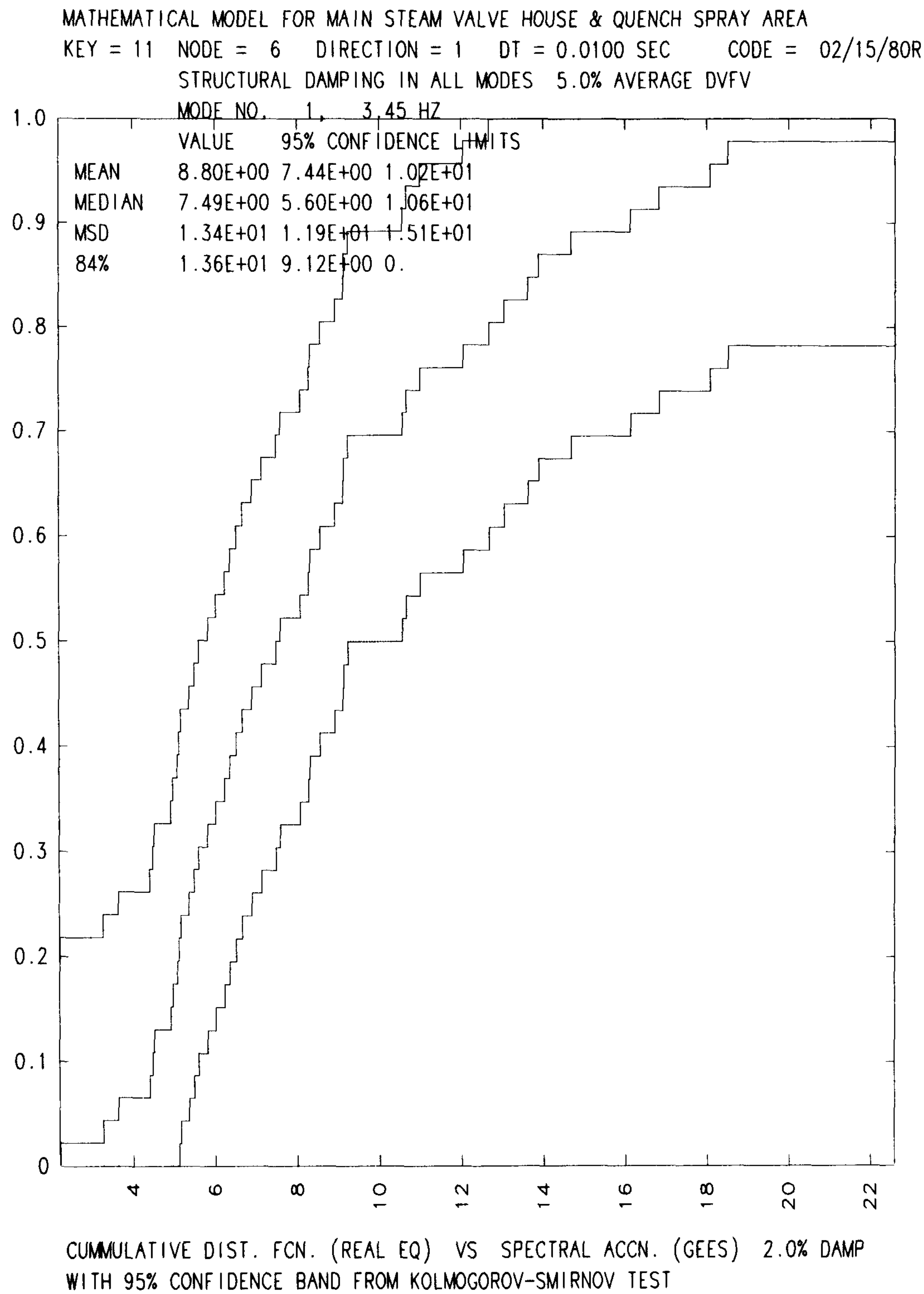

FIG. B-14. Mathematical model for main steam valve house and quench spray area (key = 11, node = 6, direction = 1).

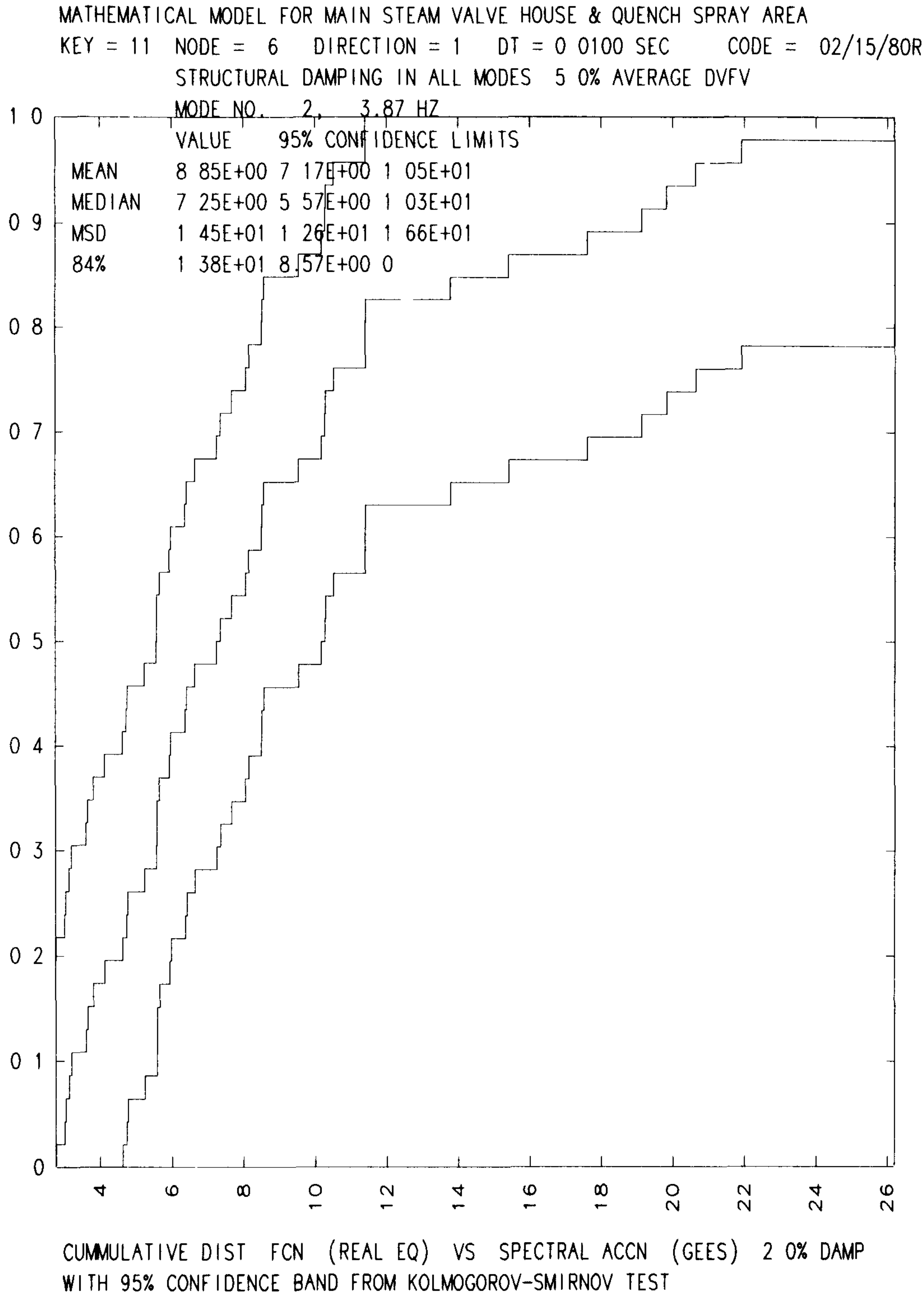

FIG. B-15. Mathematical model for main steam valve house and quench spray area (key = 11, node = 6, direction = 1).

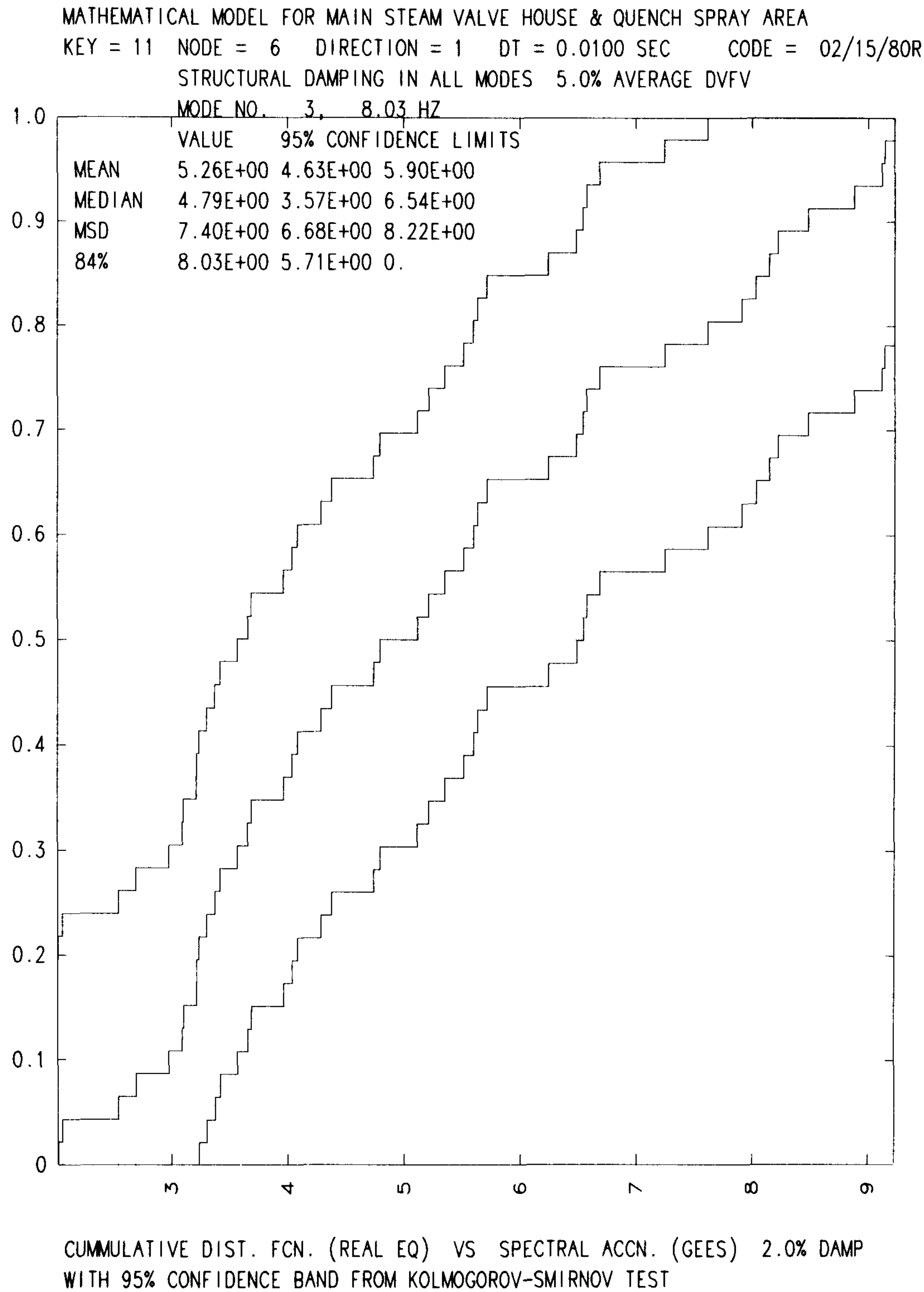

FIG. B-16. Mathematical model for main steam valve house and quench spray area (key = 11, node = 6, direction = 1).

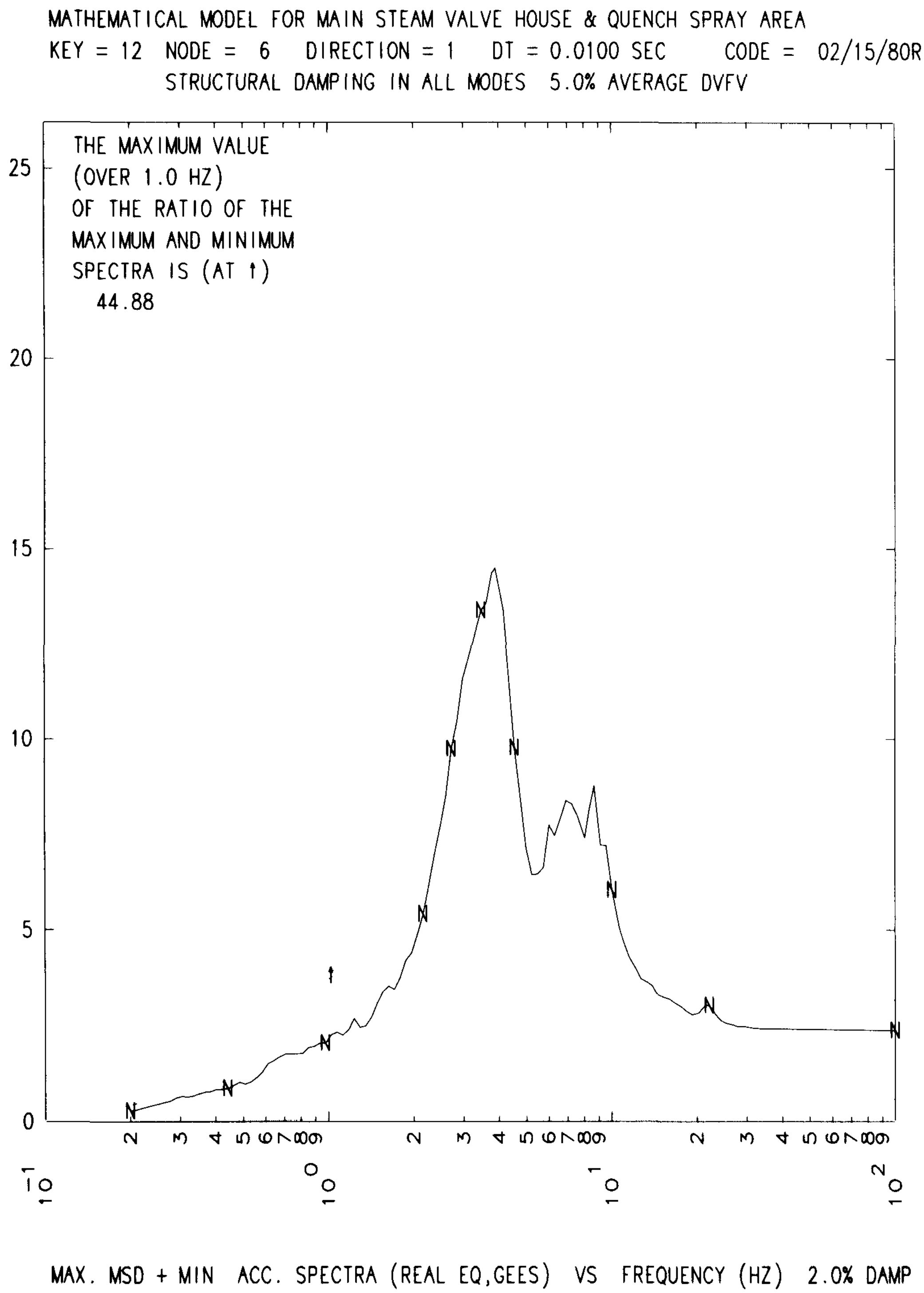

FIG. B-17. Mathematical model for main steam valve house and quench spray area (key = 12, node = 6, direction = 1).

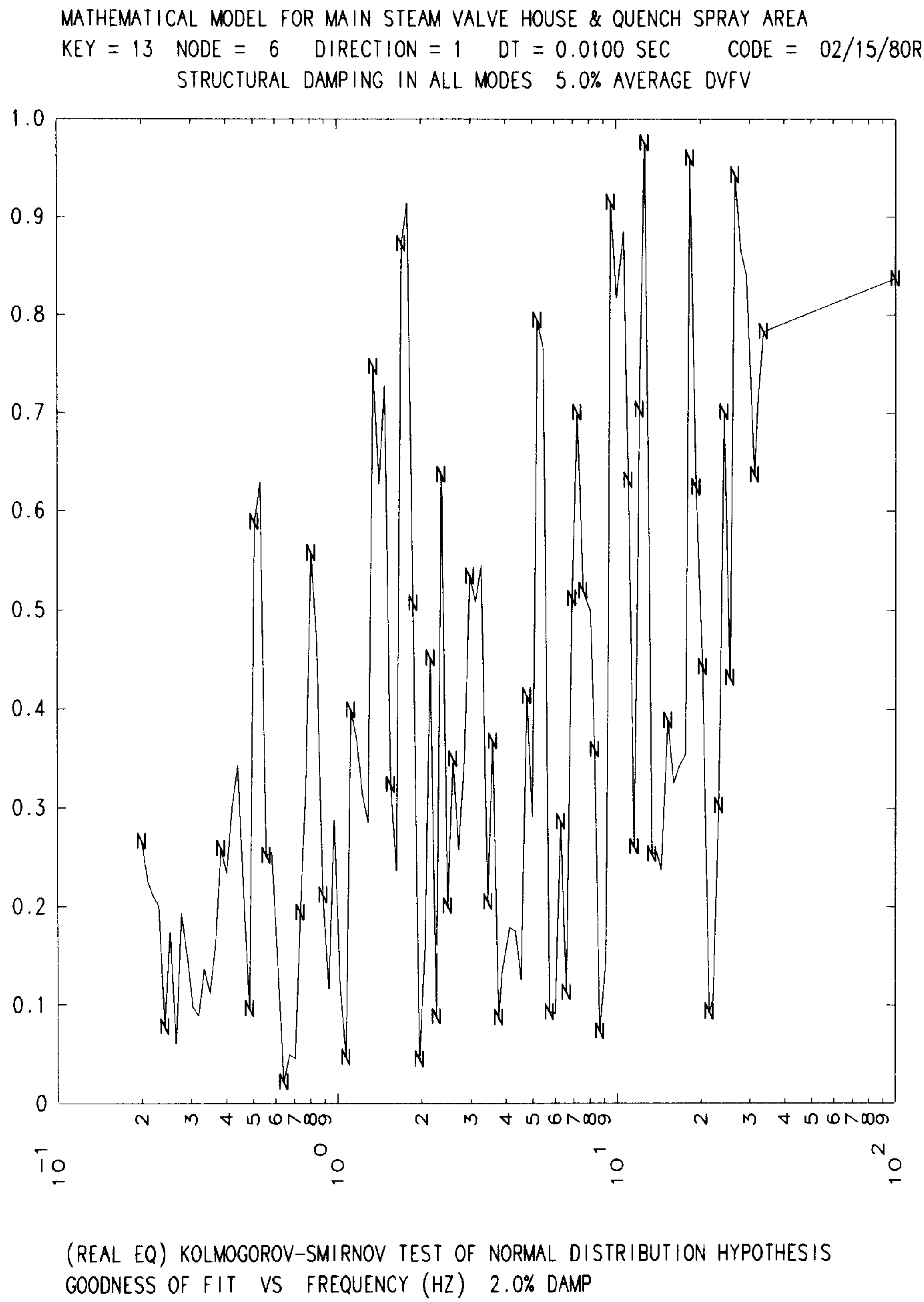

FIG. B-18. Mathematical model for main steam valve house and quench spray area (key = 13, node = 6, direction = 1).

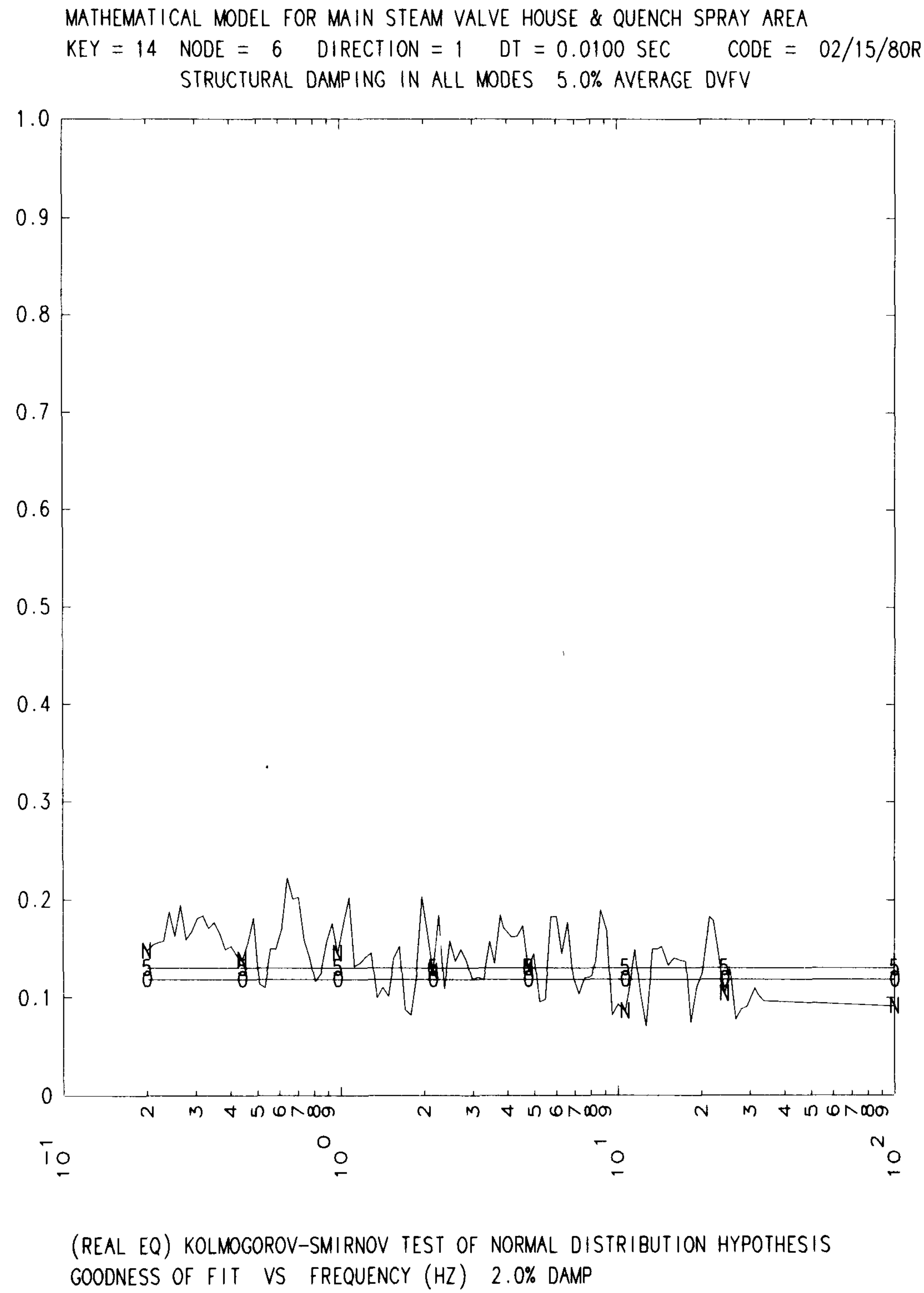

FIG. B-19. Mathematical model for main steam valve house and quench spray area (key = 14, node = 6, direction = 1).

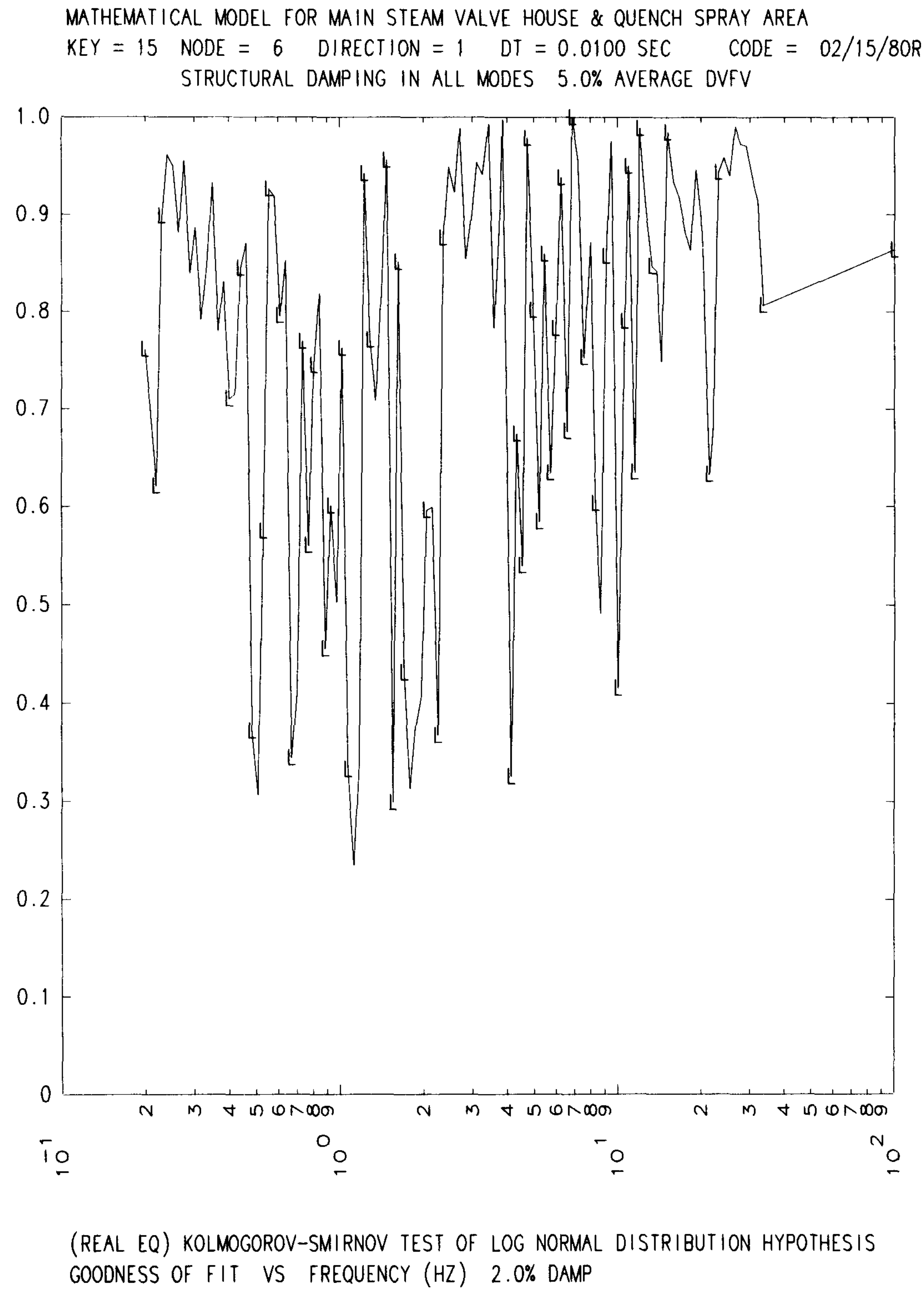

FIG. B-20. Mathematical model for main steam valve house and quench spray area (key = 15, node = 6, direction = 1).

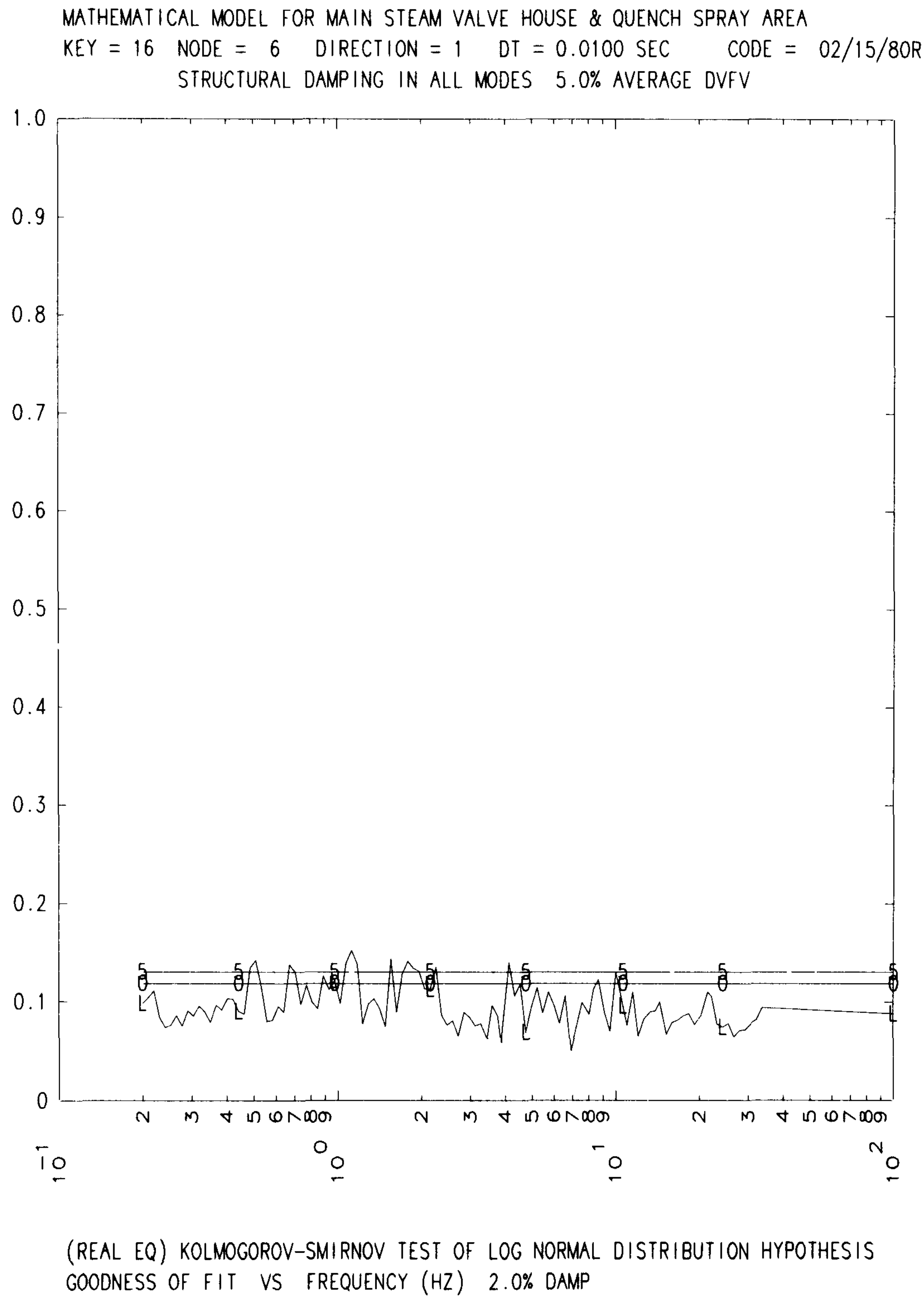

FIG. B-21. Mathematical model for main steam valve house and quench spray area (key = 16, node = 6, direction = 1).

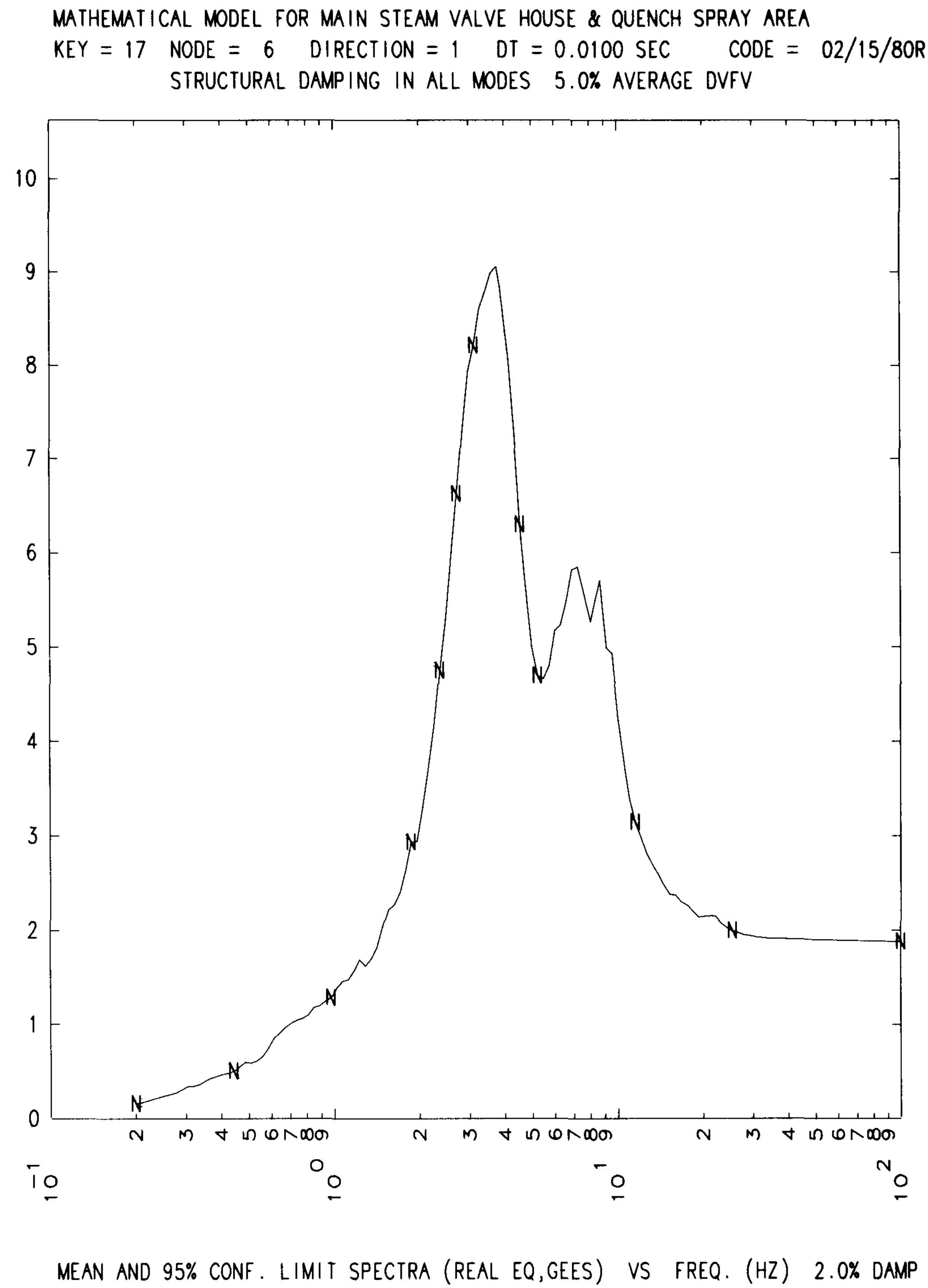

FIG. B-22. Mathematical model for main steam valve house and quench spray area (key = 17, node = 6, direction = 1).

MATHEMATICAL MODEL FOR MAIN STEAM VALVE HOUSE & QUENCH SPRAY AREA
KEY = 18 NODE = 6 DIRECTION = 1 DT = 0.0100 SEC CODE = 02/15/80R
STRUCTURAL DAMPING IN ALL MODES 5.0% AVERAGE DVFV

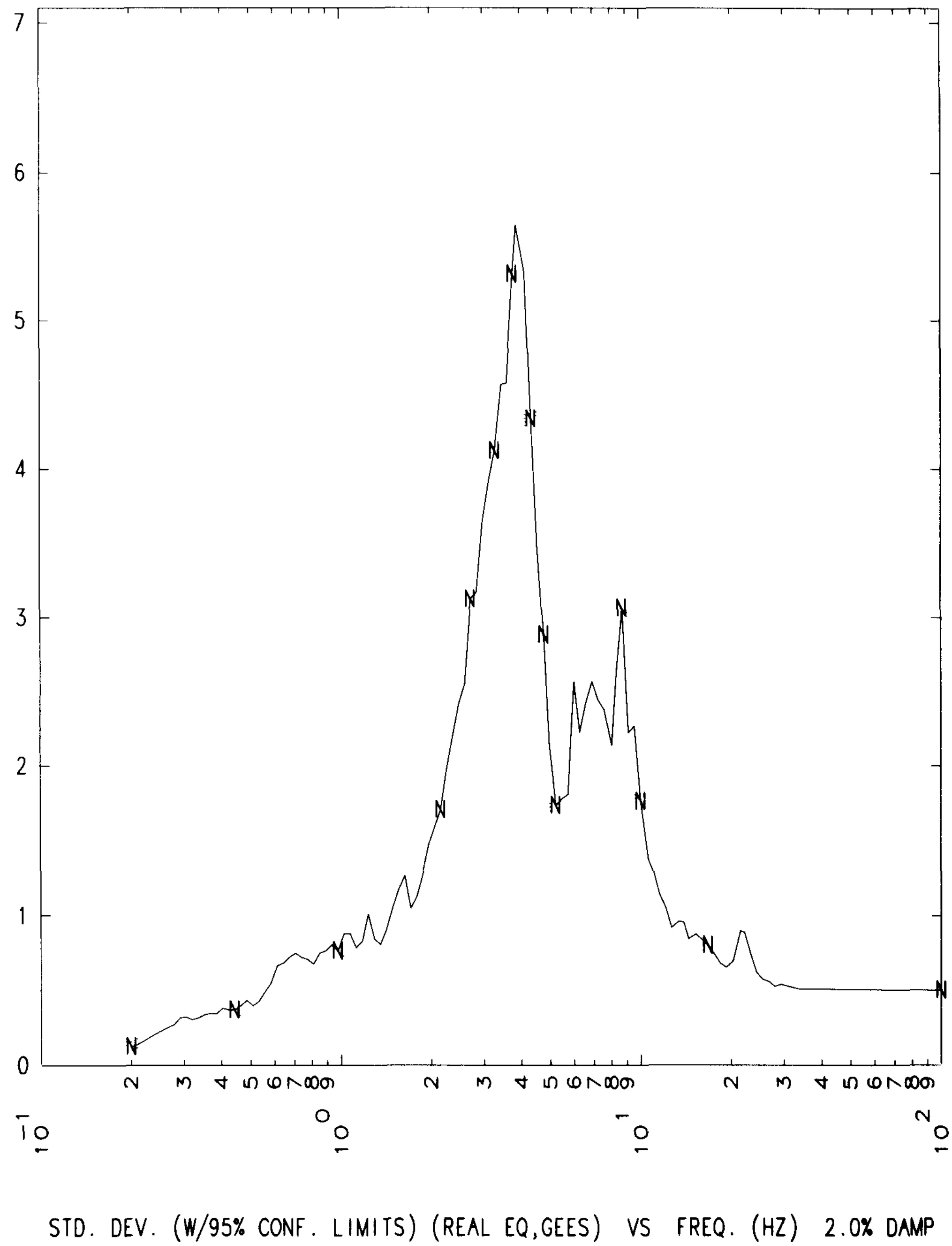

FIG. B-23. Mathematical model for main steam valve house and quench spray area (key = 18, node = 6, direction = 1).

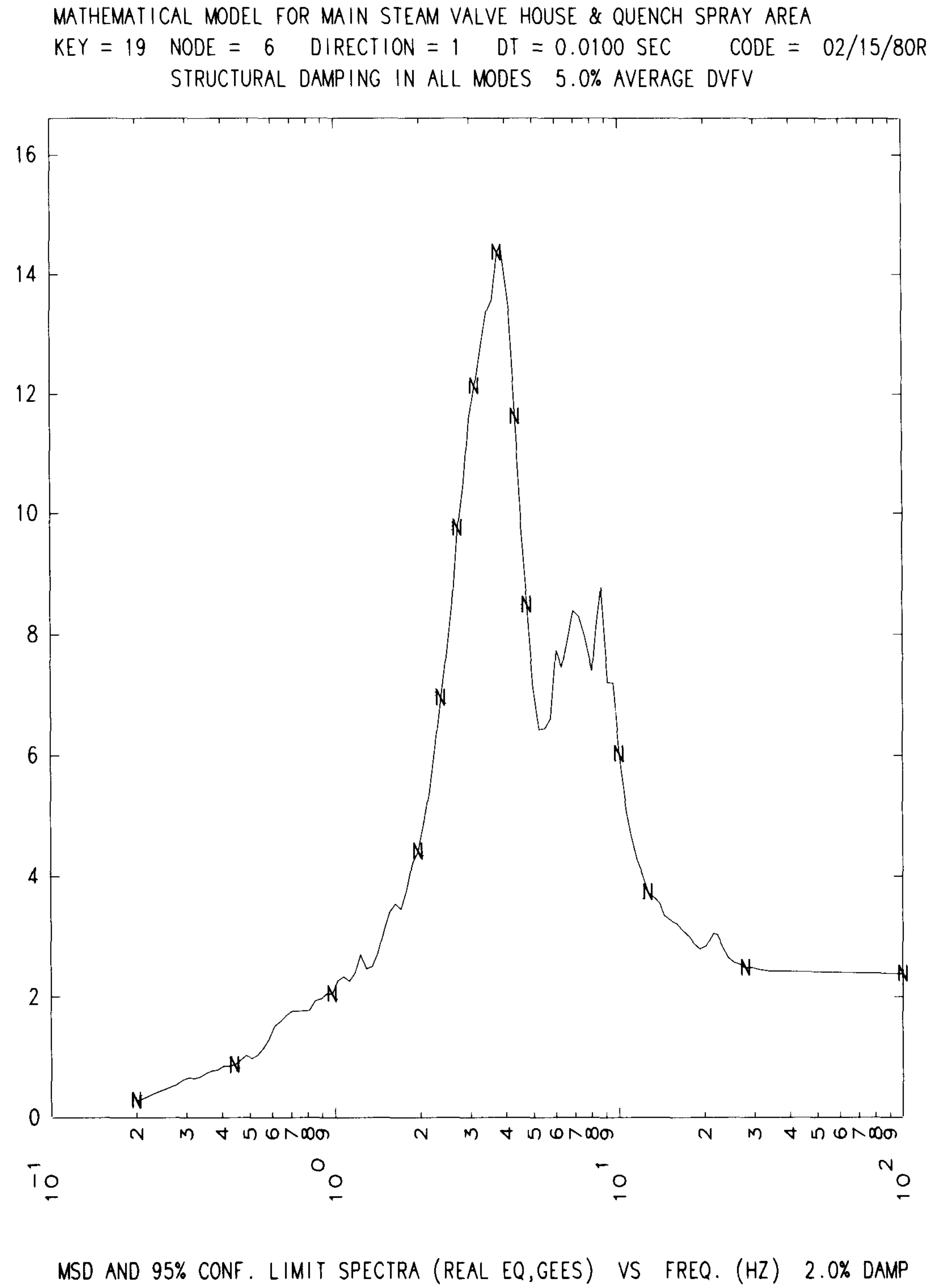

FIG. B-24. Mathematical model for main steam valve house and quench spray area (key = 19, node = 6, direction = 1).

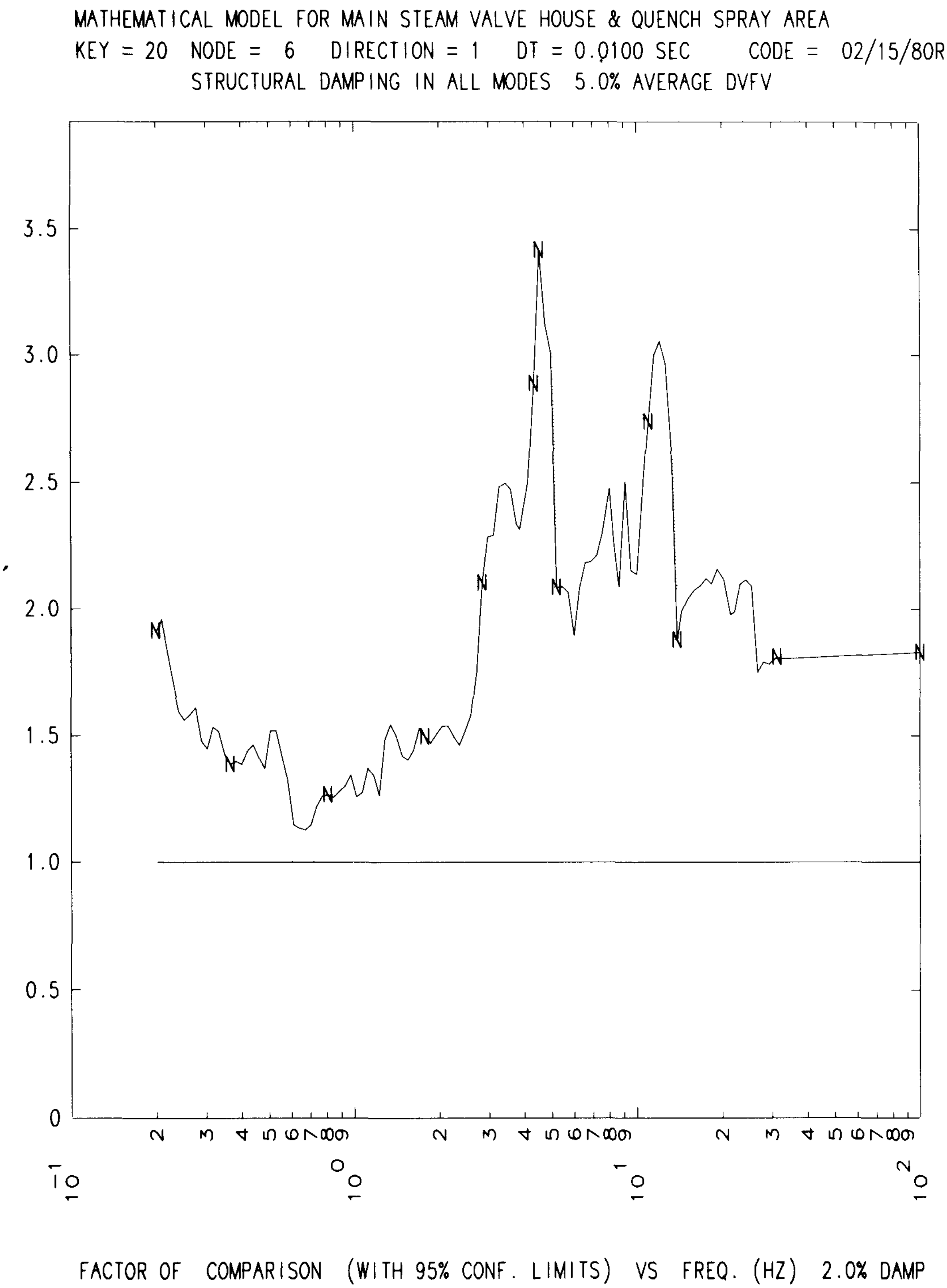

FIG. B-25. Mathematical model for main steam valve house and quench spray area (key = 20, node = 6, direction = 1).

MATHEMATICAL MODEL FOR MAIN STEAM VALVE HOUSE & QUENCH SPRAY AREA
KEY = 21 NODE = 6 DIRECTION = 1 DT = 0.0100 SEC CODE = 02/15/80R
STRUCTURAL DAMPING IN ALL MODES 5.0% AVERAGE DVFV BROADENED 15%

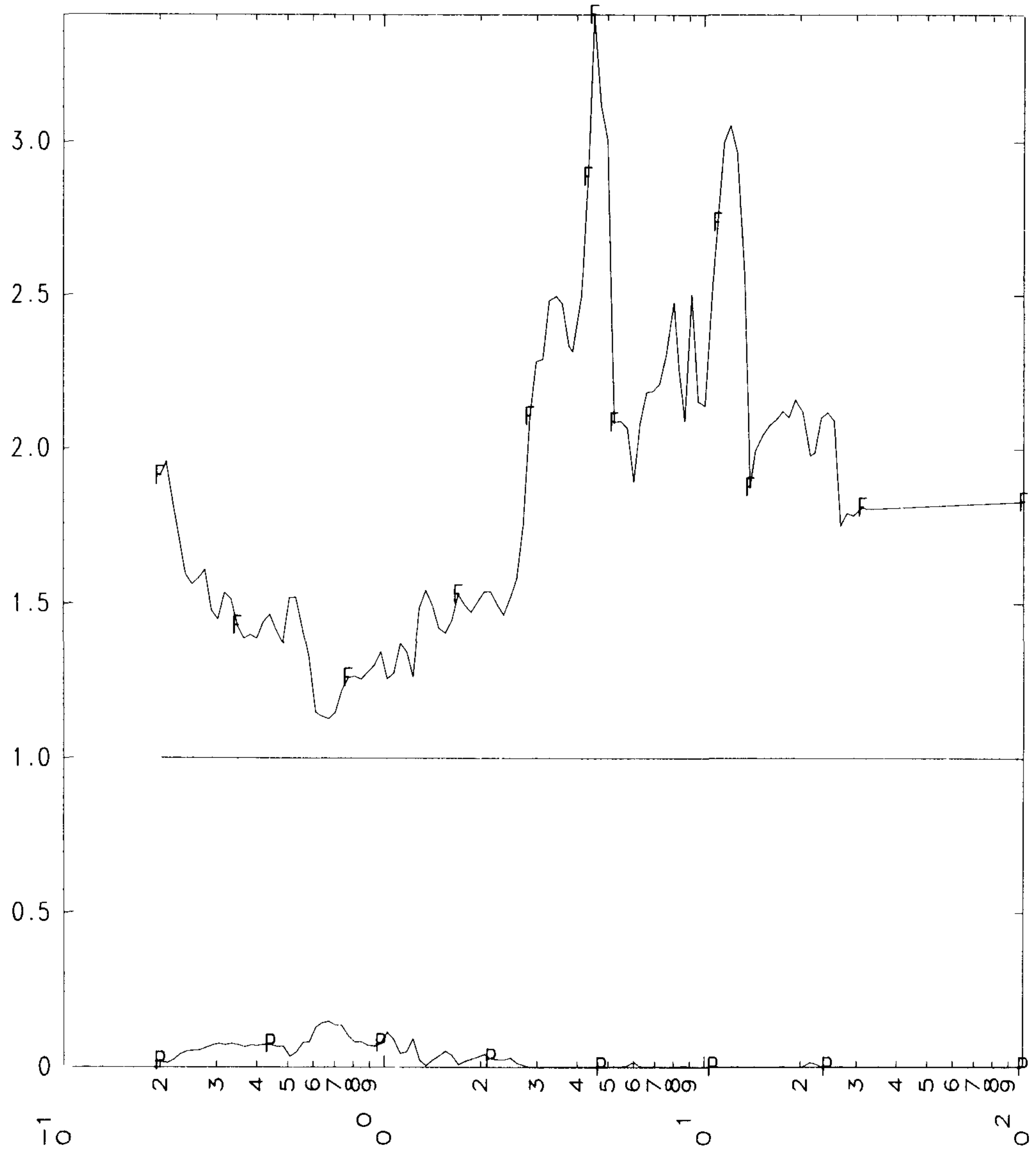

FACTOR OF COMPARISON (F) VS FREQUENCY SUPERIMPOSED ON MEASURE OF
PROBABILITY OF EXCEEDING SRSS SPECTRA FROM R.G. 1.60 SYNTHETIC TIME HIST.
PROBABILITY VS FREQUENCY (HZ) 2.0% DAMPING

FIG. B-26. Mathematical model for main steam valve house and quench spray area (key = 21, node = 6, direction = 1).

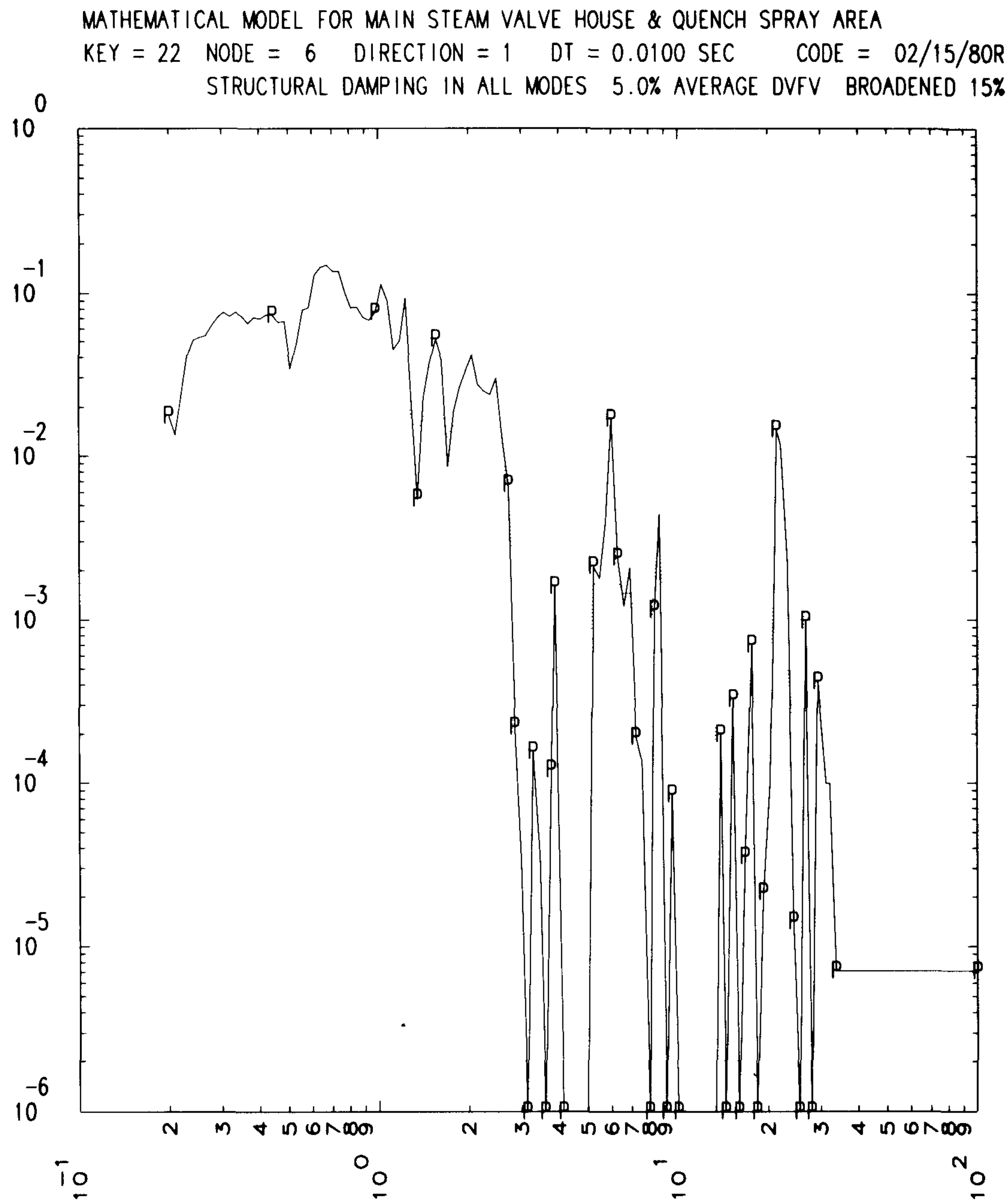

FIG. B-27. Mathematical model for main steam valve house and quench spray area (key = 22, node = 6, direction = 1).

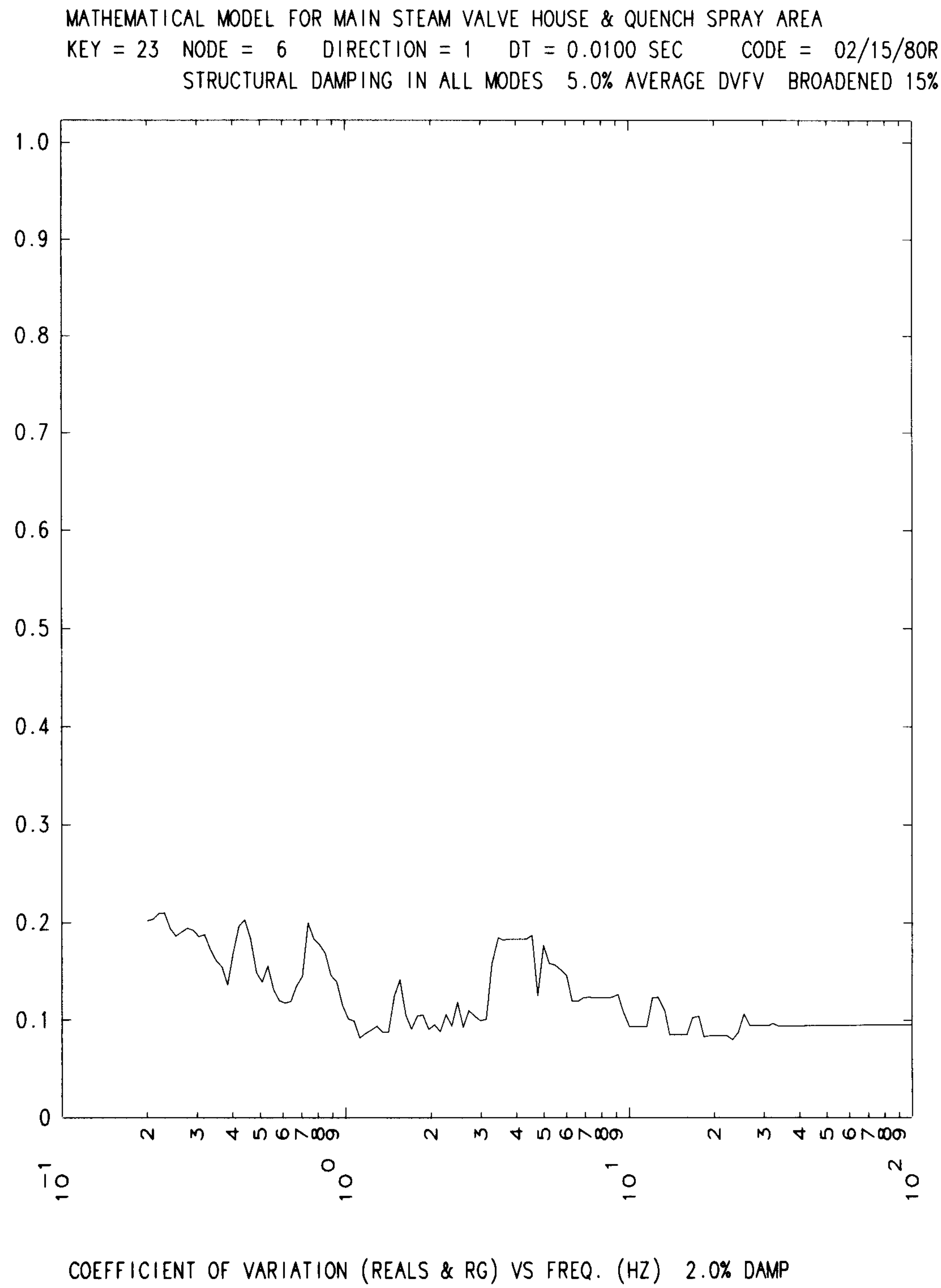

FIG. B-28. Mathematical model for main steam valve house and quench spray area (key = 23, node = 6, direction = 1).

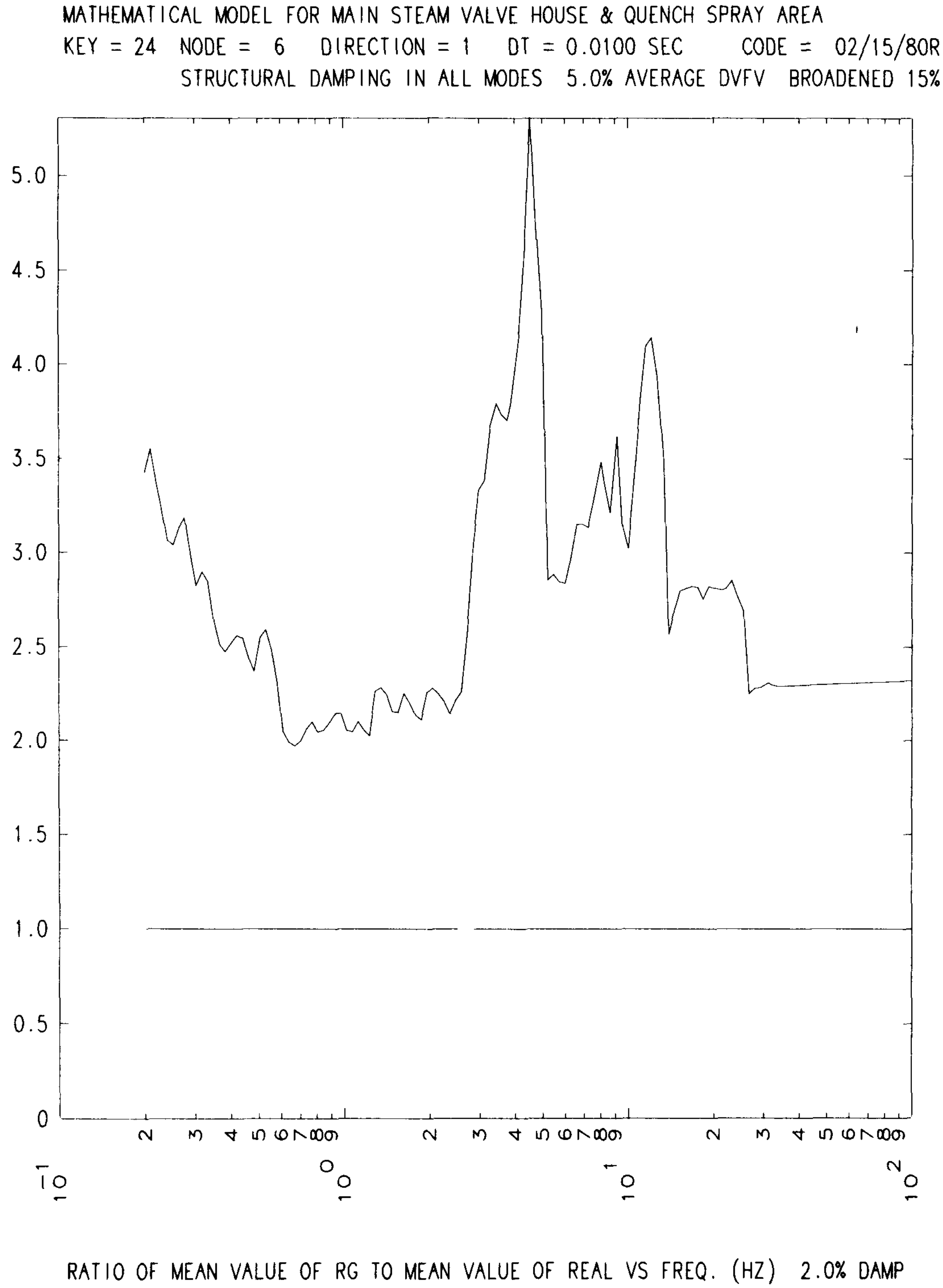

FIG. B-29. Mathematical model for main steam valve house and quench spray area (key = 24, node = 6, direction = 1).

MATHEMATICAL MODEL FOR MAIN STEAM VALVE HOUSE & QUENCH SPRAY AREA
KEY = 25 DT = 0 0100 SEC CODE = 02/15/80R
STRUCTURAL DAMPING IN ALL MODES 5 0% AVERAGE DVFV BROADENED 15%
NODE = 6 DIRECTION = 1 ABS ACCN

9 703297E+01	MINIMUM R G 1 60 EQ VALUE (SRSS)
1 599550E+02	MAXIMUM R G 1 60 EQ VALUE (SRSS)
1 648460E+00	RATIO OF MAXIMUM TO MINIMUM
1 350416E+02	MEAN OF R G 1 60 EARTHQUAKES (SRSS)
1 345856E+02	LOWER 95% CONFIDENCE LIMIT
1 354977E+02	UPPER 95% CONFIDENCE LIMIT
1 289457E+01	STD DEV OF R G 1 60 EARTHQUAKES (SRSS)
1 258003E+01	LOWER 95% CONFIDENCE LIMIT
1 322537E+01	UPPER 95% CONFIDENCE LIMIT
1 916118E+01	MINIMUM REAL EQ VALUE
1 020392E+02	MAXIMUM REAL EQ VALUE
5 325308E+00	RATIO OF MAXIMUM TO MINIMUM
6 043464E+01	MEAN OF REAL EARTHQUAKES
5 561902E+01	LOWER 95% CONFIDENCE LIMIT
6 525025E+01	UPPER 95% CONFIDENCE LIMIT
1 621619E+01	STD DEV OF REAL EARTHQUAKES
1 345001E+01	LOWER 95% CONFIDENCE LIMIT
2 042807E+01	UPPER 95% CONFIDENCE LIMIT
7 665083E+01	MEAN PLUS STD DEV OF REAL EQ
7 129393E+01	LOWER 95% CONFIDENCE LIMIT
8 290911E+01	UPPER 95% CONFIDENCE LIMIT
1 761777E+00	FACTOR OF COMPARISON
1 628510E+00	LOWER 95% CONFIDENCE LIMIT
1 894022E+00	UPPER 95% CONFIDENCE LIMIT
1 203012E-04	MEASURE OF PROBABILITY OF EXCEEDING R G 1 60 EARTHQUAKE SRSS VALUE

FIG. B-30. Mathematical model for main steam valve house and quench spray area (key = 25, node = 6, direction = 1).

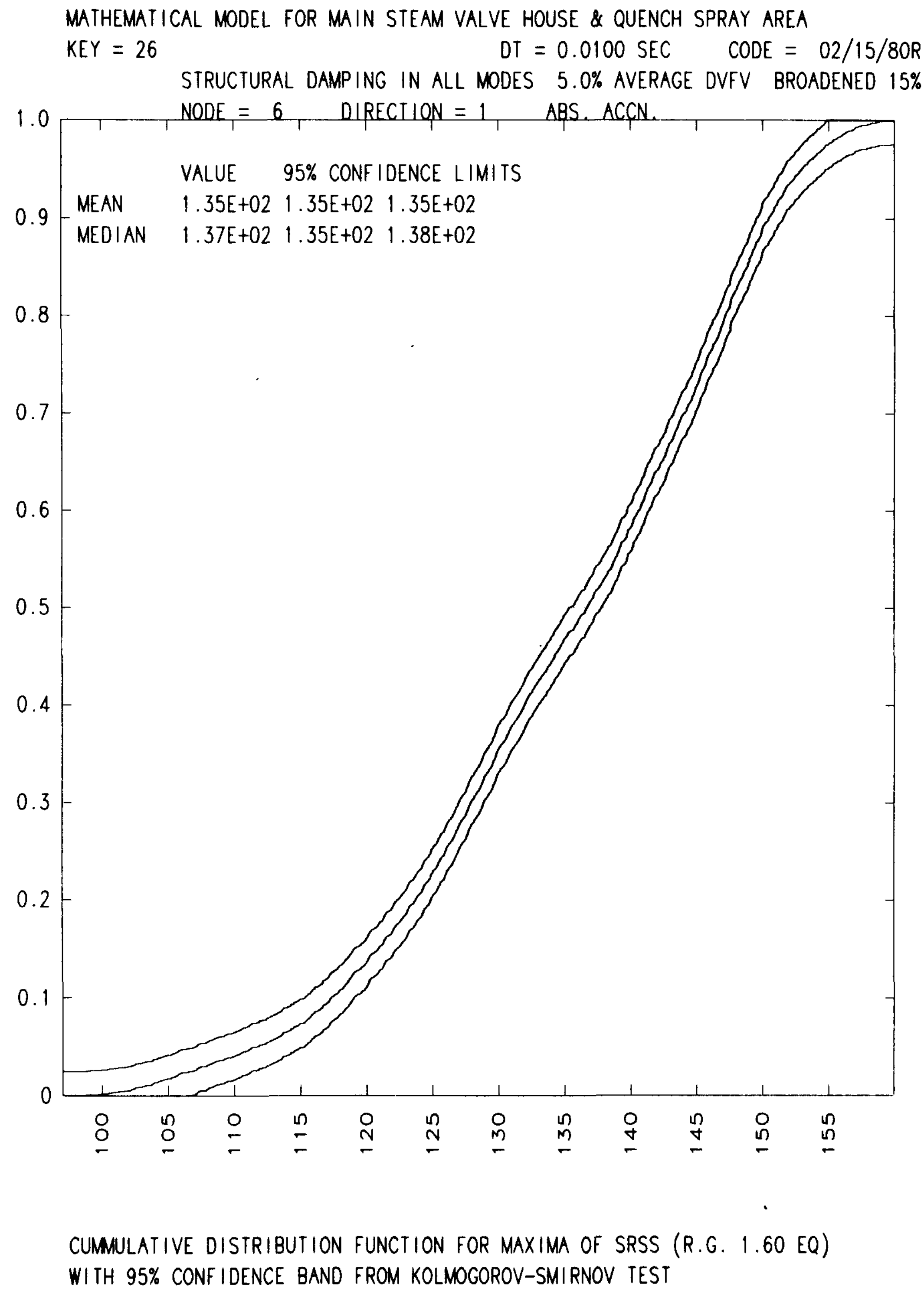

FIG. B-31. Mathematical model for main steam valve house and quench spray area (key = 26, node = 6, direction = 1).

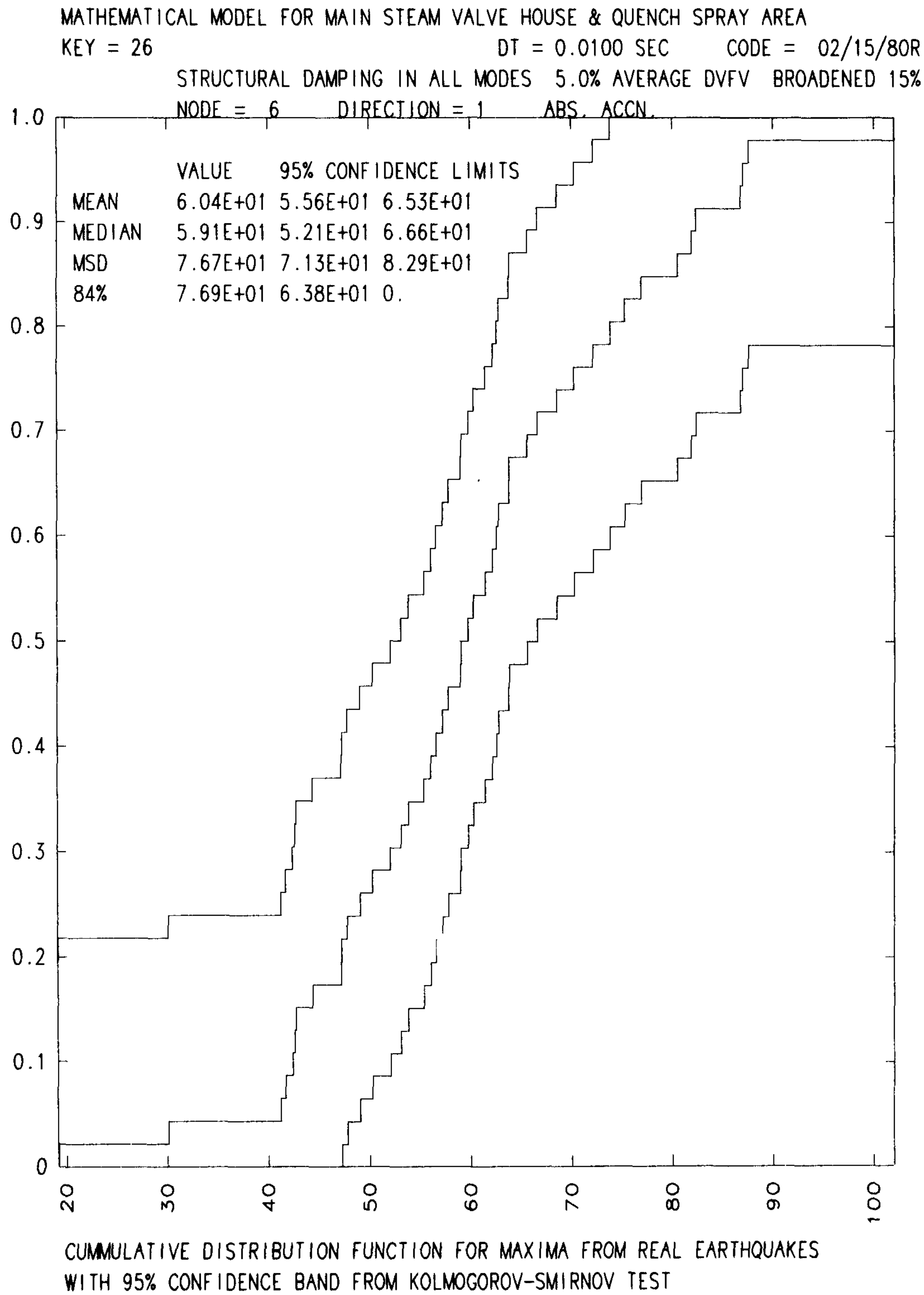

FIG. B-32. Mathematical model for main steam valve house and quench spray area (key = 26, node = 6, direction = 1).